Target-Fishing entzündungsrelevanter Arzneistoffe

sowie biochemisch-molekularpharmakologische Charakterisierung der Arzneistoff-Target Interaktion

Target-fishing of drugs relevant to inflammation

and biochemical molecular pharmacological characterisation of the drug-target interaction

Dissertation
der Mathematisch-Naturwissenschaftlichen Fakultät
der Eberhard Karls Universität Tübingen
zur Erlangung des Grades eines
Doktors der Naturwissenschaften
(Dr. rer. nat.)

vorgelegt von
Felix Behnke
aus Vaihingen/Enz

Tübingen
2011

Tag der mündlichen Qualifikation: 28.04.2011
Dekan: Prof. Dr. Wolfgang Rosenstiel
1. Berichterstatter: Prof. Dr. O. Werz
2. Berichterstatter: Prof. Dr. S. Laufer

TABLE OF CONTENTS

Abbreviations

2D-DIGE	Two dimensional difference gel electrophoresis
2D-EL	2-dimensional gel electrophoresis
5-LO	5-lipoxygenase
AA	Arachidonic acid
ABHD14B	Abhydrolase domain-containing protein 14B
ABPP	Activity-based protein profiling
ACAP	Acetaminophen (= Paracetamol)
ADP	Adenosine diphosphate
Akt	Ak-transformed kinase
AM404	N-arachodinyl-phenolamine
AR	Androgen receptor
ATM	Ataxia telangiectasia mutated kinase
ATP	Adenosine triphosphate
ATR	Ataxia telangiectasia-Rad3-related kinase
BA	Betulinic acid
BCiP	5-bromo-4-chloro-3-indolyl phosphate
Boc	tert-butoylxycarbonyl
BSA	Bovine serum albumin
CCD	Charge-coupled Device,
CDK	Cyclin-dependend kinases
c-fos	Cellular proto-oncogene encoded by the FOS gene
CG	Cathepsin G
Chk1	Checkpoint kinase 1
c-jun	Protein encoded by the JUN oncogene
CMO	Carboxymethoxylamine
COX	Cyclooxygenase
c-Raf	See Raf
c-Src	Cellular-sarcoma
Ctrl	Control
DCC	N,N-dicyclohexylcarbidiimide
DHT	Dihydrotestosterone
DIC	N,N-diisopropylcarbodiimide

DIGE	Difference gel electrophoresis
DMAP	4-Dimethylaminopyridine
DMEM	Dulbecco´s Eagle Medium
DMF	Dimethylformamide
DMSO	Dimethyl sulfoxide
DNA	Deoxyribonucleic acid
DTT	Dithiothreitol
EC_{50}	Half maximal effective concentration
ECL	Chemoluminescence
E. coli	*Escherichia coli*
EDC	1-(3-Dimethylaminopropyl)-3-ethylcarbodiimide hydrochloride
EDTA	Ethylenediaminetetraacetic acid
EGF	Epidermal growth factor
eNOS	Endothelian NO synthase
ErbB2	Erythroblastic leukaemia viral oncogene homolog 2
ERK	Extracellular-signal-regulated kinase
ERK1/2	Extracellular signal-regulated kinases 1 and 2
ESI	Electrospray ionization
FBP	Far upstream binding protein
FCS	Fetal calf serum
fig	Figure
FK-506	Synonym for rapamycin
fMLP	N-Formylmethionine leucyl-phenylalanine
FUBP	Far upstream binding protein
GnRH	Gonadotropin-releasing hormone
GTP	Guanosine triphosphate
hAR-A	Human androgen receptor isoform A
hAR-B	Human androgen receptor isoform B
HeLa	Henrietta Lacks, cervical cancer cell line
Hepes	4-(2-hydroxyethyl)-1-piperazineethanesulfonic acid
Her2/neu	Human Epidermal growth factor Receptor 2
HIV	Human immunodeficiency virus
HLE	Human leukocyte elastase

HRE	Hormone responsive elements
HRP	Horseradish peroxidase
HSA	Human serum albumin
HSP B1	Heat shock protein beta-1
HSP27	Heat shock protein 27
IC_{50}	Half maximal inhibitory concentration
IEF	Isoelectric focussing
IEP	Isoelectric pint
IL	Interleukin
iNOS	Inducible NO synthase
IPG	Immobilised pH gradient
IR3MO	Indirubine-3´-monoxime
IκB-α	Inhibitor of NF-κB
KHSRP	KH-type splicing regulatory protein
KPN-β	Karyopherin β
LB (medium)	Lysogeny broth (medium)
LC	Liquid chromatography
LNCap	Lymph Node Carcinoma of the Prostate
LO	Lipoxygenase
MAPK	Mitogen-activated protein kinase
MC	Myrtucommulone A
Mek	Mitogen-activated protein kinase kinase kinase 1
MeOH	Methanol
MK2	MAPK-activated Protein Kinase-2
MNEI	Monocyte/neutrophil elastase inhibitor
Mops	3-(N-morpholino)propanesulfonic acid
mPGES1	Microsomal prostaglandin E2 synthase 1
mRNA	Messenger RNA
MS	Mass spectrometry
mTOR	Mammalian target of rapamycin
NAMPT	Nicotinamide phosphorybosyltransferase
NBT	Nitro blue tetrazolium chloride
NFκB	Nuclear factor kappa-light-chain-enhancer of activated B cells/ nuclear factor κ B

NHS	N-hydroxysuccinimide
No.	Number
NSAID	Non-steroidal anti-inflammatory drug
OGX-427	HSP27 antisense drug
p(Ser82)HSP27	HSP27 phosphorylated on serine No. 82
p38 MAPK	p38 mitogen-activated protein kinases
P8340	Protease inhibitor cocktail
PAA	Polyacrylic acid
PARP	Poly (ADP-ribose) polymerase
PBA	Phenoxybutyric acid
PBEF	Pre-B-cell colony enhancing factor = visfatin
PBMC	Peripheral blood mononuclear cell
PBS	Phosphate buffered saline
PC12	Pheochromocytoma cell line
PCT	Pressure cycling technology
PDGF	Platelet-derived growth factor
pERK	Phosphorylated ERK (see ERK)
PG buffer	PBS containing glucose
PGC	PBS containing glucose and calcium
PI3K	Phosphatidylinositol 3-kinases
PKA	Protein kinase A
PMNL	Polymorphonuclear leukocyte
PMSF	Phenylmethanesulfonyl fluoride
PR	Progesterone receptor
PR3	Proteinase 3
PR-A	Progesterone receptor isoform A
PR-B	Progesterone receptor isoform B
prog.	Progesterone
qTOF	Quadrupole time-of-flight
Raf	Rapidly growing fibrosarcoma
Ras	Rat Sarcoma
RNA	Ribonucleic acid
RNAi	RNA interference
RPMI 1640	Roswell Park Memorial Institute medium

RT	Room temperature
RTK	Receptor tyrosine kinase
RV	Resveratrol
SDS	Sodium dodecyl sulfate
SDSb	SDS buffer (see SDS)
SDS-PAGE	SDS polyacrylamide gel electrophoresis
Ser	Serine
Serpin B1	Serine protease inhibitor B1
SHBG	Sex hormone binding globulin
SHP-2	Member of the protein tyrosine phosphatase (PTP) family
Src	Sarcoma
Tbl	Table
TBS	Tris buffered saline
TBST	Tris buffered saline containing Tween
test.	Testosterone
THF	Tetrahydrofuran
TNFα	Tumor necrosis factor alpha
TOF	Time-of-flight
Tris	Tris(hydroxymethyl)aminomethane
TTR-RBPs	Turnover and translation regulatory mRNA-binding proteins
UV	Ultra violett
v/v	Volume per volume
VIM	Vimentin
VIS	Visfatin
Vol	Volume
VSMC	Vascular smooth muscle cells
w/v	Weight per volume

1 Introduction

1.1 Importance of drug target identification and validation

Today, two strategies may be in principal pursued for treatment of diseases, namely (i) surgical and (ii) pharmacological intervention. The human anatomy as base for a rational surgical intervention has been known in detail for a very long time. Despite the notable scientific progresses in the last decades, the pharmacological-, biochemical- and molecular biological processes as base for a rational pharmacotherapy are instead rather poorly understood and very complex. Although certain molecular pathways have been largely characterised, pharmacotherapy focusses on only about 100 proteins. Since the human proteome is estimated to consist of 30,000 - 200,000 different proteins [1-2], today's pharmacotherapy is only limited to a small fraction of possible targets.

To be efficacious, a drug has to bind a target structure and thereby influence its activity. Today, medicinal chemistry focusses mainly on the identification and development of new drugs to known targets (i.e., target-oriented drug discovery). Therefore high throughput screenings are performed to identify lead compounds for appropriate targets and furthermore optimise these lead compounds to obtain drugs with high efficacy and selectivity. Although this strategy results in a large number of drugs, it suffers from a number of drawbacks: (i) It focusses only on a few known targets, thus only a limited number of diseases can be addressed by the drugs obtained by this methodology. (ii) Side effects caused by interaction with other targets (off-targets) can not be recognised in the early stages of drug development. (iii) Compounds (e.g., natural compounds) that are known to have beneficial effects in certain diseases as well as low side effects are neglected if they do not interact with a determined target.

Furthermore, although modern drugs are designed and optimised for one particular target, they often show side effects that are inexplicable with the interaction to the known target. For instance, statins as lipid lowering drugs show also anti-inflammatory properties [3-4].

While drugs that affect multiple targets were seen as so called "dirty drugs" due to their complex variety of side effects, scientists today try to develop systematically so called "multi-target drugs" for the treatment of complex diseases with multiple pathogenic

factors [5-9]. Regardless of whether a drug is designed to affect only one or multiple targets, a thorough understanding of all targets is required for a rational use in pharmacotherapy.

Usually, targets for known compounds are discovered by testing them in functional assays for estimated targets. This strategy suffers from the same drawbacks as target-focussed drug development, and again only a small part of possible targets are covered. However, diverse techniques and new approaches offer the opportunity to search systematically target candidates for drugs and natural compounds, which may be of particular interest for those drugs which have shown efficacy in certain pathologic conditions. Also, these methods might help to characteris biochemical and molecular biological processes by identifying unknown receptors for endogenous mediators (i.e., drugs as tools). These methods are: (i) affinity based approaches, like the target-fishing [10-11], which allow to identify new targets having a certain affinity to the ligand, and (ii) activity based approaches, like activity-based protein profiling (ABPP) [12-17], which allow to identify targets that are affected in their activity by the ligand. Thus, these methods are independent of the state of scientific knowledge and can thereby contribute to the discovery of new therapeutic options.

1.2 The target-fishing approach

Pull-down assays are suitable and valuable tools to evaluate drug-target interactions as well as a vast variety of other ligand-protein interactions. In so-called target-fishing experiments a drug covalently bound to an insoluble matrix is incubated with a cell lysate as source of target protein(s). Thus, proteins which are bound to the drug (ligand) can be isolated and identified by appropriate protein analytics (Fig. 1). Examples for the successful application of this technique are the identification of human histone deacetylase as target for trapoxin [18] and identification of the mammalian target of rapamycin (mTOR) as the target of the immunosuppressant FK-506 (rapamycin) [19]. Therefore, the target-fishing approach allows the identification of new, so far not considered targets for known pharmacological active compounds.

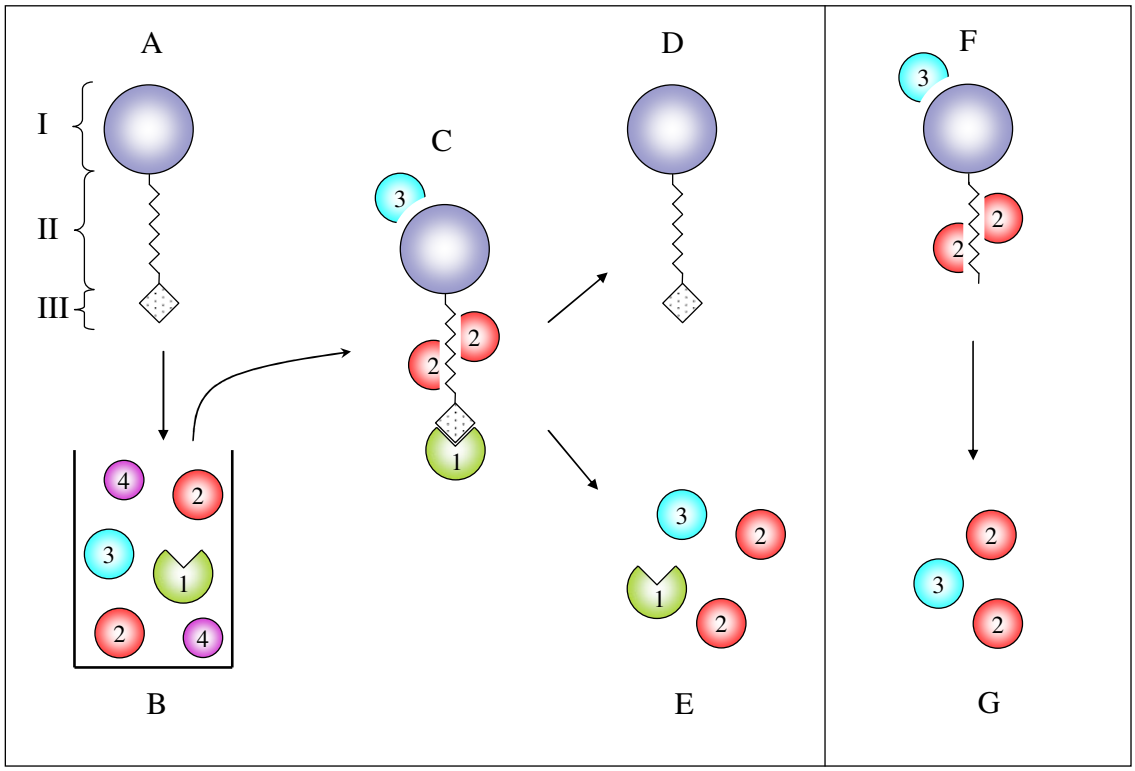

Figure 1: Outline of the target-fishing approach. The fishing construct (A) consists of drug/ligand (III) that is bound via a linker (II) to an insoluble particle (I). After incubation with a cell lysate (B), proteins are bound to the fishing construct (C). Bound proteins can be released after an elution step (E). To distinguish between specific bound proteins (1) and those protein that bind to the linker (2) or the matrix (3), the same experiment is performed with a control construct without ligand (F). Proteins eluted from this construct (G) are then known to come from unspecific interactions.

For successful target fishing experiments, several parameters have to be chosen thoroughly. The choice of the matrix, the linker, the immobilisation and derivatisation reactions of the ligand as well as buffer compositions, type of protein source and elution conditions directly influence the results of a fishing experiment.

1.2.1 Ligand immobilisation

One prerequisite for successful target-fishing is an appropriate immobilisation of the ligand. Therefore, the following critical requirements have to be considered: (i) The ligand has to possess a functional group which allows its immobilisation on a certain matrix (e.g. -NH_2, -OH, -COOH, -SH groups). (ii) This functional group has to be unique in the molecule in order to achieve a selective immobilisation on only one defined position. (iii) The ligand must not possess additional functional groups that facilitate reactions with other molecules of the ligand. (iv) The functional group used for

immobilisation of the ligand must not be essential for its pharmacological activity in order to ensure an appropriate ligand-target interaction. Since only few ligands accomplish all these requirements, synthetic approaches to insert protection groups, derivatise ligands or completely synthesise ligand derivatives are needed.

1.2.2 Fishing matrices

Coupling ligands to insoluble particles (matrix) is an essential step for subsequent target fishing experiments. Thus, several aspects have to be considered to choose the correct matrix for a certain drug or natural compound, as the chemical composition of the matrix itself, the activation form and the ligand capacity. For the matrix composition, agarose (Sepharose®) is the most common substance used as matrix in affinity based methods and proteomic approaches. Agarose matrices are developed for the immobilisation of peptides or proteins via convenient one step reactions. However, they are not suitable for more complex immobilisation strategies. In addition, their use is limited by their poor chemical resistance. The solvent for immobilisation reactions on agarose matrices has to consist of at least 50% (v/v) water. Hence, reactions that require lipophilic ligands or reagents that are not soluble in aqueous solutions can not be performed with agarose matrices. Alternatives are represented by matrices consisting of polymethacrylic acid (methacrylat), which are characterised by a higher chemical resistance. Furthermore, they are available with about 10-fold higher ligand binding capacity. Table 1 summarises the chemical properties of commercial available matrices.

Name	Matrix	Activation form	Ligand capacity	Spacer	Bead size
EAH Sepharose® 4B [1]	Agarose	-NH_2	7 – 12 µmol/ml [A]	1,6-diaminohexane	90 µm (45-165 µm)
Epoxy-activated Sepharose® 6B [1]	Agarose	Epoxy	19 – 40 µmol/ ml [A]	1,4-bis (2,3-epoxypropoxy-) butane	90 µm (45-165 µm)
Toyopearl AF-Amino-650M [2]	Methacrylat	-NH_2	100 +/- 30 µmol/ml [B]	n.n.	40 -90 µm
Toyopearl AF-Epoxy-650M [2]	Methacrylat	Epoxy	0.6 – 1.0 mmol/g	n.n.	40 -90 µm

Table 1: Chemical properties of commercial available matrices: [1] Amersham/ GE Healthcare; [2] Tosho Bioscience; [A] calculated per ml drained matrix; [B] Calculated per ml wet resin

Besides their chemical composition, matrices differ in their activation form. To perform an immobilisation reaction on a matrix a functional so-called active group is required, on the surface of the matrix. The most common active groups for pull-down assays are primary amino and oxirane (=epoxy) groups. Amino-activated matrices are used to immobilise carboxylic acid containing ligands over an amide bond whereas epoxy-activated matrices are used to immobilise ligands with hydroxylic-, primary amino- or thiol groups creating an ether moiety, secondary amine or a thioether bond.

1.2.3 Linker molecules

Linker molecules are needed to connect ligands to an appropriate matrix. A linker for target-fishing experiments has to comply with conditions like low protein binding and optimal length to allow an effective interaction between the ligand and the binding site of the target. However, linker molecules could have even more specialised functions. Thus, there are linkers allowing a covalent cross linking between the fishing construct and the matrix or chemo- or photosensitive parts that allow cleaving the ligand off the fishing construct.

1.2.3.1 Photoreactive linker systems

Photochemical reactions offer a smart, non-invasive possibility for intervention in biochemical approaches, thus limiting effects of interfering reagents. Known applications of photoreactive linker systems are so called photoaffinity approaches where a molecule that has been bound to an affinity matrix is captured by a covalent connection after UV irradiation [20], or the release of synthesised peptides from a matrix after solid state synthesis [21] by cleaving a UV light sensitive linker system. For the target-fishing approach an insertion of a pre-determined breaking point would allow to elute target proteins by cleaving off the ligand from the matrix by UV light irradiation (Fig. 2). Hence, problems regarding unspecific protein-matrix interactions are essentially by-passed and appropriate target analytics are facilitated.

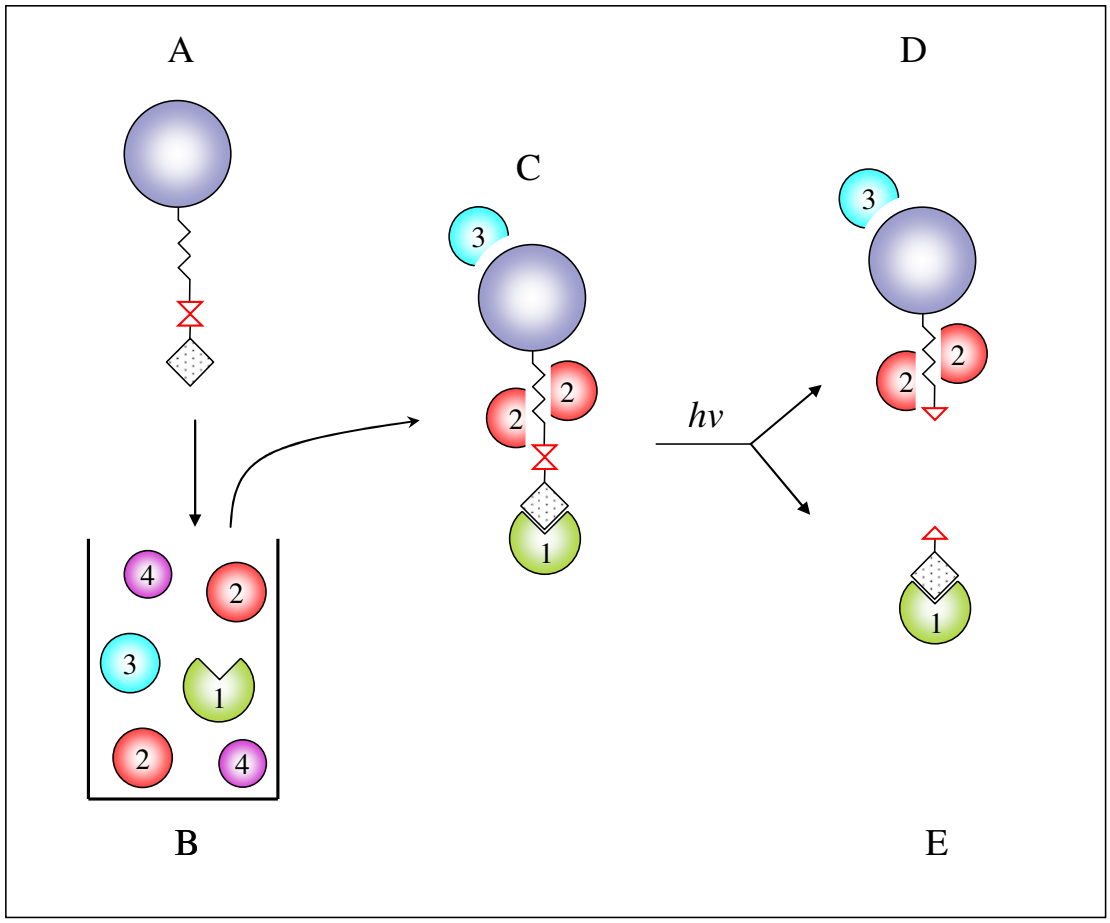

Figure 2: Application of photoreactive linker systems in the target-fishing approach: The fishing construct (A) is incubated with proteins from a cell lysate (B). After incubation, the construct (C) is irradiated with UV light. The photoreactive linker system is cleaved and specific bound proteins (1) are released (E), while unspecific bound proteins (2, 3) remain on the matrix (D).

One of the most interesting reactions in this context is the Norrish-Type II reaction which was first described in 1937 [22]. The mechanism of this reaction is an intramolecular movement of a γ-hydrogen atom in aldehydes or ketones after UV light irradiation (Fig. 3). The resulting diradicals are subsequently fragmented into a corresponding enol and alkene.

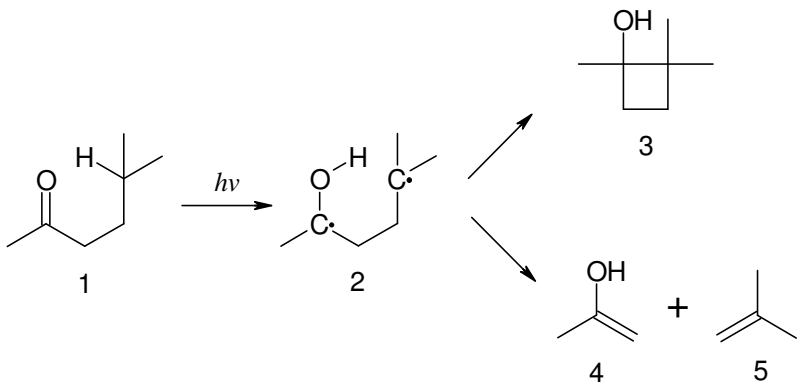

Figure 3: Norrish-type-II-reaction: UV light exposure of a ketone with a γ-hydrogen atom (1) results in a diradical (2) after an intramolecular movement of a hydrogen atom. The diradical can either form the corresponding cyclobutanol (3) or is fragmented into a corresponding enol (4) and alkene (5).

Ortho-nitrobenzylic systems offer all requirements for sufficient cleavage via Norrish type II reaction. Since o-nitrobenzylic systems possess adequate daylight stability, their use is limited by the very long cleavage half times [23]. In 1995, Holmes et al. developed an UV light cleavable linker system to cleave small peptides of a matrix after solid phase synthesis [21] on basis of o-nitrobenzylic systems. Although several improvements to existing linker systems could be achieved they still have disadvantages which hindered their use in proteomic approaches. Long cleavage times with up to 24 h [21, 24] would support enzymatic degradation and protein processing, thus complicate subsequent protein analytics.

1.2.4 Cell lysates

For the fishing approach, a source of abundant target structures is required. Cell lysates of isolated blood cells as well as of immortalised cell lines are routinely used. Incubation of immobilised ligands with these lysates allows the binding of potential targets to the ligands. After several washing steps, the proteins can be eluted by addition of detergents or chaotropic agents. Since specific (ligand-bound) proteins are eluted together with unspecific (matrix- or linker-bound) proteins, highly appropriate separation methods must be performed. Unspecific protein binding occurs mainly due to binding to the matrix or to the linker, thus appropriate controls are needed to discriminate whether a certain protein is fished through specific ligand-target interactions.

1.2.5 Elution conditions

Elution of proteins is performed by addition of appropriate reagents. The most specific way to elute proteins from ligands is the addition of free ligand in an excess to elute targets in a competitive way. However, since fishing experiments are usually performed in aqueous buffer solutions, ligands have to be water soluble to be suitable for this technique. Thus, this elution method cannot be used for the most drugs or natural compounds.

Additional methods are used to elute proteins by changing the ionic strength, such as high salt buffers or by changing the conformation of the proteins, such as sodium dodecylsulfate (SDS) buffer or urea buffers. Since protein denaturation by SDS is needed to perform gel electrophoretic separation by SDS polyacrylamide gel electrophoresis (SDS-PAGE) and urea buffers are needed for protein separation by isoelectric focussing (IEF), subsequent protein analytics is most efficient when elution reagents are chosen according to the subsequently used separation technique.

1.2.6 Analysis of target-fishing experiments

For the identification of a selectively fished target, fished proteins have to be separated by gel electrophoresis. After separation, differentiation between specific and unspecific bound proteins can be accomplished by comparing proteins fished by the ligand containing construct and the control. Selected proteins can be identified further by mass spectrometric proteomic approaches to receive a peptide fingerprint. Bioinformatic evaluations are used subsequently to identify the fished protein by matching the peptide fingerprint with a protein data bank (Fig. 4).

1.2.6.1 Electrophoretic separation of fished proteins

Electrophoresis is a technique to separate charged molecules in an electrical field. The classical approach to separate proteins by electrophoresis is the SDS-PAGE using a tris-/glycine-buffered system [25]. Two dimensional (2D) electrophoresis is a technique with increased resolution, where proteins are first sorted by their isoelectric point in the first dimension and then separated by SDS-PAGE in the second dimension.

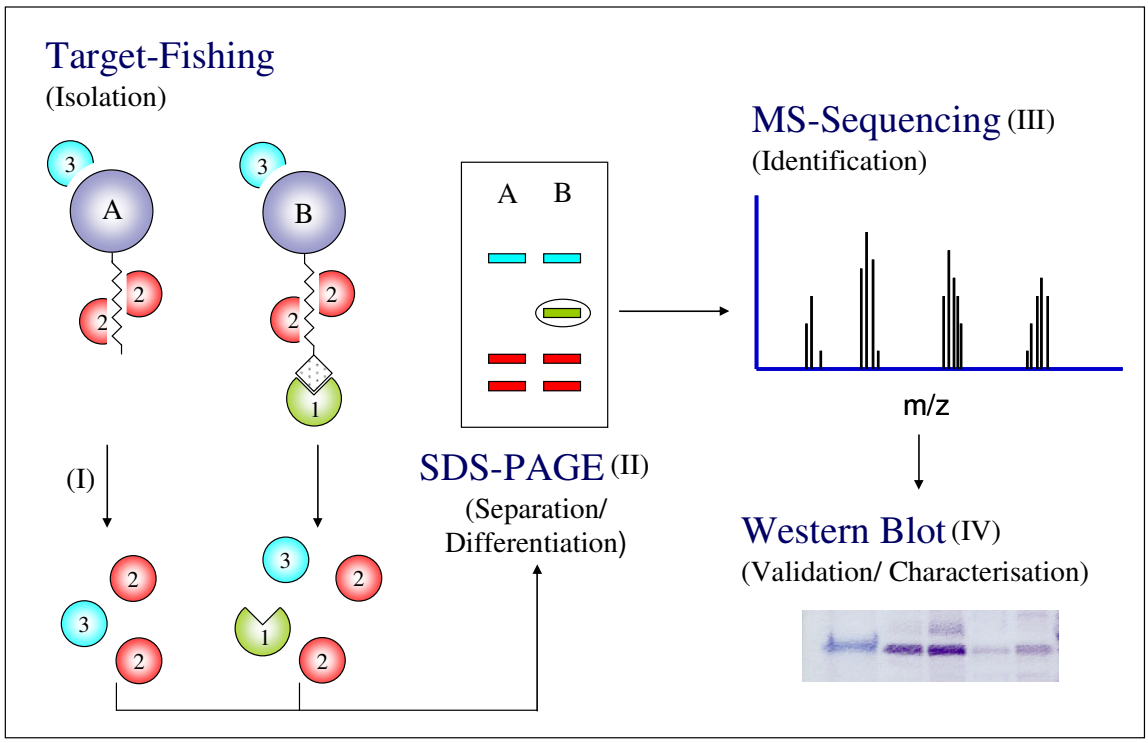

Figure 4: Outline of the workflow for the analysis of a target-fishing experiment. First, a fishing experiment with a drug (B) and a reference construct (A) is performed. After elution, (I) proteins can be separated and it can be differentiated between specific and unspecific bound proteins (II). Specific bound proteins can be subsequently identified by mass spectrometric approaches (III). Validation and characterisation is performed by Western blot analysis (IV).

Difference gel electrophoresis (DIGE) is a technique that revolutionised 2D-electrophoresis in the 1990s. A general problem of 2D-electrophoresis is its poor reproducibility. In fact, running the same samples under the same conditions on different gels leads to differing spot patterns, making comparison of 2D gels with different samples a very challenging task. In 1997, Ünlü et al. described a method using two fluorescence dyes for labelling proteins of two different samples prior to 2D electrophoresis [26]. The so called Cy3 and Cy5 dyes are N-hydroxysuccinimide (NHS) ester-activated cyanine dyes meeting crucial requirements: (i) these dyes react with the same moieties of proteins, namely the epsilon amino groups of lysine residues, (ii) they don't change the

charge and thereby the isoelectric point of proteins, (iii) they have similar molecular weight, and (iv) they have distinct fluorescence characteristics such as linearity, sensitivity and a wide dynamic range [27-28] (Fig. 5).

Labelling two different protein samples with these two dyes allows running them on the same 2D gel. With this procedure, problems regarding different spot patterns on different gels are completely by-passed. Since its invention, DIGE became a prominent standard procedure for comparison of expression patterns in tissue proteomics, subcellular proteomics and for various proteomic profiling approaches [29-32].

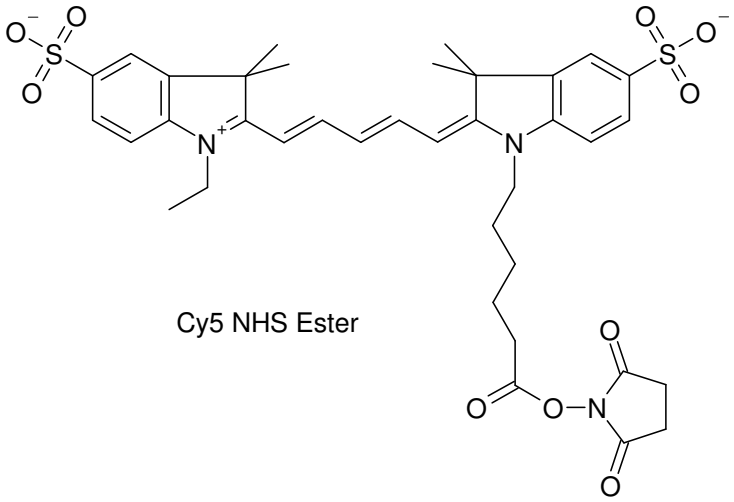

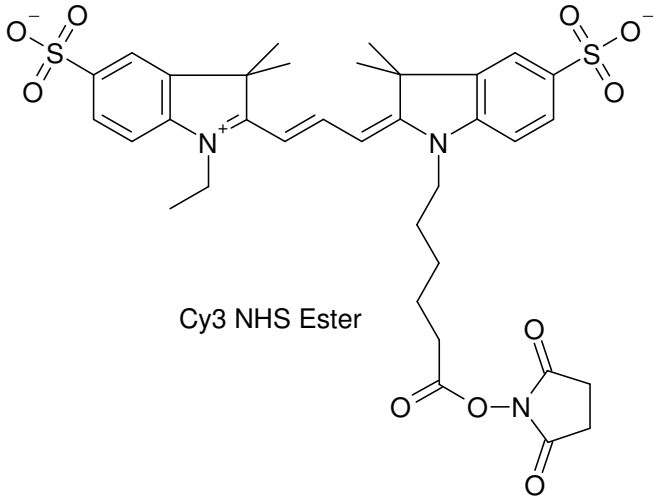

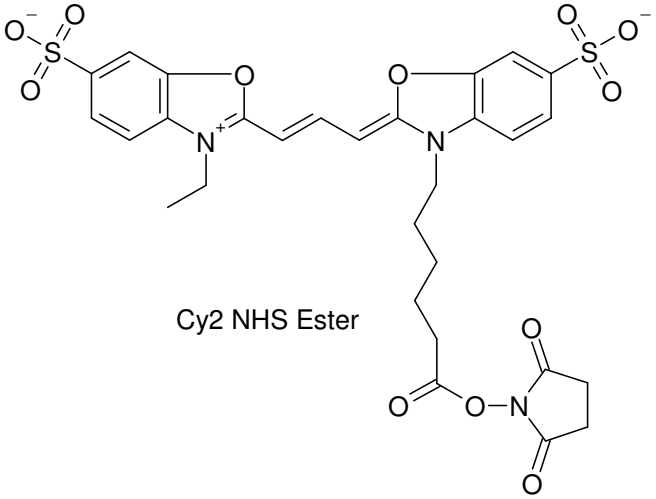

Figure 5: Chemical structures of the CyDye fluors.

1.2.7 Target validation and characterisation

After the identification of a putative target, one has to consider that there are direct as well as indirect bound targets. Direct specific binding means that the targets interact directly with the ligand as shown in Fig. 6. In contrast, an indirect binding means that the target could be bound to an adapter protein that is directly bound to the ligand. To elucidate whether a target is directly or indirectly bound to a ligand, fishing experiments using the isolated protein instead of cell lysates can be performed. Only direct interacting targets can be isolated under such conditions since potential adapter proteins are not present in these experiments.

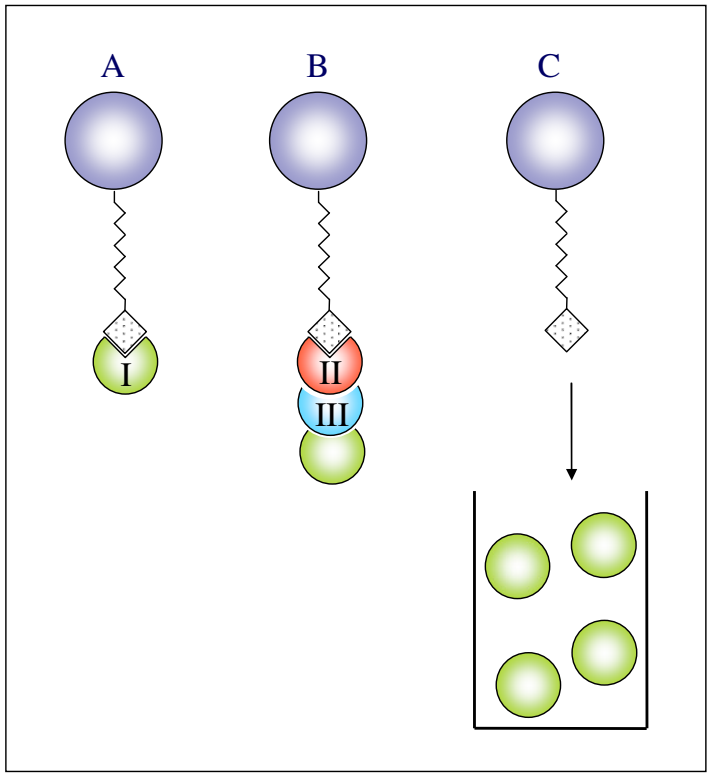

Figure 6: Outline of binding events after a target-fishing experiment. A identified putative target (I) can either bind directly (A) or via one ore more adapter proteins (II, III) (B) to the immobilised ligand. To determine which of both binding events takes place, a fishing experiment with the isolated target protein is performed. Thus, only direct binding events can take place under these experimental settings.

The target-fishing approach is a tool to identify new target proteins. However, whether or not this target is affected in its functionality by the ligand can not be elucidated by target-fishing. Therefore, additional experiments, methods and assays are needed to evaluate and validate functional effects of the discovered ligand-target interaction.

1.2.8 Importance of the target-fishing approach

Although a fishing approach represents a valid technique for target identification and can potentially give novel insights into the pharmacological properties of a certain drug, it is used rather seldom. On the one hand, this is due to the fact that the properties of the fished protein to be analysed are not known in advance and this makes the (blind) optimisation of analytical methods a challenging task. On the other hand, an interdisciplinary scientific network consisting of biochemists, synthetic chemists and proteomic specialists is needed. This has slowed-down the development of reliable target-fishing approaches, and thus suitable methodologies for fishing have been seldom established.
In this thesis the target-fishing approach has been optimised to identify new targets of synthetic and natural compounds which possess anti-inflammatory effects that are not readily explicable on the basis of known targets.

1.3 Inflammation

Inflammation is a physiological, non-specific immune response characterised by five cardinal signs: redness, heat, swelling, pain and loss of function. The aim of the physiological inflammatory response is to limit and delete injurious stimuli and to restore tissue function. Therefore, acute inflammation does not represent a disease; instead it is a self limiting physiological process in response to an injurious stimulus. However, the persistence of inflammatory stimuli or faulty regulation of the inflammatory response may lead to chronic and pathologic conditions. Furthermore, chronic inflammation affects and sustains tumour development and progression [33-35]. Thus, pharmacological anti-inflammatory approaches are not only intended as treatment for acute conditions, but are rather an essential part of the therapies of a wide range of diseases, such as chronic inflammation, pain, bacterial infections, autoimmune diseases and cancer.
On the cellular level, inflammation is a complex process involving several biochemical events and is initiated by the release of pro-inflammatory mediators such as cytokines (e.g. interleukin-1, tumour necrosis factor-α), plasma proteins (e.g. bradykinin and thrombin), lipid mediators (leukotrienes, prostaglandins) and histamine in response to an inflammatory stimulus. As a consequence of the action of the inflammatory mediators, the postcapillary venule permeability is increased, permitting leukocyte migration

into tissues. In addition, tissue-infiltrated leukocytes release additional pro-inflammatory agents. Among these, mediators derived from arachidonic acid (all-cis 5,8,11,14-eicosatetraenoic acid, AA), the so-called eicosanoids, play a key role in the regulation of inflammatory processes and are therefore considered a valuable target for pharmacological intervention. AA is part of phospholipid membranes. After appropriate stimulation, AA is enzymatically liberated by phospholipases A_2. Free AA itself can act as mediator but is also a substrate for subsequent enzymatic reactions. AA can be transformed by (i) cyclooxygenases (COXs) to prostaglandins and thromboxanes, (ii) by lipoxygenases (LOs) (predominantly 5-LO) to leukotrienes or (iii) by different cytochrome P450 enzymes to epoxyeicosatrienoic acids [36].

1.4 Synthetic and natural anti-inflammatory drugs as candidate ligands for the fishing approach

1.4.1 Acetaminophen (Paracetamol)

Acetaminophen (ACAP) (Fig. 7) is one of the most used analgesic drugs worldwide. Nevertheless its exact mode of action remains unclear and is still under discussion. ACAP was first synthesised in 1878 by Morse [37] and has been used as antipyretic drug since 1887 [38]. Its broad distribution started in the 1950s after the abandons of phenacetin. Today there is still a large interest on ACAP. The amount of publications concerning ACAP increased 60-fold in the last 40 years whereas medical publications in general only increased threefold in the same time. Interestingly about 70% of the literature focusses on side effects and clinical use and only 5% consider pharmacodynamics [39]. This leads to a big discrepancy between the wide spread use of this drug and the knowledge about its pharmacologic action.

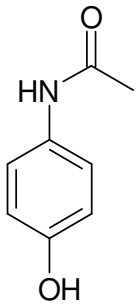

Figure 7: Chemical structure of ACAP

Although ACAP is not considered as a classical non-steroidal anti-inflammatory drug (NSAID) it possesses beneficial effects in certain inflammatory diseases [40-41]. Today, several targets have been discussed to be affected by ACAP. Several effects on the eicosanoid pathway, prominently COX-1 and COX-2 inhibition, have been described [42-46]. However, neither an inhibition of the COX function nor an inhibition of the peroxidase function [47] of COX-1 or COX-2 could explain all pharmacological effects of ACAP. Also the opioidergic system as well as the serotonergic- and the cannabinoid system were discussed to be affected by ACAP [45-46]. In addition there are studies suggesting that ACAP is only a prodrug of the active form AM404 (N-arachodinylphenolamine). The fact that AM404 is found in the central nerve system (CNS) but not in blood after ACAP administration could at least explain the central effects of ACAP [48-50].

In 2002, a new perspective of ACAP was proposed regarding COX as targets. Chandrasekharan et al. described that there is a COX-3 that could be selectively inhibited by ACAP [51]. Scientists recognised that this work contains experimental inadequacies as well as a lack of general scientific standards [44, 52]. Chandrasekharan et al. claimed that in canine COX-3 there is an intron that is not present in the COX-1 mRNA having 75% sequence homology with the corresponding intron in human. In fact, this intron exists in the human genome but its retention leads to a frame shift and a nonfunctional protein with 8.7 kDa and not to a functional, additional COX. For the specific inhibition of COX, it was obtained an IC_{50} value of 460 µM for COX-3 and over 1000 µM for COX-1 and COX-2. Since it has been known that the sensitivity of COXs against inhibitors depends on their activity [53] and the COX-3 showed only 20% of the activity of COX-1 and only 4% activity in comparison with COX-2, the stronger inhibition of COX-3 by ACAP is explained by its poor activity, and not by a “selective” sensitivity to ACAP.

In conclusion neither effects on the opioidergic-, the serotonergic- or the cannabinoid system nor inhibition of COXs can explain the anti-inflammatory effects of ACAP. Thus, the mechanism of action for one of the most used drugs worldwide remains unclear up to date.

1.4.2 Resveratrol

Resveratrol (RV, 3,5,4´-trihydroxystilbene) (Fig. 8) is a polyphenolic phytoalexin first isolated from *Polygonum cuspidatum* by Nonomura et al. in 1963 [54]. However, it was widely unnoticed until Siemann et al. reported its presence in red wine in 1992 [55]. Speculations that this could explain the "French paradox"[I] [56] brought RV back into the focus of interest [57].

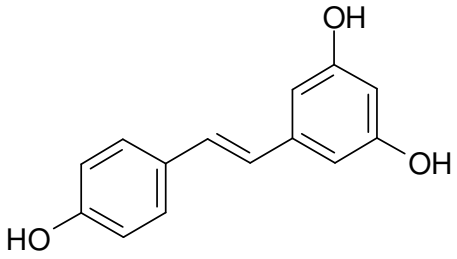

Figure 8: Chemical structure of resveratrol

So far RV has been known to influence a wide range of cellular effects. As a polyphenolic compound, RV shows redox activity and antioxidative capacities [58-60]. RV is known to reduce carcinogenesis at different levels (e.g. cancer initiation, -promotion, and -progression) [59-65] as well as inflammatory diseases [66-67]. Several targets for the anti-cancer effects of RV have been determined, such as inhibition of the DNA polymerase [65], inhibition of the ribonucleotide reductase activity [64-65], activation of the DNA checkpoint pathways including ataxia telangiectasia mutated/ ataxia telangiectasia-Rad3-related (ATM/ATR) kinase and checkpoint kinase 1(Chk1) [63] as well as angiotensin II and epidermal growth factor (EGF) mediated Ak-transformed (Akt) kinase activation [68-69]. Anti-inflammatory activities of RV are shown to be due to inhibition of both the COX and LO pathway as well as microsomal prostaglandin E2 synthase 1 (mPGES1) expression [70]. Furthermore RV was found to slow the progres-

[I] The "French paradox" describes the observation that the French people have a relative low incidence of coronary heart disease, although they have a diet relatively rich in cholesterol and saturated fat.

sion of Alzheimer disease [71], to mimic caloric restriction and to extend the lifespan of mice [72]. However the versatile anti-inflammatory properties of RV [66-67, 73-76] can only be partially explained by the known targets.

1.4.3 Indirubin-3´-monoxime

Indirubine-3´-monoxime (IR3MO) is a 3,2´-bisindole from *Indigo naturalis*. In traditional Chinese medicine Danggui Longhui Wan, a recipe consisting of 11 ingredients is known to relieve symptoms of chronic myelomic leukaemia [77-78]. In 1966, scientists identified Qing Dai, known as *Indigo naturalis* as the active compound of this recipe. Besides high levels of the blue dye indigo, *Indigo naturalis* contains also an indigo isomer called indirubine (Fig. 9).

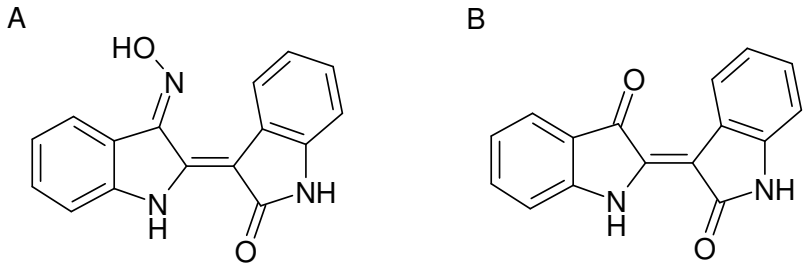

Figure 9: Chemical structure of indirubin-3´-monoxime (A) and indirubine (B)

In 1999, Hoessel et al. showed that the antileukaemic activity is related to the inhibition of several cyclin-dependend kinases (CDKs) [79]. CDKs play a critical role in cell cycle regulation. CDKs are activated by binding to cyclins and building holoenzymes. Indirubin inhibits CDK activity in the micromolar range.

Since indirubin shows poor solubility and absorbance but gastrointestinal toxicity, medicinal chemists attempted to synthesise optimised derivatives of indirubin [80-81]. Among others, IR3MO was synthesised. Besides better solubility and absorption, IR3MO showed a 5- to 50-fold improved inhibitory activity to various CDKs. Besides its antitumoural activity, IR3MO also possesses anti-inflammatory properties [82-83]. However, a molecular or biochemical basis for the observed anti-inflammatory effects does not exist.

1.4.4 Myrtucommulone A

Myrtucommulone A (MC) (Fig. 10) is a nonprenylated acylphloroglucinol contained in leaves of *Myrtus communis*. In folk medicine *Myrtus communis* is known for its antiseptic and anti-inflammatory properties. Extracts have been reported to be antibacterial, antihyperglycemic and analgesic [84].

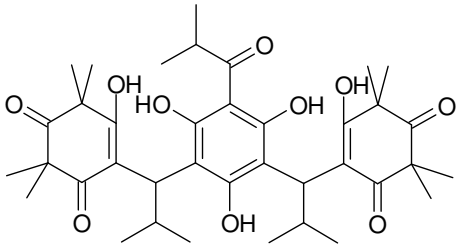

Figure 10: Chemical structure of myrtucommulone A

The anti-inflammatory activity of MC is related to interference with several molecular targets and the activity of mPGES1 [85], COX-1, 5-LO as well as human leukocyte elastase (HLE) release were shown to be influenced by MC [86]. While anti-inflammatory aspects of MC have been known for a long time and are basically understood, the antiapoptotic action was first reported in 2008 [87]. MC was shown to induce cell death with an EC_{50} values in the low micromolar range. Several characteristics of apoptosis such as caspase-3, -8 and -9 activation as well as Poly (ADP-ribose) polymerase (PARP) cleavage could be shown selectively for cancer cell lines [87]. Nevertheless, direct molecular targets of MC related to apoptosis induction are still not known.

1.4.5 Betulinic Acid

Betulinic acid (BA) (Fig. 11) is a plant-derived pentacyclic triterpene. BA is the C-28 oxidised form of betulin (3β-lup-20(29)-en-3, 28-diol). Betulin was first isolated in 1788 and was therefore one of the first isolated natural compounds at all. Although betulin is present in a vast variety of plants it is named after the white birch tree (*Betula alba*) whose bark consists up to 30% (dry weight) betulin [88]. BA itself is also present in a large number of plants [89-90]. Since the BA content in plants is rather low, it is obtained by oxidising betulin isolated from *Betula alba* [89]. The bark of *Betula alba* was traditionally used by native Americans for the treatment of several diseases [90]. In

1994, Fujioka et al. stated that BA is able to inhibit the replication of the human immunodeficiency virus (HIV) [91]. As result of this work, the BA analogue bevirimat is under further investigation in a phase II clinical trial for the treatment of HIV-1 infections [92-93].

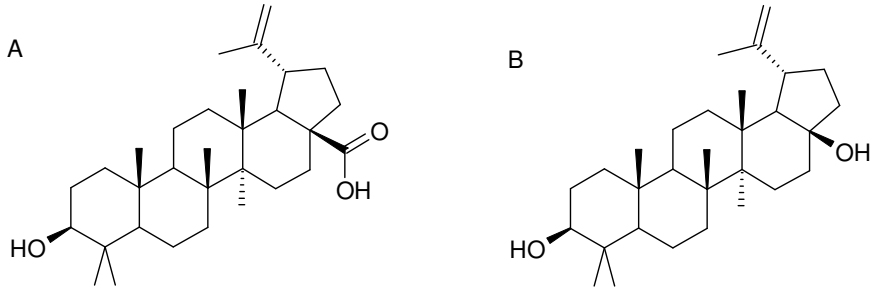

Figure 11: Chemical structure of betulinic acid (A) and betulin (B)

Beside its antiviral activity, BA also possesses antitumoural effects first described in 1995 [94]. Although there are conflicting results concerning the exact mode of action of BA, several components of the intrinsic apoptotic pathway could be identified to be affected by BA [89-90]. While the mechanisms of action in inhibition of HIV replication and antitumoural effects are quite well understood, the described anti-inflammatory effects [95] are by today inexplicable.

1.5 Gender bias in inflammation

Traditionally, anti-inflammatory pharmacotherapies do not discriminate between men and women. However, it has been recognised in the last decades that several inflammatory diseases show a higher prevalence for one of the two genders [96-102] (Tab. 2). Also, enormous changes in regard to prevalence and gravity of certain inflammatory diseases are observed at puberty, during pregnancy or during the climacteric period [103-104], suggesting that sex hormones may play a key role in the regulation of inflammation and immune reactions, though also other factors may be involved (genetic-, anatomical-, physiological- [105-106], psychological- [107-108] and sociocultural factors [109-110]). Hence, a comprehensive understanding of gender differences on a molecular level is needed to facilitate gender specific pharmacotherapy.

Disease	Ratio female:male	reference
Rheumatoid arthritis	2:1 to 3:1	Alamanos 2005
Systemic lupus erythematodes	9:1	D´Cruz 2007
Scleroderma	4:1	Whitcare 2001
Myasthenia gravis	3:1	Whitcare 2001
Multiple sclerosis	3:2	Whitcare 2001
Systemic sclerosis	3:1	Chifflot 2008

Table 2: Prevalence of inflammatory diseases in male and female subjects.

1.6 The steroid hormones testosterone and progesterone as ligands for target-fishing experiments

Testosterone and progesterone are sex hormones primarily involved in the regulation of sexual maturation and reproduction. Testosterone is primarily produced in the gonads while progesterone is produced in the ovaries. For their classical mode of action, the signalling of both hormones is mediated by corresponding steroid hormone receptors. These receptors act as ligand inducible transcriptional enhancing factors. Thus, binding of a steroid hormone to a corresponding cytosolic receptor causes dimerisation of the receptor, translocation to the nucleus and binding to hormone responsive elements (HREs) of the DNA [111-115]. For the progesterone receptor (PR) and the androgen receptor (AR) two isoforms are known, respectively. For the PR, PR-A and PR-B are known isoforms differing in their promoter usage [116]. The two AR isoforms hAR-A and hAR-B are structural analogues to the two PR isoforms [117]. However, the exact contribution and functional differences of PR and AR isoforms are not known.

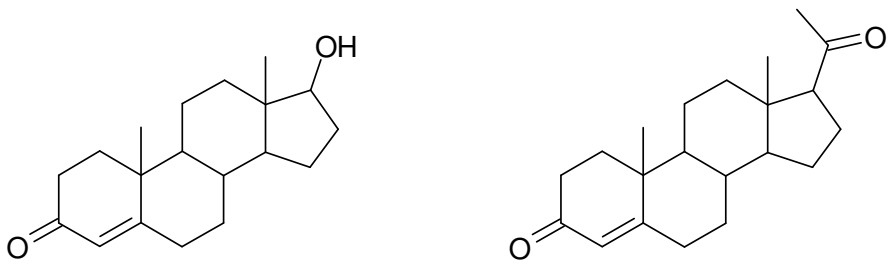

Testosterone Progesterone

Figure 12: Chemical structure of testosterone and progesterone

Although the genomic effects mediated by AR and PR have been extensively investigated and are understood in terms of triggering mechanisms, there are hormonal effects that can not be explained by the classical genomic regulation. In fact, testosterone and progesterone are known to induce very rapid effects (seconds to minutes), also in cells devoid of the classical hormone receptor, which are clearly not compatible with a genomic regulation. These recent evidences indicate the existence of additional targets for testosterone and progesterone that are responsible for these so-called non-genomic effects. Examples of non-genomic hormonal effects are: (i) a rapid change of intracellular Ca^{2+} after androgen exposure in Sertoli-, LNCap- and T-cells [118-121]. (ii) Changes in membrane fluidity in mammary cancer cells [122-123] resulting in an increased Na^{+}/K^{+}-ATPase and Ca^{2+}-ATPase activity [124-126]. (iii) Activation of second messenger pathways such as cellular-sarcoma (c-Src) mediated mitogen-activated protein kinases (MAPK) activation in prostate cancer cells [127-128] or sex hormone binding globulin (SHBG) receptor mediated activation protein kinase A (PKA) in breast cancer cells [129-130]. (iv) Rapid regulation of gonadotropin-releasing hormone (GnRH) release in neuronal cells [131-135]. (v) Extracellular-signal-regulated kinase (ERK) mediated regulation of 5-LO activity in neutrophils [96].

Although some targets have been suggested to explain at least some of these effects, clear evidences for the existence of additional receptors responsible for the non-genomic actions of these sex-hormones are still missing.

2 Aim of the study

Today, two strategies may be in principal pursued for treatment of diseases, namely (i) surgical and (ii) pharmacological intervention. The human anatomy as base for a rational surgical intervention has been known in detail for a very long time. Despite the notable scientific progresses in the last decades, the pharmacological-, biochemical- and molecular biological processes as base for a rational pharmacotherapy are instead rather poorly understood and very complex. Although certain molecular pathways have been largely characterised, pharmacotherapy focusses on only about 100 proteins. Since the human proteome is estimated to consists of 30,000 - 200,000 different proteins [1-2], today's pharmacotherapy is only limited to a small fraction of possible targets.

For a rational pharmacotherapy, a comprehensive understanding of the molecular pharmacological interactions of drugs with the respective targets is necessary. However, the mechanism of action of many drugs commonly used in therapy is so far only partially understood. The overall molecular actions of many drugs and natural compounds often appears like a patchwork obtained by testing these compounds in a limited number of well established systems. Thus, there is a lack of knowledge caused by a lack of methods that allow a systematic and reliable discovery of drug targets.
The aim of this work was to refine and improve the target-fishing approach in order to receive a reliable, standardised and convincing tool for the identification of new targets for natural compounds and synthetic agents used as drugs. The following methodological issues were approached: (i) evaluation of various matrix types, (ii) development of new immobilisation strategies, (iii) systematic evaluation of fishing and elution conditions, (iv) development of photoreactive linker systems, (v) establishment of the 2D-DIGE approach and its optimization in relation to the particular requirements of target-fishing eluates. Furthermore, this work aimed also to confirm the success of these technical improvements by performing fishing-experiments using selected baits with pharmacological potential (i.e. acetaminophen, resveratrol, indirubin-3´-monoxime, myrtucommulone A, betulinic acid, progesterone and testosterone) and by the subsequent evaluation and validation of the ligand-target interactions.

3 Materials and Methods

3.1 Materials

3.1.1 Chemicals

Name	Supplier
1-(3-Dimethylaminopropyl)-3-ethylcarbodiimide hydrochloride	Acros Organics (Geel, Belgium)
1,6-Diisocyanatohexane	Acros Organics (Geel, Belgium)
2-[4-(2-Hydroxyethyl)-1-piperazine]ethanesulfonic acid	AppliChem GmbH (Darmstadt, Germany)
2-Cyclopentenone	Acros Organics (Geel, Belgium)
4-Aminophenol	Acros Organics (Geel, Belgium)
5,5´-Dithio-bis(2-nitrobenzoic acid)	AppliChem GmbH (Darmstadt, Germany)
5-Bromo-4-chloro-3-indolyl phosphate, p-toluidine salt	AppliChem GmbH (Darmstadt, Germany)
5α-Dihydrotestosterone	Sigma-Aldrich Inc. (St. Luis, MO, USA)
Acrylamide solution 30% (37.5:1)	AppliChem GmbH (Darmstadt, Germany)
AG® 501-X8 Resin	Bio-Rad Laboratories, Inc. (Hercules, CA, USA)
Agar-Agar	Merck KGaA (Darmstadt, Germany)
Ammonium persulfate	AppliChem GmbH (Darmstadt, Germany)
Ampholyte Bio-Lyte3/10®	Bio-Rad Laboratories, Inc. (Hercules, CA, USA)
beta-Mercaptoethanol	Carl Roth GmbH + Co. KG (Karlsruhe, Germany)
Betulinic acid	Alexis Corporation (Lausen, Switzerland)
BioRad DC Protein Assay Kit	Bio-Rad Laboratories, Inc. (Hercules, CA, USA)
Boc-Ala-Ala-Nva-SBzl (PR3 substrat)	EPC
Bromophenol Blue	Merck KGaA (Darmstadt, Germany)
Calciumchloride	AppliChem GmbH (Darmstadt, Germany)
Chaps	AppliChem GmbH (Darmstadt, Germany)
Chemoluminescence films (Amersham HyperfilmTM ECL	GE Healthcare GmbH (Freiburg, Germany)
Cy 2,3,5 5nmol CyDye DIGE Fluor minimal Dye labelling Kit	GE Healthcare GmbH (Freiburg, Germany)
Cy3 Bis NHS ester	GE Healthcare GmbH (Freiburg, Germany)
Cy5 Bis NHS ester	GE Healthcare GmbH (Freiburg, Germany)

Name	Supplier
Cytochalasin B	AppliChem GmbH (Darmstadt, Germany)
Dextran	Sigma-Aldrich Inc. (St. Luis, MO, USA)
Dimethylformamide 99.8% extra dry	Acros Organics (Geel, Belgium)
Dioxane	Carl Roth GmbH + Co. KG (Karlsruhe, Germany)
Disodium hydrogen phosphate dihydrate	Merck KGaA (Darmstadt, Germany)
Dithiothreitol	AppliChem GmbH (Darmstadt, Germany)
Dulbecco's modified Eagle's medium (DMEM)	PAA Laboratories GmbH (Pasching, Austria)
Dulbecco's buffer substance	Serva Electrophoresis GmbH (Heidelberg, Germany)
Epoxy-activated Sepharose® 6B	GE Healthcare GmbH (Freiburg, Germany)
Escin	Sigma-Aldrich Inc. (St. Luis, MO, USA)
Ethylenediaminetetraacetic acid	AppliChem GmbH (Darmstadt, Germany)
Eupergit C250L	Degussa / evonik industries (Darmstadt, Germany)
Fatty acid free BSA	Sigma-Aldrich Inc. (St. Luis, MO, USA)
Fetal calf serum (FCS)	Sigma-Aldrich Inc. (St. Luis, MO, USA)
FK-866	Biozol Diagnostica Vertrieb GmbH (Eching, Germany)
Flamingo Fluorescent Gel Stain 10x	Bio-Rad Laboratories, Inc. (Hercules, CA, USA)
Formaldehyde	Sigma-Aldrich Inc. (St. Luis, MO, USA)
Galacturonic acid	Sigma-Aldrich Inc. (St. Luis, MO, USA)
Glycerol	Caesar & Lorentz GmbH, (Hilden, Germany)
(L)-Glycine	AppliChem GmbH (Darmstadt, Germany)
Hepes solution (for cell culture)	PAA Laboratories GmbH (Pasching, Austria)
Horse serum	PAA Laboratories GmbH (Pasching, Austria)
HybondTM-C Extra nitrocellulose membranes	GE Healthcare GmbH (Freiburg, Germany)
Indole-3-carbinol	Sigma-Aldrich Inc. (St. Luis, MO, USA)
Iodoacetamide	Sigma-Aldrich Inc. (St. Luis, MO, USA)
IPG Strips (ReadyStrip™) 17 cm 3-10NL	Bio-Rad Laboratories, Inc. (Hercules, CA, USA)
Leupeptin hemisulfate salt	Sigma-Aldrich Inc. (St. Luis, MO, USA)
(L)-Glutamine solution (for cell culture)	PAA Laboratories GmbH (Pasching, Austria)
(L)-Lysin	Acros Organics (Geel, Belgium)

Name	Supplier
Lupeol	Alexis Corporation (Lausen, Switzerland)
Lymphocyte Separation medium LSM 1077	PAA Laboratories GmbH (Pasching, Austria)
Magnesium chloride	Merck KGaA (Darmstadt, Germany)
Milk powder (blotting degree)	Carl Roth GmbH + Co. KG (Karlsruhe, Germany)
Mineral Oil	Bio-Rad Laboratories, Inc. (Hercules, CA, USA)
N,N-Dicyclohexylcarbodiimide	AppliChem GmbH (Darmstadt, Germany)
N,N'-Diisopropylcarbodiimide	Acros Organics (Geel, Belgium)
N-[Tris(hydroxymethyl)methyl]glycine	AppliChem GmbH (Darmstadt, Germany)
Sodium chloride	Merck KGaA (Darmstadt, Germany)
Nitro blue tetrazolium (NBT)	Roche Applied science (Mannheim, Germany)
Nonidet® P40	AppliChem GmbH (Darmstadt, Germany)
Penicillin / Streptomycin solution (for cell culture)	PAA Laboratories GmbH (Pasching, Austria)
peqGOLD IV Protein Molecular weight Marker	PEQLAB Biotchenology (Erlangen, Germany)
Phenylmethylsulphonyl fluoride	AppliChem GmbH (Darmstadt, Germany)
Ponceau S red	Sigma-Aldrich Inc. (St. Luis, MO, USA)
Propylamine	Sigma-Aldrich Inc. (St. Luis, MO, USA)
Protease Inhibitor Cocktail P8340	Sigma-Aldrich Inc. (St. Luis, MO, USA)
RPMI (Roswell Park Memorial Institute) medium	PAA Laboratories GmbH (Pasching, Austria)
Sclerotiorin	Biozol Diagnostica GmbH (Eching, Germany)
Silver nitrate	Sigma-Aldrich Inc. (St. Luis, MO, USA)
Sodium azide	Merck KGaA (Darmstadt, Germany)
Sodium bicarbonate	Sigma-Aldrich Inc. (St. Luis, MO, USA)
Sodium carbonate	Merck KGaA (Darmstadt, Germany)
Sodium dihydrogen phosphate, anhydrous	Merck KGaA (Darmstadt, Germany)
Sodium dodecyl sulfate	AppliChem GmbH (Darmstadt, Germany)

Name	Supplier
Sodium nitrite	Merck KGaA (Darmstadt, Germany)
Sodium pyruvate solution (for cell culture)	PAA Laboratories GmbH (Pasching, Austria)
Soybean trypsin inhibitor (STI)	Sigma-Aldrich Inc. (St. Luis, MO, USA)
Tetramethylethylenediamine (TEMED)	Carl Roth GmbH + Co. KG (Karlsruhe, Germany)
Testosterone	Sigma-Aldrich Inc. (St. Luis, MO, USA)
Tetrahydrofuran (THF)	Carl Roth GmbH + Co. KG (Karlsruhe, Germany)
Thiourea	AppliChem GmbH (Darmstadt, Germany)
Toyopearl AF-Amoni 650M	Tosho Bioscience GmbH (Stuttgart, Germany)
Toyopearl AF-Carboxy 650M	Tosho Bioscience GmbH (Stuttgart, Germany)
Toyopearl AF-Epoxy 650M	Tosho Bioscience GmbH (Stuttgart, Germany)
Trichloroacetic acid	Merck KGaA (Darmstadt, Germany)
Triethanolamine	Merck KGaA (Darmstadt, Germany)
Tris(hydroxymethyl)aminomethane	AppliChem GmbH (Darmstadt, Germany)
Triton X-100	Carl Roth GmbH + Co. KG (Karlsruhe, Germany)
Trypan Blue	AppliChem GmbH (Darmstadt, Germany)
Trypsin / EDTA solution (for cell culture)	PAA Laboratories GmbH (Pasching, Austria)
Tween 20	Carl Roth GmbH + Co. KG (Karlsruhe, Germany)
Urea	AppliChem GmbH (Darmstadt, Germany)
X-Ray Developing solution	Calbe Chemie GmbH (Calbe, Germany)
X-Ray Fixing solution	Calbe Chemie GmbH (Calbe, Germany)

Table 3: List of used chemicals

3.1.2 Primary Antibodies

Name	Supplier
Karyopherin beta	Calbiochem; Merck Chemicals
Vimentin	Novus Biologicals
Visfatin	Santa Cruz Biotechnology, INC.
Heat shock protein 27	Santa Cruz Biotechnology, INC.
Phosphorylated heatshock protein 27	Santa Cruz Biotechnology, INC.
Serine protease inhibitor B1	Santa Cruz Biotechnology, INC.
Proteinase 3	Santa Cruz Biotechnology, INC.
Cathepsin G	Biomol International, LP
Extracellular-signal regulated protein kinase	Cell Signaling Technology®
Rat sarcoma (protein)	Cell Signaling Technology®
Rat fibrosarcoma/ rapidly growing fibrosarcoma (protein)	Cell Signaling Technology®
Rat fibrosarcoma/ rapidly growing fibrosarcoma (protein)	Cell Signaling Technology®
Rat fibrosarcoma/ rapidly growing fibrosarcoma (protein)	Cell Signaling Technology®
Protein kinase B	Cell Signaling Technology®
Androgen receptor	Santa Cruz Biotechnology, INC.
Progesterone receptor	Santa Cruz Biotechnology, INC.
KH-type splicing regulatory protein	Abnova Corporation
Cyclooxygenase-1	Biozol Diagnostica Vertrieb GmbH
Cyclooxygenase-2	Enzo® Life Sciences

Table 4: List of used primary antibodies

3.1.3 Secondary Antibodies

Name	Supplier
Anti-goat IgG FC	Rockland Inc.
Anti-mouse IgG FC specific	Sigma-Aldrich
Anti-rabbit IgG (whole molecule)	Sigma-Aldrich
Anti-goat IgG (whole molecule)	Sigma-Aldrich
Anti-rabbit IgG (whole molecule)	Sigma-Aldrich
Anti-chicken IgY (IgG) (whole molecule)	Sigma-Aldrich
Anti-mouse IgG (whole molecule)	Sigma-Aldrich

Table 5: List of used secondary antibodies

3.1.4 Recombinant proteins

Name	Supplier
Visfatin	Randox Laboratories Ltd.
HSP27	Biomol GmbH

Table 6: List of used recombinant proteins

3.2 Methods

3.2.1 Isolation of primary human blood cells (PMNL, PBMC, monocytes and platelets)

Venous blood was collected from adult healthy volunteers, with consent, and subjected to centrifugation (4000 × g/20 min/20 °C) for preparation of leukocyte concentrates (Blood Center, University Hospital Tuebingen, Germany). Leukocyte concentrates from different donors were pooled and diluted 1:1 (v/v) with PBS buffer (1 mM KH_2PO_4, 3 mM Na_2HPO_4, 150 mM NaCl, pH 7.4). PMNL, PBMC and platelets were isolated by dextran sedimentation (5% (w/v) dextran in ice cold PBS for 45 min at RT) followed by centrifugation on lymphoprep cushions (1000 × g, 10 min, RT, without brake). PMNL, PBMC and platelets were collected by taking respective fractions after centrifugation (1000 × g, 10 min 4°C for PMNL and PBMC; 2000 × g, 10 min, 4°C for platelets).

For isolation of PMNL, hypotonic lysis of erythrocytes was performed as described [136]. Cells were washed two times prior use by addition of PBS buffer pH 7.4 and centrifugation.

For isolation of monocytes, the mononuclear cell fraction (PBMC) was washed and resuspended in RPMI 1640 medium supplemented with 2 mM glutamine, 100 µg/ml streptomycin, 100 U/ml penicillin, 10% fetal calf serum (FCS). Cells were plated at a density of 2×10^7 cells/ml in culture flasks for 2 h (37°C, 6% CO_2). Non-adherent cells (i.e., lymphocytes) were removed by gentle washing with PBS buffer. Adherent monocytes were harvested by scraping and resuspended in PBS or PG buffer (PBS containing 0.1% (w/v) glucose) respectively.

Cells were counted after addition of trypan blue solution 1:1 (v/v) (0.2% (w/v) Trypan blue, 0.9% (w/v) NaCl) under a light microscope using a “Bürker” haemocytometer.

3.2.2 Culture of immortalised cells

All cell lines were cultured at 37 °C and 6% CO_2 in incubators with saturated humidity. Cells were cultured according to supplier instructions as followed (Tab. 7).

Cell line	Medium	Splitting conditions
LNCap	RPMI 1640 medium containing 10% heat inactivated FCS, 100 U/ml penicillin, 100 µg/ml streptomycin, 10 mM Hepes and 1 mM sodium pyruvate	Subconfluent cultures (70 - 80%) were split 1:5 using 0.05% trypsin and 0.02% EDTA in PBS buffer
Jurkat A3	RPMI 1640 medium containing 10% heat inactivated FCS, 100 U/ml penicillin, 100 µg/ml streptomycin	Cells were split 1:5 at a density of 8×10^5 cells/ ml
HeLa	RPMI 1640 medium containing 10% heat inactivated FCS, 100 U/ml penicillin, 100 µg/ml streptomycin	Subconfluent cultures (70 - 80%) were split 1:8 using 0.05% trypsin and 0.02% EDTA
PC12	Dulbecco´s Eagle Medium (DMEM) containing 10% heat inactivated FCS, 5% heat inactivated horse serum, 100 U/ml penicillin and 100 µg/ml streptomycin	Subconfluent cultures (80 - 90%) were split 1:5

Table 7: Conditions for cultivation of immortalised cells

3.2.3 Preparation of cell lysates

3.2.3.1 Preparation of whole cell lysates

Whole cell lysates were prepared by addition of 1 ml lysis buffer (50 mM Hepes pH 7.4, 200 mM NaCl, 1 mM EDTA, 1% Triton® X-100, 10 µg/ml leupeptin, 2 mM PMSF, 120 µg/ml soybean tripsin inhibitor (STI)) per g drained cell pellet, following 3 × 10 sec sonification. Lysed cells were centrifuged (15,000 × g, 1 h, 4 °C) to remove cell debris and the supernatants were used for fishing experiments.

3.2.3.2 Isolation of soluble proteins

Soluble proteins were isolated by addition of 1 ml lysis buffer (50 mM Hepes pH 7.4, 200 mM NaCl, 1 mM EDTA, 0.1% Triton® X-100, 50 µl P8340 protease inhibitor cocktail) per ml cell pellet following 3 x 10 sec sonification. Lysed cells were centrifuged (100,000 × g, 1 h, 4°C) to remove cell debris. The supernatant containing solubilised proteins was taken for fishing experiments.

3.2.3.3 Preparation of *E. coli* lysate

To prepare *E. coli* lysate, *E. coli* (BL21 strain, from a glycerol stock stored at -80°C) were added to 20 ml of LB medium (0.5% yeast extract, 1% NaCl, 1% peptone) and incubated for 24 h at 37 °C on a shaker. Then, 5 ml of cell suspension were added to 500 ml fresh LB media and incubated for additional 24 h at 37 °C.
Cells were harvested by centrifugation (7,700 × g, 15 min, 4 °C) and lysed by addition of equal volumes of lysis buffer to the pellet and subsequent sonification (3 × 15 sec) (Branson B-12, Branson Ultrasonics Corporation, Danbury, CT). After centrifugation (40,000 × g, 20 min, 4 °C), the supernatant was collected and protein concentration was set to 1 mg/ml by adding appropriate volumes of lysis buffer.

3.2.4 Immobilisation of small molecule ligands to insoluble matrices (beads)

All resins where prewashed with 3 × 5 ml Milli-Q water and with 1 × 5 ml of the ligand solution solvent on a G4 glass filter crucible. For immobilisation, ligand solution (300 µmol in 2 ml solvent) and 1.5 mmol carbodiimide were added to 1 ml prewashed amino-functionalised methacrylic acid resin (Toyopearl AF-Amino-650M, Tosho Bioscience). The reaction was performed at room temperature (RT) at pH 4.5 over night. Remaining free amino groups of the resin were blocked with acetic acid (150 µmol, with 1.5 mmol N,N-diisopropylcarbodiimide (DIC) at RT over night). Between every reaction step, the resin was washed with 20 ml solvent (depending on the solubility of the ligand, see below).

When the reaction was complete, the resin was washed 3 times with 5 ml solvent (depending on the solubility of the ligand, see below) and then 3 times with 5 ml acetate buffer (0.1 M sodium acetate, 0.1 M acetic acid, pH 4, 0.5 M NaCl) and Tris buffer (0.1 M Tris-HCl pH 8, 0.5 M NaCl), alternately, to remove ionic-bound ligand. The beads were finally washed with 5 ml 20% (v/v) ethanol and stored at 4 °C in 20% (v/v) ethanol until use.

Depending on the solubility of the ligand, the following solvents where used: Dioxane (50 – 100% (v/v)), DMF, THF, methanol. Water soluble carbodiimides such as 1-(3-Dimethylaminopropyl)-3-ethylcarbodiimide hydrochloride (EDC) where used if water was necessary as solvent, otherwise N,N-dicyclohexylcarbidiimide (DCC) or DIC where used. An additional washing step with methanol after the coupling reaction was performed to remove the corresponding urea derivative of the carbodiimide, when unpolar carbodiimides (such as DCC or DIC) were used.

For detailed immobilisation conditions of selected small molecule ligands, see results part 4.2.

3.2.4.1 Immobilisation strategies for ligands

Depending on the chemical nature and presence of functional residues, the following reactions were used to immobilise small molecules.

3.2.4.1.1 Immobilisation of ligands on amino functionalised matrices over carboxylic acid residues

Coupling of molecules containing carboxylic residues to amino functionalised matrices is a standard reaction performed in the synthesis of peptides via a solid phase approach (Fig. 13) [137-138]. Reactions were performed with a 10- to 100 fold excess of ligand (calculated in relation to free binding sides of the matrix). Times and conditions of the reaction were adapted to the requirement of each ligand, on the base of the respective chemistry. Thus, for compounds showing a good solubility in aqueous systems (e.g. 50% or more water), the reaction was performed using agarose beads and required a water soluble carbodiimide such as EDC. For lipophilic compounds (such as steroids or

terpenes), organic solvents (preferable dioxane, THF or DMF) and methacrylic acid resins were used, and DIC was applied as carbodiimide.

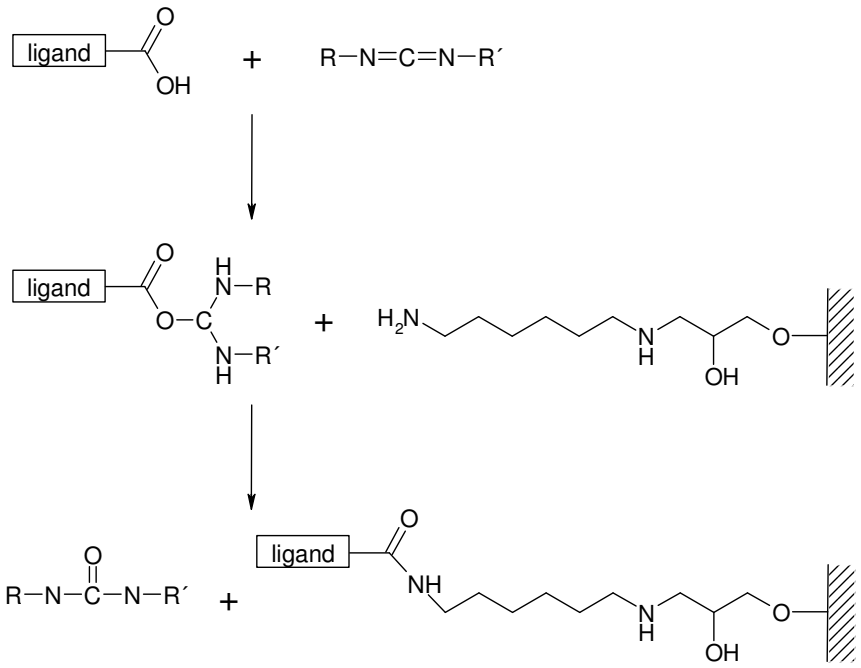

Figure 13: Immobilisation of ligands containing carboxy residues to amino activated matrices

3.2.4.1.2 Immobilisation of ligands on carboxylic acid functionalised matrices over amine residues

Immobilisation of molecules containing amine residues to carboxylic acid functionalised matrices was performed under the same conditions as described in (3.2.4.1.1).

3.2.4.1.3 Immobilisation of ligands to epoxy-functionalised matrices

Ligands containing $–NH_2$ or –OH residues were immobilised by incubating appropriate amounts of solubilised ligand with beads, under alkaline conditions (Fig. 14). In general, over night incubation at RT and pH values between 9 and 13 were required for a sufficient coupling.

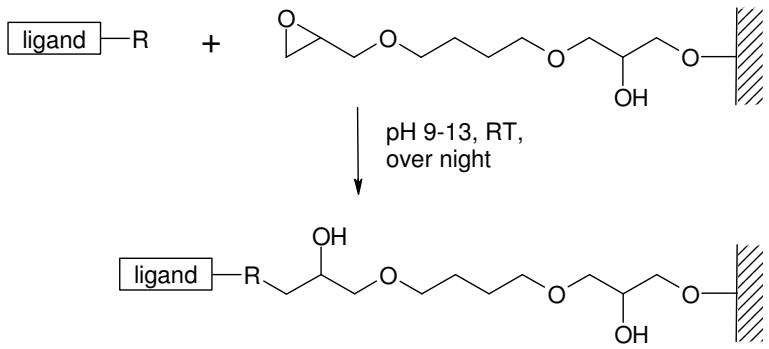

Figure 14: Immobilisation of ligands containing hydroxy and amino residues to epoxy-activated matrices. R could be –OH, -NH_2 or –SH.

3.2.4.1.3.1 Immobilisation of Acetaminophen (ACAP)

A.) N-glutaroyl-phenolamine and glutaric acid were immobilised by dissolving 74.3 mg (333 µmol) N-glutaroyl-phenolamine and 43.6 mg (333 µmol) glutaric acid in 10 ml 40% (v/v) dioxane. 290 mg 1-(3-dimethylaminopropyl)-3-ethylcarbodiimide hydrochloride and 10 µl HCl (1 M) were added. The coupling reaction was performed as described in chapter 3.2.4.

B.) Acetaminophen/ Phenol immobilisation: immobilisation of ACAP and phenol to epoxy activated beads was performed by dissolving 1 mmol of ACAP and phenol in dioxane respectively. 75 mg beads were given to this solution and the pH value was adjusted to pH 14 by addition of 10 µl NaOH (10 M).

C.) Aminophenol/ Aniline: Aminophenol and aniline were immobilised by dissolving 109.1 mg (1 mmol) Aminophenol and 93.14 mg aniline in 2 ml dioxane respectively. The pH value was adjusted by addition of 20 µl HCl 2 M. After addition of 1 ml Toyopearl® AF 650M carboxy slurry the reaction was started by addition of 30 mg EDC.

3.2.5 Fishing experiments / pull-down assays

3.2.5.1 Pull down assay of proteins from cell lysates

For pull-down assays, 50 µl beads (corresponding to 100 µl of 50% (v/v) bead slurry) were used. Beads were washed 3 times by centrifugation (7000 × g, 5 min, 4 °C for Sepharose® beads; 5000 × g, 3 min, 4° C for polyacrylic acid beads) and were resuspended in 500 µl binding buffer (different binding buffers were used, depending on the experimental requirements, see results). Incubation of the beads with the cell lysate was performed for 4 h at 4 °C on a rotator in 750 µl binding buffer.
All steps regarding derivatisation or incubation of beads were performed on a tube rotator to ensure appropriate agitation and to prevent sedimentation of the beads during these steps.

3.2.5.2 Pull down of recombinant proteins

For pull-down of isolated recombinant proteins, beads where prepared as described in (3.2.5.1). To prevent adhesion of the isolated protein to plastic surfaces or unspecific binding to the beads, *E. coli* lysate or BSA (0.25 mg total protein content in 750 µl assay volume) were used.

3.2.5.3 Elution of fished proteins

3.2.5.3.1 SDS elution

The beads were washed 3 times with 500 µl binding buffer. Fished proteins were eluted by addition of 50 µl SDS-PAGE loading buffer (20 mM Tris pH 8.0, 2 mM EDTA, 0.5% (w/v) SDS, 10% (v/v) 2-mercaptoethanol) to 50 µl beads and 5 min incubation at 95 °C. Eluted proteins were separated from the beads by centrifugation (7000 × g, 5 min, 4°C) and then analysed (see 3.2.6).

3.2.5.3.2 Urea elution

The beads were washed 3 times with 500 µl binding buffer. Fished proteins were eluted by addition of 50 µl 4 M urea to 50 µl beads and 30 min incubation at 4°C. Eluted proteins were separated from the beads by centrifugation (7000 × g, 5 min, 4°C) and incubated for 5 min at 96 °C after addition of 50 µl SDS-PAGE loading buffer (20 mM Tris pH 8, 2 mM EDTA, 0.5% (w/v) SDS, 10% (v/v) 2-mercaptoethanol).

3.2.5.3.3 Elution via cleavage of photoreactive linker systems

For detailed conditions of protein elution via cleavage of photoreactive linker systems see Results part (4.1.5.1).

3.2.6 Protein analytics

3.2.6.1 One dimensional gel electrophoresis (SDS-PAGE)

For electrophoretic separation, protein samples were mixed with equal volumes of SDS buffer (20 mM Tris-HCl, pH 8, 2 mM EDTA, 5% (w/v) SDS, 10% (v/v) 2-mercaptoethanol), heated for 5 min at 96 °C and then 2 µl bromphenol blue solution (50% (v/v) glycerol, 0.1% (w/v) bromophenol blue) were added to 10 µl sample. Proteins were separated by SDS-PAGE using self cast gels with 8 - 14% (v/v) acrylamide (according to the protein size). For a maximum resolution, constant currents of 90 V for the stacking-gel and 120 V for the separation-gel were applied.

3.2.6.2 Western blot analysis

Proteins were blotted (tank blotting method) from polyacrylamide gels to nitrocellulose membranes (90 V const., 90 min, in transfer buffer containing 48 mM Tris, 40 mM Glycine mM, 0.1 mM SDS, 20% (v/v) methanol). Correct loading of gels and transfer

of proteins were confirmed by Ponceau S staining (0.1% (w/v) Ponceau S, 5% (v/v) acetic acid for 5 sec).

Membranes were blocked with BSA blocking buffer (50 mM Tris-HCl, pH 7.4, 100 mM NaCl, 0.1% Tween 20, 5% (w/v) BSA) for 1 h at RT, washed with TBS buffer (50 mM Tris-HCl, pH 7.4, 100 mM NaCl) for 10 min at RT and then incubated with the respective primary antibody overnight at 4 °C. Antibodies were diluted in BSA blocking buffer, as indicated.

3.2.6.2.1 NBT/BCiP development of membranes

The membranes were washed (3 × 10 min) with TBS buffer and incubated with a 1:1000 dilution of alkaline phosphatase-coupled secondary antibodies for 1 h at RT. After washing 3 × 10 min with TBS buffer, 1 × 10 min TBST buffer ((50 mM Tris/HCl, pH 7.4, 100 mM NaCl, 0.1% (v/v) Tween 20), 1 × 10 min in detection buffer (100 mM Tris/HCl, pH 9.5; 100 mM NaCl, 5 mM $MgCl_2$), proteins were visualised by incubation of membranes with 0.4 mM nitro blue tetrazolium chloride (NBT) and 0.75 mM 5-bromo-4-chloro-3-indolyl phosphate (BCiP) in detection buffer.

3.2.6.2.2 ECL development of membranes

The membranes were washed (3 × 10 min) with TBST buffer and incubated with a 1:10,000 dilution of horseradish peroxidase (HRP)-conjugated secondary antibodies 1 h at RT. After washing (2 × 5 min, 1 × 15 min, 2 × 5 min with TBST buffer respectively), proteins were visualised by addition of HRP-substrate (Amersham™ ECL Western blotting detection reagent, GE Healthcare). Chemoluminescence films (Amersham Hyperfilm™ ECL) where exposed for the indicated times and developed using an X-Ray table-top processor (CP 1000 AGFA Healthcare N.V., Mortsel, Belgium)

3.2.6.2.3 ETTAN™ DIGE development of membranes

The membranes were rinsed two times with TBST buffer and subsequently washed (2 × 5 min) with TBST buffer. Afterwards, the membranes were incubated with ECL Plex CyDye™-conjugated secondary antibodies (1 h, RT, Cy3-conjugated anti-mouse dilution: 1:2500 in TBS buffer; Cy5-conjugated anti-mouse dilution: 1:4000 in TBS buffer). After washing (3 times for 5 sec plus 4 × 5 min with TBST buffer in the dark) the membranes were rinsed with TBS buffer and dried at 37 °C for 1 h.
Bands were visualised using an ETTAN™ DIGE Imaging system (GE Healthcare), using Cy3 (excitation filter: 540 nm; emission filter: 595 nm) and Cy5 (excitation filter: 635 nm; emission filter: 680 nm) channels. Incubation with CyDye™ labelled antibodies and following steps were performed in the dark to avoid bleaching of the fluorophoric group.

3.2.6.3 Silver staining

Silver staining was performed by fixing the gels immediately after the electrophoretic run in fixing solution (45% (v/v) methanol, 45% (v/v) H_2O, 5% (v/v) acetic acid) for 30 min. Gels were then washed for 30 min in water and sensitised by addition of $Na_2S_2O_3$ solution (1 mg/ml) for two minutes. After two more washing steps (1 min, each) with Milli-Q water, the staining solution ($AgNO_3$, 1 mg/ml) was added for 30 min. Again, two washing steps with water (1 min, each) were performed and then the developing solution (2.5% Na_2CO_3, 0.03% formalin in H_2O) was added for the time required to reach an optimal intensity of the staining. The staining reaction was stopped by a quenching step using 1% (v/v) acetic acid. Prior further steps, gels were washed with water for 10 min.

All solutions were prepared using Milli-Q water. All steps were performed on an orbital shaker at RT. Staining and sensitising solutions were prepared freshly and kept on ice until use. For large 18 × 20 cm gels and 2D gels, sensitising and staining steps were performed on ice.

3.2.6.4 CyDye™ labelling for differential gel electrophoresis (DIGE)

For 2D-DIGE, proteins were eluted with 4 M urea pH 8.5. The protein concentration was determined using an urea-compatible protein determination kit (BioRad DC Assay-Kit). For preparation of the CyDye™ working solution, 2 mM CyDye™ stock solution was diluted 1 to 2.5 with 3 µl water-free DMF (<0.005 ppm water). The pH was adjusted between 8.5 and 9.5 by adding 50 mM NaOH. For the coupling of the CyDye™ to the proteins, CyDye™ working solution (1 µl for 10 µg protein) was added to the samples and incubated for 30 min at 4 °C. The reaction was stopped by addition of 1 µl 10 mM lysin. CyDye™ labelled samples were stored at -80 °C until the isoelectric focussing (IEF).

3.2.6.5 Isoelectric focussing (IEF)

IEF was performed on 17 cm immobilised pH gradient (IPG) strips with a non linear pH gradient from pH 3 to pH 10 (Ready Strip™ IPG Strip). Proteins were diluted with PCT buffer (8 M urea, 2 M thiourea, 4% (w/v) chaps, ampholyte pH 3-10 0.7% (v/v), dithiothreitol (DTT) 65 mM, 10 µg/ml bromophenol blue). To prevent protein degradation by proteases, 50 µl P8340 protease inhibitor cocktail per gram protein was added to the sample. 300 µl sample solution containing up to 300 µg labelled and multiplexed proteins was pipetted into a 17 cm focussing tray. An IPG strip was placed on the sample to rehydrate with the sample solution for 12 h at 50 V and 10 °C (BioRad Protean® IEF cell, Herecules, CA).

step	voltage [V]	time	slope
1	0-250	1 min	linear
2	250	2 h	linear
3	250-500	1 min	linear
4	500	2 h	linear
5	500-1000	1 min	linear
6	1000	1 h	linear
7	1000-4000	1 h	linear
8	4000	2 h	linear
9	4000-10,000	2 h	linear
10	10,000	30 kVh	linear

Table 8:Voltage slope for IEF with 17 cm IPG strips

After rehydration, electrode wicks were moistened with 5 µl PCT-buffer and placed on the electrodes. IEF was performed using the following voltage conditions (Tab. 8). Focussed stripes where stored at -80°C until development of the second dimension.

For development of the second dimension, a SDS-PAGE was performed to separate proteins on the base of their molecular weight. IPG-strips were equilibrated by incubation for 2 × 7 min in equilibration buffer I (6 M urea, 4 (w/v) SDS, 0.05 M tris pH 8.8, 30 (v/v) glycerol, 1% (v/w) DTT), 2 × 7 min in equilibration buffer II (6 M urea, 4 (w/v) SDS, 0.05 M Tris pH 8.8, 30 (v/v) glycerol, 4% (w/v) iodoacetamide), and 1 × 10 s in SDS-PAGE running buffer (200 mM glycine, 25 mM Tris, 3 mM SDS). The IPG strip was placed on top of an 18 × 20 cm polyacrylamide gel containing 12% acrylamide overlayed by a 2 cm stacking gel. The IPG-strip was ingrained into an agarose gel (0.5% (w/v) agarose, 0.001% bromophenol blue in SDS-PAGE running buffer (25 mM Tris, 190 mM glycine, 3.5 mM SDS). For evaluation of molecular weights of proteins, a filter paper (5 mm diameter) was moistened with 5 µl of protein markers (peqLab, peqGOLD IV) and ingrained together with the IPG-strip. Gels were developed with a constant current of 16 mA for the stacking gel and 24 mA for the separation gel for a run time of about 8 h (BioRad PowerPac™ HV, Hercules, CA).

All urea containing buffers were purified from carbamoylated contaminations and salt impurities by incubating with ion exchange resin (BioRad AG® 501-X8 Resin). Appropriate amounts of AG 501-X8 ion exchange resin were determined by observation of a colour change from gold/yellow to transparent/colourless, due to depletion of the ion exchange capacity.

3.2.6.6 Acquisition of results

Silver stained gels and X-ray films of ECL-developed Western blot membranes were acquired with a CCD camera system (CabUVis, Hitachi HV-C20M 3CCD, Sarstedt AG Co., Nümbrecht, Germany). NBT/BCiP developed Western blots were digitised with a common flat bed scanner.

DIGE pictures were obtained by an ETTAN™ DIGE Imager system (GE Healthcare) and evaluated via ImageQuant™ TL software. Appropriate dyes were scanned in their corresponding channels (Tab. 9). Required exposure times were set to 0.040 – 0.400 sec for Western blot experiments, depending on the signal intensities, and to 1.000 – 4.000 sec (= highest possible exposure time) for 2D DIGE gels.

Dye	Exication filter	Emission filter
Cy 2	480 nm	530 nm
Cy 3	540 nm	595 nm
Cy 5	635 nm	680 nm

Table 9: Exication and emmision wavelengths of the ETTAN DIGE™ channels

Spots on scanned 2D-DIGE gels were detected using the DeCyder 7.0 software. DeCyder 7 algorithm was used to calculate appropriate spot values. The threshold was set as 2.0. Spots exceeding a slope of 1.0 were considered artificial.

MS analytics of fished proteins was done in cooperation with the Proteom Center at Univ. Tuebingen via in-gel digestion and nanoflow liquid chromatography tandem MS (nano-LC-ESI-MS/MS) on a QSTAR Pulsar hybrid qTOF mass spectrometer (AB-MDS Sciex) as described previously [139]. Bioinformatic analysis of the identified peptides was subsequently done with Matrix Science Mascot.

3.2.7 Functional enzyme assays

3.2.7.1 Determination of phosphorylated proteins

Isolated neutrophils (10^7 cells /100 µl PGC buffer (PBS containing 0.1% (w/v) glucose and 1 mM $CaCl_2$) were incubated with the indicated compounds at 37 °C for the indicated time. The reaction was stopped by addition of 100 µl of 2×SDS buffer (20 mM Tris pH 8, 2 mM EDTA, 0.5% SDS, 10% 2-Mercaptoethanol) and incubated for 6 min at 95°C. After sonification for 10 sec, total cell lysates were analysed for ERK1/2, phosphorylated ERK1/2 (Thr-202/Tyr-204), phosphorylated AKT (Ser473), HSP27 and phosphorylated HSP27 (Ser82) by SDS-PAGE and Western blotting.

3.2.7.2 Serine protease activity assays

3.2.7.2.1 Proteinase 3 (PR3) activity assay

Proteinase 3 purified enzyme (0.1 µg) was diluted in 100 µl assay buffer (0.1 M Mops, 0.5 M NaCl, 0.1 mM 5,5´-dithiobis-(2-nitro-benzoic acid), pH 7.5) in a 96 well plate. The enzyme was preincubated with the indicated compounds for 15 min at RT. The enzymatic reaction was started by addition of 0.1 mM substrate (Boc-Ala-Ala-Nva-SBzl) in 100 µl assay buffer. Enzyme activity was measured by detection of the reduced cosubstrate (2-nitro-5-thiobenzoate dianion) on a microplate reader (VersaMax^{TM}, Molecular Devices Inc., Sunnyvale, CA) at 410 nm for 1 h at RT.

3.2.7.2.2 Cathepsin G (CG) activity assay

CG was freshly isolated from PMNL (2.5×10^7 cells/ml in PGC buffer) by stimulation with 10 µM cytochalasin B and 2.5 µM fMLP for 5 min at 37 °C and subsequent centrifugation (1200 × g, 5 min, 4°C). The supernatant (10 µl/sample) was used as source of CG and added to 180 µl assay buffer (0.1 M Hepes pH 7.4, 0.5 M NaCl). The enzyme was preincubated with the indicated inhibitors for 15 min at 37 °C. The enzymatic reaction was started by addition of CG substrate (1 mM N-Suc-Ala-Ala-Pro-Phe-pNA) and the conversion of the substrate was directly measured by detection of the proteolytic product (p-nitrophenol) on a microplate reader (VersaMax^{TM}, Molecular Devices Inc., Sunnyvale, CA) at 410 nm for 1 h at RT.

Compounds were solubilised in ethanol or DMSO. The final concentration of solvents in the assay was kept below 0.1% (v/v) for 3.2.7.1 and 1% (v/v) for 3.2.7.2.

4 Results

4.1 Development of methods to improve fishing approaches

4.1.1 Evaluation of different matrix types:

A summary of the chemical composition of different matrix types is given in the introduction (1.2.2). In our experiments, agarose beads show an insufficient chemical resistance against organic solvents limiting their application and the possibilities of modification reactions. While agarose beads get partially solubilised or show a dramatic change in their structure using moderately unpolar solvents such as dioxane, methanol, THF or DMF, methacrylic acid matrices turned out to be stable under these conditions. Strongly unpolar aromatic solvents, such as toluene, as well as extreme pH values and high temperatures facilitate solubilisation of these beads. However, methacrylic acid matrices afford the widest range of possibilities and were therefore used in subsequent experiments.

4.1.2 Generation of carboxymethoxylamine beads for immobilisation of ligands via keto- or aldehyde groups.

Since there are no commercially available matrices to immobilise ligands via keto- or aldehyde residues to beads, we established an approach to derivatise existing matrix types to allow subsequent immobilisation of aldehydes and ketones [II].

For this purpose, N-boc-carboxymethoxylamine was covalently coupled to amino functionalised beads under standard coupling conditions (see 3.2.4). After deprotection of the oxime group (10% (v/v) TFA, on, RT) the ligand can be coupled under mild reaction conditions (MeOH, Pyridin, RT, on) to the beads (Fig. 15).

[II] The development of carboxymethoxylamine activated beads was done in cooperation by dipl. chem. M. Golkowski and the group of Prof. Dr. T. Ziegler, Institute of Organic Chemistry, University Tübingen

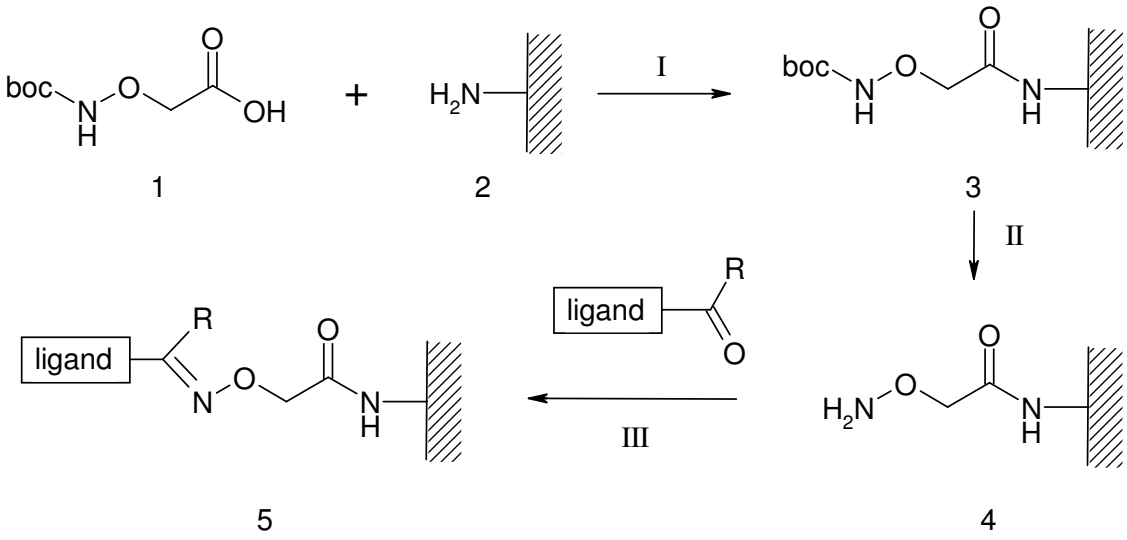

Figure 15: Matrix surface derivatisation for aldehyde and ketone immobilisation. N-boc-carboxymethoxylamine (1) is coupled under standard conditions (I) (DIC, RT, on in dioxane, pH 4) to the amino functionalised matrix (2). The Boc group was removed by addition of TFA (10 % (v/v), RT, on) (II) to receive the free methoxyl function (4). The ligand was used in a 1:1 ratio and coupled by addition of two equivalents pyridine in MeOH at RT over night (III).

Testosterone was used as model compound for this derivatization strategy since it possesses one single keto group and thereby offers the possibility for a selective immobilisation. Successful immobilisation of testosterone was controlled by addition of 35% (v/v) ethanolic sulfuric acid and subsequent heating (75°C, 10 min) which leads to a fluorescent product. Fluorescence of the steroid was detected by UV light exposure at 366 nm. Neither the beads alone nor the carboxymethoxylamine derivatised beads showed any fluorescence. A solution of testosterone as positive control as well as testosterone coupled to the beads show distinct fluorescence as result of a successful ligand coupling (Fig. 16).

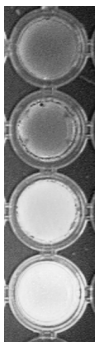

Figure 16: Verification of testosterone immobilisation on carboxymethoxylamin (CMO)-activated beads. Testosterone shows fluorescence after treatment with ethanolic H_2SO_4 35% and subsequent heating at 75°C for 1 h. A solution of testosterone in MeOH as well as the testosterone coupled CMO-beads show fluorescence, whereas CMO-activated or unmodified beads themselves are not fluorescent.

Further studies in cooperation with M. Golkowski (Dept. of Organic Chemistry, Univ. Tuebingen) showed that other compounds like ketoprofen as well as complex structures like erythromycin can be immobilised selectively and without derivatization reaction using this strategy (data not shown).

4.1.3 Evaluation of fishing conditions

For the evaluation of the fishing conditions, a huge number of buffers containing different types and quantities of salts or detergents were tested. However, buffer systems containing PBS or Hepes as buffer substance, a pH-Value of 7.4 and 0.9% NaCl turned out to be sufficient. The use of Hepes resulted in a higher number of bound protein, but since it is known to form radicals [140] it was substituted by PBS for experiments where extensive UV radiation was applied.
Addition of non ionic detergents in concentrations up to 1% reduced unspecific protein binding. Overnight incubation with cell lysates (pre-cleared by ultracentrifugation) led to the best fishing results.

4.1.4 Evaluation of elution conditions

In order to evaluate various elution conditions, experiments were performed using immobilised ACAP that was incubated with PBMC and PMNL cell lysates. Elution using SDS-buffers results in a large number of eluted proteins that exceed the separation capacity of a standard 8 × 6 cm polyacrylamide gel. Elution using NaCl (1 M) was less stringent but not more specific. Thus, the analysis of proteins is limited to the estimated 50 most abundant proteins. Using a solution of ACAP (50 mM) to elute proteins fished by ACAP in a competitive way leads to very low amounts of eluated proteins (Fig. 17).

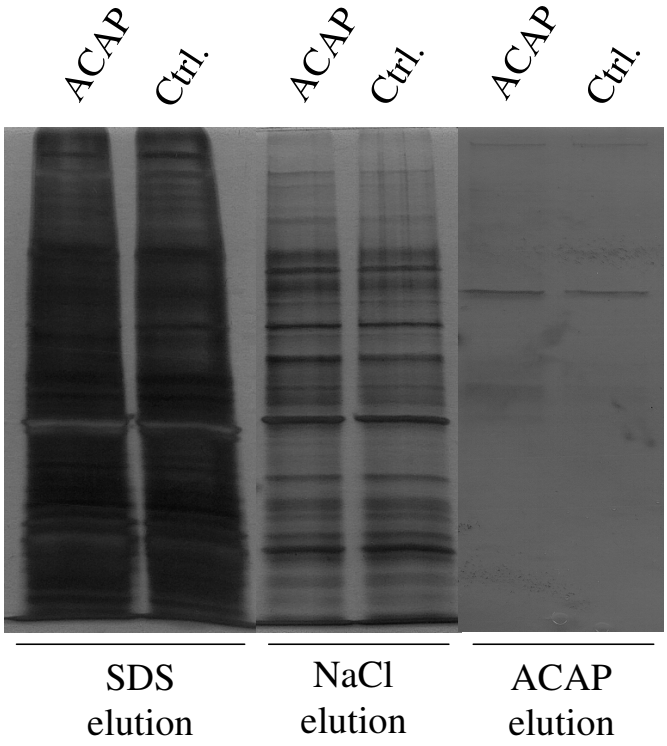

Figure 17: Evaluation of different elution conditions. Electrophoretical separation of fishing-eluates derived by elution of ACAP-matrices after incubation with lysates of PMNL using SDS, NaCl and ACAP buffer and detection of the proteins by silver staining.

4.1.5 Improvement of the target-fishing approach

The major disadvantage of the target-fishing is the high number of unspecific bound proteins. Two different strategies were followed in order to improve this approach. On the one hand, an UV light cleavable linker system was developed to by-pass unspecific binding events. On the other hand, the electrophoretic separation capacity was improved by using a 2D-DIGE approach.

4.1.5.1 Development of a photoreactive linker system

The synthesis of the o-nitrophenyl linker was done according to Holmes et at 1996 [21, 141] in cooperation with Thomas Kutter (Dept. of Organic Chemistry, Univ. Tuebingen) (Fig. 18).

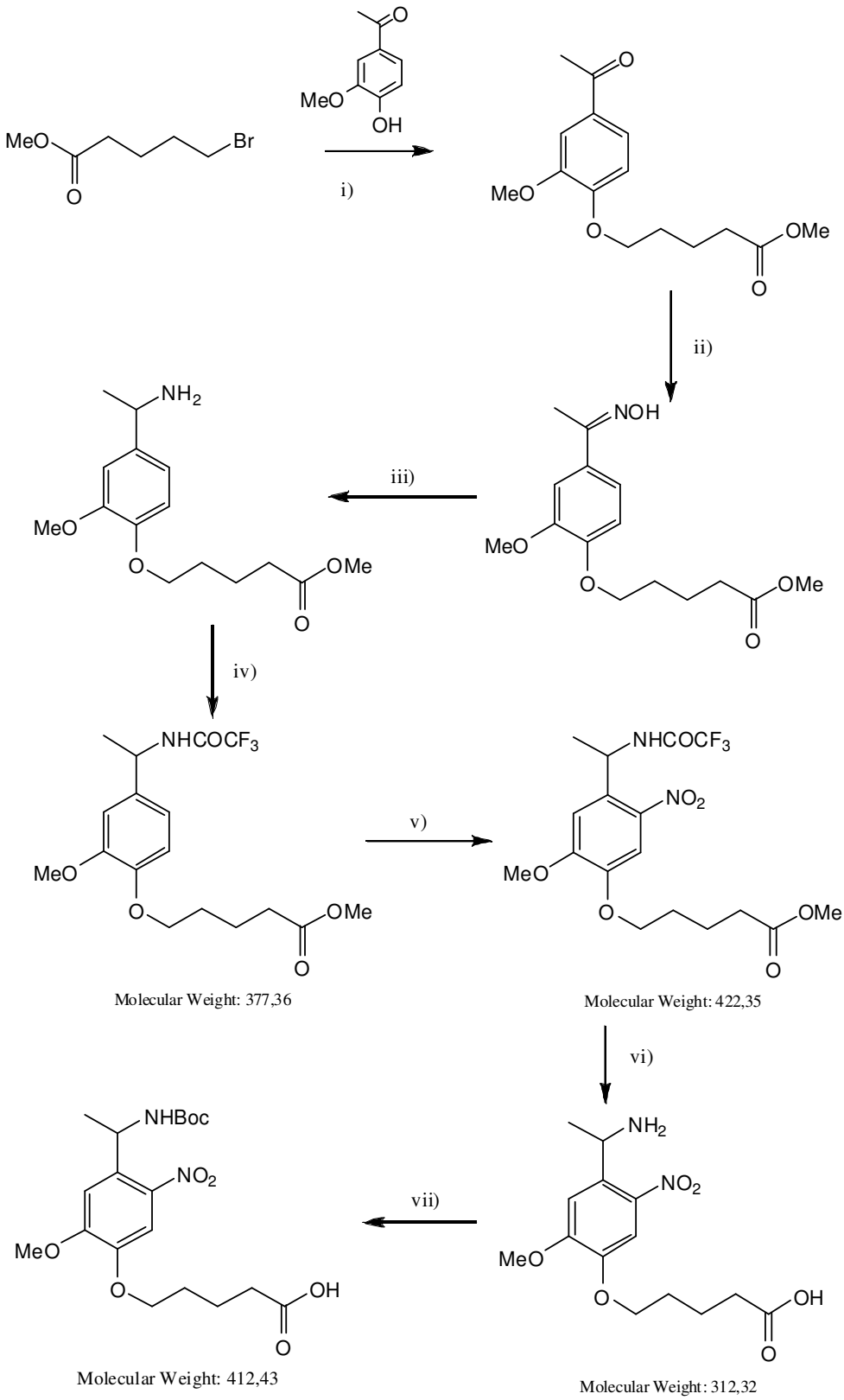

i) K_2CO_3, DMF, RT ii) NH_2OH*HCl, Py, RT iii) $Pt(IV)O_2$, H_2, AcOH, RT iv) TFA_2O, DCM, -10°C v) HNO_3, -10°C vi) NaOH, MeOH, H_2O RT vii) Boc_2O, DMAP, EtOAc, RT

Figure 18: Synthesis of the Boc protected nitrobenzylic photoreactive linker system with C5 spacer.

Modifications of known linker systems were needed in order to achieve a better solubility and biocompatibility. Therefore, the photoreactive core of the molecule was retained, whereas subsequent changes of alkyl chain length and the protection group were tested [III]. A *tert*-butoylxycarbonyl- (Boc) protected o-nitrobenzylic linker with a C5 chain spacer turned out to be optimal in immobilisation- and cleavage reactions.

4.1.5.2 Development of an immobilisation strategy for UV light cleavable linker systems

The Boc-protected linker was immobilised using standard peptide chemistry [137-138] (3.2.4). To ensure that the ligand is only bound via the photoreactive linker and not directly to the beads, the immobilisation was performed in four steps: (i) immobilisation of the linker to the functionalised beads, (ii) blocking of remaining functional groups, (iii) removal of the Boc-group and (iv) releasing the ligand.

The immobilisation of the linker, the ligand and the blocking of remaining free amino groups was performed in three steps using three times the same reaction (Fig. 19). For the immobilisation, the linker solution (300 µmol in 2 ml DMF) and 1.5 mmol diisopropylcarbodiimide (DIC) were added to 1 ml pre-washed amino-functionalised methacrylic acid resin (Toyopearl® AF-Amino-650M; Tosho Bioscience). The reaction was performed at room temperature and pH 4.5 over night. Remaining free amino groups of the resin were blocked with acetic acid (150 µmol, with 1.5 mmol DIC at room temperature over night). Afterwards the boc group was removed (10% TFA in H_2O, 90 min at RT) to receive the free amino group of the linker. The ligand was coupled by adding 2 ml ligand solution (330 µmol ligand, 1.5 mmol DIC) to the resin and incubating it over night at pH 4.5 and room temperature. Washing steps were performed between every reaction step by washing the resin with 20 ml DMF on a G4 glass filter crucible.

[III] Synthesis of putative UV-linker molecules was done in cooperation by dipl. chem. T. Kutter and the group of Prof. Dr. T. Ziegler, Institute of Organic Chemistry, University Tübingen

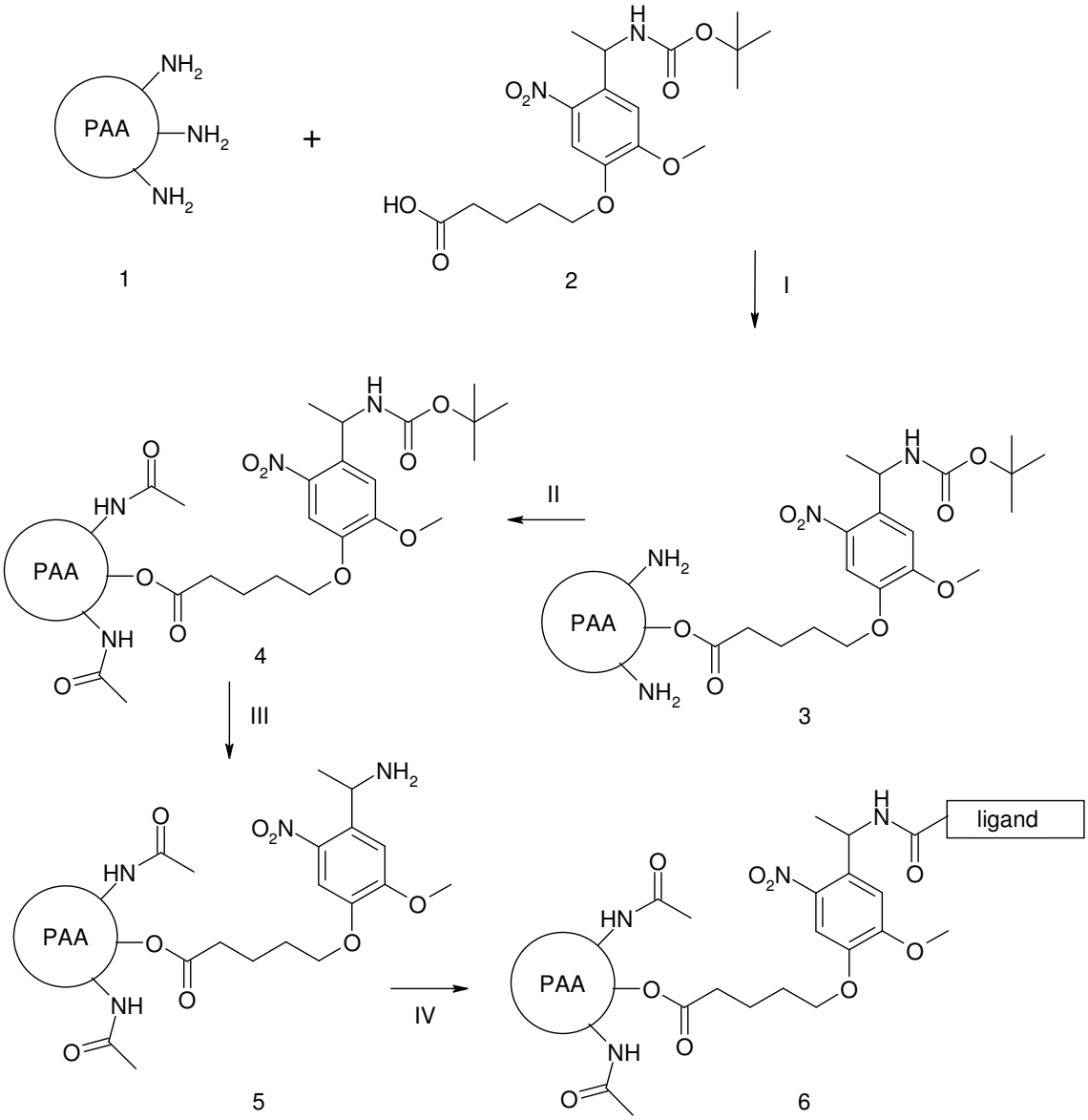

Figure 19: Immobilisation strategy for photoreactive linker systems. The Boc protected linker (2) is coupled under standard conditions (I) (DIC, RT, on in dioxane, pH 4) to the amino activated matrix (PAA, 1). Remaining free amino groups of compound 3 are blocked with acetic acid (II) (DIC, RT, on in dioxane, pH 4). The protection group of (4) was removed by addition of TFA (10% (v/v), RT, on) (III) and the ligand was then coupled in the last step (IV).

4.1.5.3 Fishing conditions for UV light cleavable linker systems

A standard buffer system used for pull-down experiments and protein fishing is a HEPES binding buffer composed of 50 mM Hepes pH 7.4, 200 mM NaCl, 1 mM EDTA, 1% (v/v) triton® X-100. Since HEPES is known to form radicals [140] we chose a phosphate-based buffer system composed of PBS pH 7.4 containing 1 mM EDTA, 200 mM NaCl, 1% (v/v) triton® X-100 to elute protein via UV light cleavage of the linker.

4.1.5.4 Elution conditions for UV light cleavable linker systems

Previous works have described the usage of nitrobenzylic linker systems for cleaving peptides from a matrix after a solid phase synthesis [21]. In this work cleavage of the linker was performed by UV radiation using a 1000 W UV lamp. In our experiments, a power of 100 W led to destruction of the proteins due to ionising radiation (Fig. 20). On the other hand, UV lamps with a power between 4 W and 16 W and a distinct wavelength of 366 nm used for TLC plate evaluation were not strong enough to cleave the linker system. To combine the benefits of both, the high power of the 100 W UV lamp and the distinct wavelength of the low power UV lamps, the filter plates of the low power UV lamp were removed and mounted to the 100 W UV lamp. Thus, the high energy of the 100 W UV lamp could be used while ionising radiation is refrained by the filter plates.

Elution of proteins by cleavage of the linker was performed in a cooled 24-well plate on an orbital shaker. After fishing and subsequent washing procedures 100 µl beads were suspended in 100 µl PBS binding buffer and irradiated for 90 min.

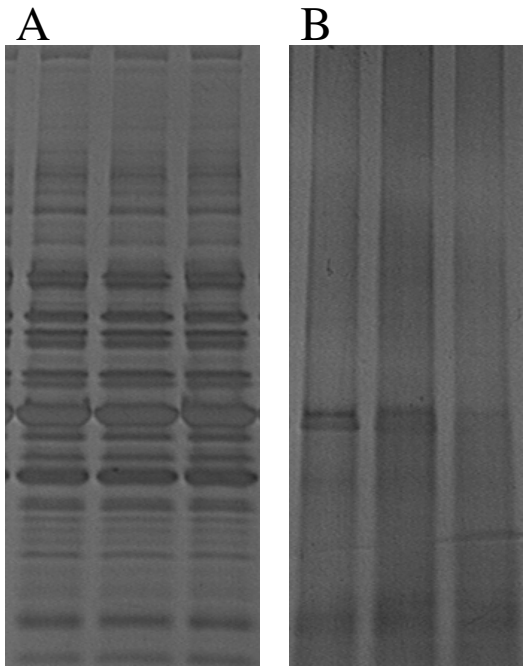

Figure 20: SDS-PAGE of testosterone fished proteins from PMNL cell lysates with (B) and without UV light exposure (A) (1 h, 100 W, 4°C).

To validate the functionality of our UV light cleavable linker system and appropriate cleavage conditions, a model system consisting of testosterone as ligand and the androgen receptor (AR) as known target was established. After a protein fishing experiment

using LNCap lysate as protein source, the AR is bound to the matrix surface (Fig. 21A). Extended blocking approaches as well as stringent washing conditions could not prevent the AR matrix interaction (Fig. 21A).

The use of the UV light cleavable linker system by-passed the AR matrix interaction by releasing only proteins that are bound on a ligand that is released after UV irradiation. Thus, AR still binds to the matrix but is not eluted whereas testosterone-bound AR can be released by cleaving off the testosterone from the matrix (Fig. 21B).

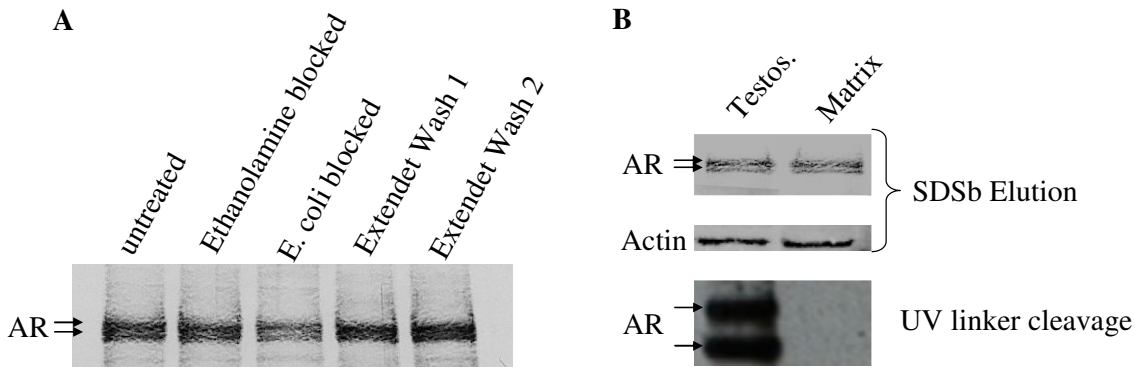

Figure 21: (A) Western blot of fishing eluates from testosterone-matrices in LNCap cell lysates with different blocking and extended washing conditions. Untreated: fishing performed according to the standard protocol (3.2.5); Ethanolamine blocked: Blocking of free primary amino groups by coupling ethanolamine to the matrix; *E. coli* blocked: *E. coli* lysate (1 mg/ml protein) was used to block protein binding moieties of the matrix; Extended wash 1: Washing steps using alternately 300 fold column volume of acetate buffer (pH 4, 0.5 M NaCl) and Tris buffer (pH 8, 0.5 M NaCl); Extended wash 2: Washing steps using 300 fold column volume of binding buffer containing 1% Triton® X-100. (B) Western blot of fishing experiments in LNCap cell lysates using testosterone-matrice with UV light cleavable linker: Elution was performed with SDSb or via cleavage of the photoreactive linker system. Data shown are representative of at least three independent experiments.

4.1.5.5 Establishment of 2D-DIGE for pull down assays

2D-DIGE is a protein separation and detection method with high sensitivity and a high resolution. It allows simultaneous quantification of two or more groups of differentially labelled proteins. 2D-DIGE was established to compare protein expression patterns of different cell types. Therefore, it has to be optimised to comply with the requirements of the target-fishing approach.
Although eluates from target-fishing experiments contain a limited pre-selected number of proteins, the sample complexity exceeded the resolution of standard, one dimensional gel electrophoresis (Fig. 17). Hence, alternatives to the classical one-dimensional SDS-PAGE had to be developed and optimised for the analysis of target-fishing eluates.

4.1.5.6 Elution conditions for 2D-DIGE

For the 2D-DIGE approach, classical elution conditions with SDS buffers are not suitable since SDS masks the isoelectric points of the proteins. Thus, IEF and CyDye compatible alternatives had to be found. A buffer containing 4 M urea with pH 8.5 was the highest concentration that could be achieved at 4 °C and showed adequate elution strength and compatibility with subsequent CyDye labelling reactions.

4.1.5.7 Labelling conditions for 2D-DIGE:

Since 2D-DIGE approaches are developed for whole cell lysates, labelling conditions for the fishing eluates had to be adopted to the very low protein concentrations and to the specific buffer compositions of fishing experiments (detailed labelling conditions are described in the methods part). Figure 22A shows the successful labelling of a fishing eluate with Cy5 (lane1/red) and Cy3 (lane 2/ green) and a “one-to-one” mixture of sample 1 and 2 in lane 3. As shown in figure 22A the presence of identical proteins in a Cy3- and Cy5-labelled sample results in a colour change to yellow as result of a green-red overlay.

For the determination of the detection limit of CyDye-labelled protein, BSA was labelled with the Cy3- and Cy5-dye respectively. The labelled BSA was separated via SDS-PAGE, fixed and scanned in the corresponding channels with an ETTAN^{TM} DIGE scanner. The labelled BSA could be seen in the scanned picture at amounts up to 5 pg protein or 500 fmol (Fig. 22B).

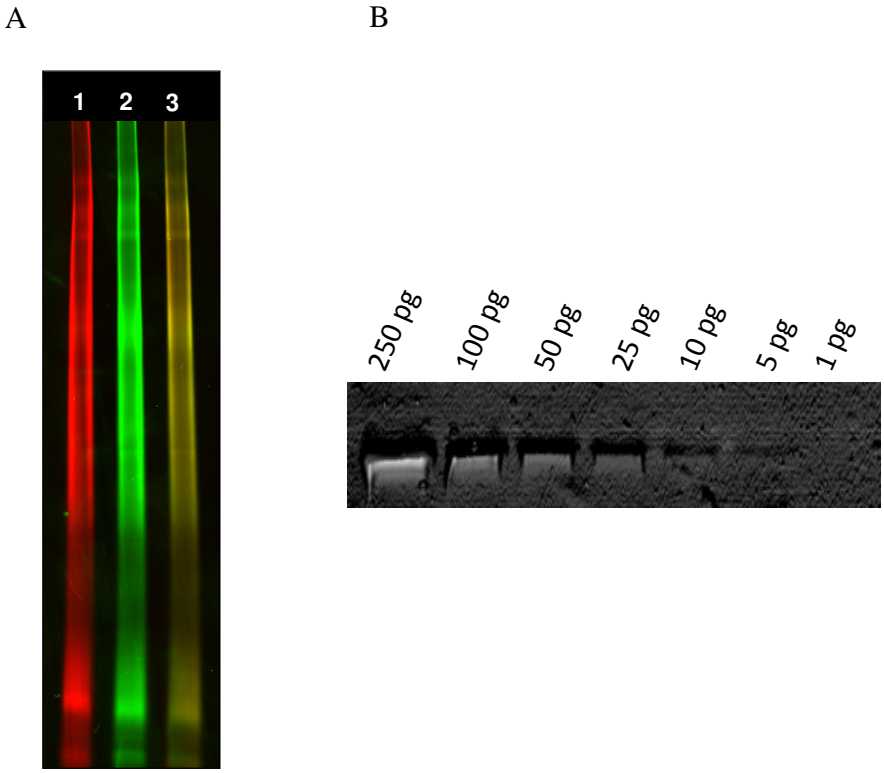

Figure 22: (A): SDS-PAGE of Cy2- and Cy3-labelled proteins fished from a PMNL cell lysate (lane 1 and 2) and a mixture of Cy2-and Cy3-labelled Cell lysates (line 3). (B) SDS-PAGE of CyDye-labelled BSA. Data shown are representative of at least three independent experiments.

4.1.5.8 IEF conditions for 2D-DIGE:

For the separation in the first dimension, IPG-strips were chosen for isoelectric focussing. The tray loading method combined with an active rehydration step resulted in the best performance for separating fishing eluates.

First experiments with 7 cm IPG strips showed that only few proteins have a very high or a very low isoelectric point and that most of the protein spots are located in a more or less neutral pH range. Therefore IPG strips with a non-linear pH gradient between pH 3 and pH 10 were used to achieve maximal separation in further experiments.

4.1.5.9 Development of the second dimension for 2D-DIGE

Equilibration steps between IEF and second dimension separation via SDS-PAGE were optimised to ensure a sufficient protein transfer from IPG-strips to the polyacrylamide gel (conditions are shown in 3.2.6). separation in the second dimension was performed with a standard Tris-glycine SDS-PAGE system [25].

4.1.5.10 2D-DIGE result evaluation:

2D-DIGE gels were digitised by scanning with an ETTAN™ DIGE scanner (for instrument settings see 3.2.6.6). Differentially fished proteins were detected by comparison of both scanning channels in ImageQuant™ TL and DeCyder™ software.

4.2 Target-fishing experiments

4.2.1 Acetaminophen (ACAP)

Since the exact pharmacological mode of action of ACAP is still not clear, ACAP was chosen as ligand for target-fishing. Para-aminophenol conjugated with prolonged carbonic acid amides are known to be still pharmacological active [49]. Thus, N-glutaroyl-aminophenol containing ACAP as substructure was chosen as ligand since the free, second carboxylic acid allows specific linking to EAH Sepharose® 6B presumably keeping its pharmacological activity (Tab. 10). However, this fishing construct did not lead to the discovery of potential target candidates. Two additional constructs as well as corresponding control constructs were generated. On the one hand, ACAP was coupled using its phenolic hydroxyl residue to epoxy-activated Sepharose® to receive a construct with an underivatised amide. Since the glutaroyl-ACAP showed poor solubility in common solvents, p-aminophenol was coupled to carboxy-activated methacylic acid beads. This immobilisation strategy offered two benefits: on the one hand the carboxy-activated matrix offers by far more functional groups than the EAH Sepharose®. On the other hand, p-aminophenol shows good solubility leading to a high immobilisation rate. An overview of the used ACAP fishing constructs is given in table 10.

Nevertheless none of the used constructs led to fishing of potential target proteins. Several cell lysates from PMNL, PBMC, platelets, Hela, Jurkat, PC12 and LNcap cells as well as different pre-clearing, washing and preparation methods of these lysates were tested without positive results. Also different separation methods like small (6 cm) and large (18 cm) scale 1D electrophoresis, 2D electrophoresis and 2D DIGE always led to identical spot patterns of immobilised ACAP and corresponding controls.

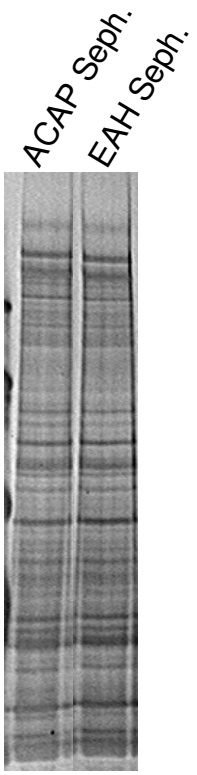

Figure 23: Identical protein-band pattern for proteins fishes with ACAP (immobilised on EAH-Sepharose® 4B) and EAH-Sepharose® 4B without ligand. Fishing in PMNL cell lysate. See also Fig. 17.

To evaluate the functionality of the ACAP-mimicking N-glutaroyl-aminophenol fishing construct, fishing experiments in lysates of PBMC (COX-2) and of platelets (COX-1) were performed. Western blot analysis of the eluates shows that there is no higher affinity for COX-1 or COX-2 to ACAP in comparison to the matrix control (Fig. 24).

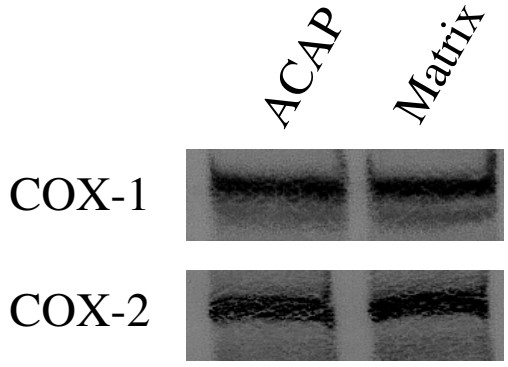

Figure 24: COX-1 and COX-2 Western blot analysis of fishing eluates using an ACAP-mimicking fishing construct as ligand.

	Ligand	Fishing construct
N-glutaroyl-aminophenol (A) immobilised on amino activated beads (EAH Sepharose® 4B) (A´) and glutaric acid as control (B, B´)	A 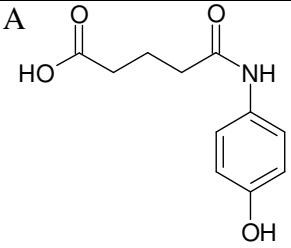	A´ 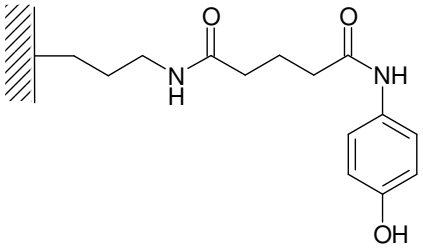
	B 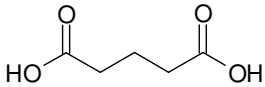	B´ 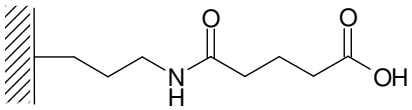
Acetaminophen (C) immobilised on epoxy activated beads (Toyopearl AF-Epoxy-650M) over the 4´OH group (C´) and phenol as control (D, D´)	C 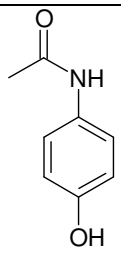	C´ 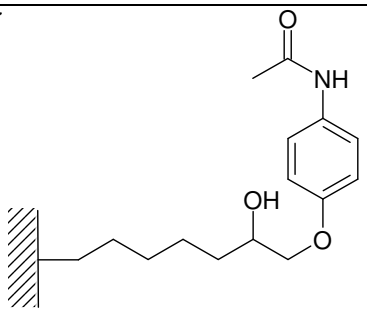
	D 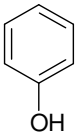	D´ 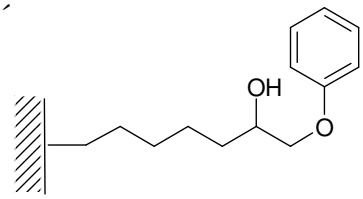
p-Aminophenol (E) immobilised on carboxy activated beads (E´) and aniline as control (F, F´)	E 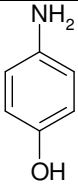	E´ 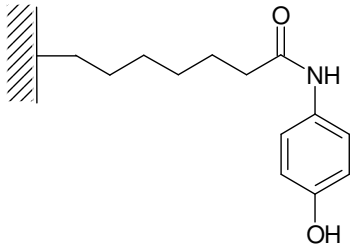
	F 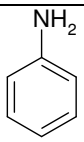	F´ 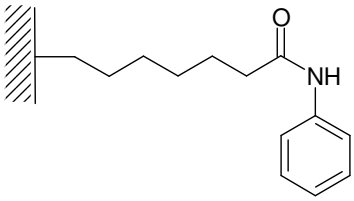

Table 10: Immobilisation strategies for ACAP target-fishing: To obtain comprehensive fishing results for ACAP, the compound was immobilised in three different ways. First, N-glutaroyl-aminophenol, containing ACAP as substructure was immobilised to EAH Sepharose® 4B (A, B). Second, ACAP itself was immobilised via its 4´-hydroxylic group (C, D) and p-aminophenol was immobilised to carboxy functionalised methacrylic acid beads as third construct (E,F).

4.2.2 Indirubin-3-monoxime (IR3MO)

4.2.2.1 Immobilisation of IR3MO

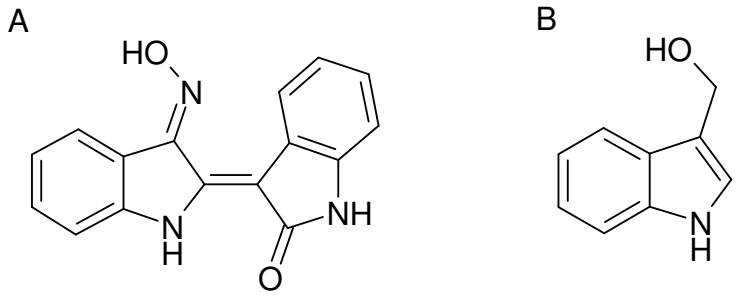

Figure 25: Chemical structure of indirubin-3´-monoxime (A) and indole-3-carbinol (B)

In contrast to indirubin, IR3MO possesses a monoxime moiety on the 3´-position that enhances its bioavailability (Fig. 25). Thus, the monoxime moiety does not affect the pharmacological properties of indirubin and can therefore be used for the immobilisation. Unfortunately, monoxime moieties are characterised by a very poor reactivity. Thus, no reactions are so far known to immobilise monoximes. However, Kurbanov et. al. showed in 1999 that ketoximes can be alkylated by reaction with α-epoxides [142]. Therefore, the immobilisation of IR3MO was performed using epoxy-activated beads (Toyopearl AF-Epoxy-650M). For the immobilisation, IR3MO [IV] was solved in a 1:1 (v/v) mixture of 5 N aqueous NaOH and acetone. The reaction took place at 60 °C for 72 h under continual rotation.

[IV] IR3MO substance and VSMC lysates were kindly provided by the group of Prof. Dr. V. M. Dirsch, Department of Pharmacognosy, University of Vienna, Austria

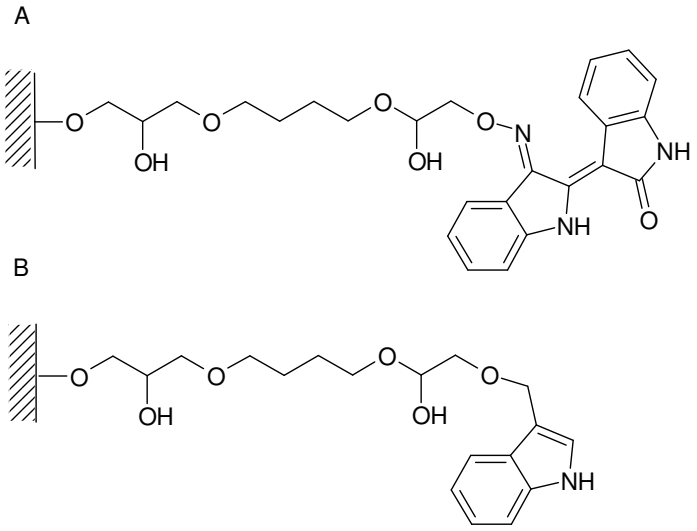

Figure 26: Structure of fishing constructs for IR3MO (A) and I3C (B) as control.

Indole-3-carbinol (I3C) was chosen as a substructure of IR3MO as negative control for IR3MO. Since I3C possesses a primary hydroxyl group, the immobilisation could be performed under standard conditions with epoxy activated beads (see 3.2.4.1.3) (Fig. 26).

4.2.2.2 Target-fishing experiments with IR3MO

Since known anti-inflammatory and antitumoral effects of IR3MO were observed in vascular smooth muscle cells (VSMCs) by our cooperation partners [IV] (unpublished data), lysates of VSMCs as well as PMNL and PBMC lysates were used for fishing experiments. Although there are visible spots in the DIGE experiments, protein amount of the fishing eluates were too low for detection by silver staining or subsequent MS approaches (Fig. 27). Additional experiments with cell lysates containing higher protein concentrations showed no significant improvement.

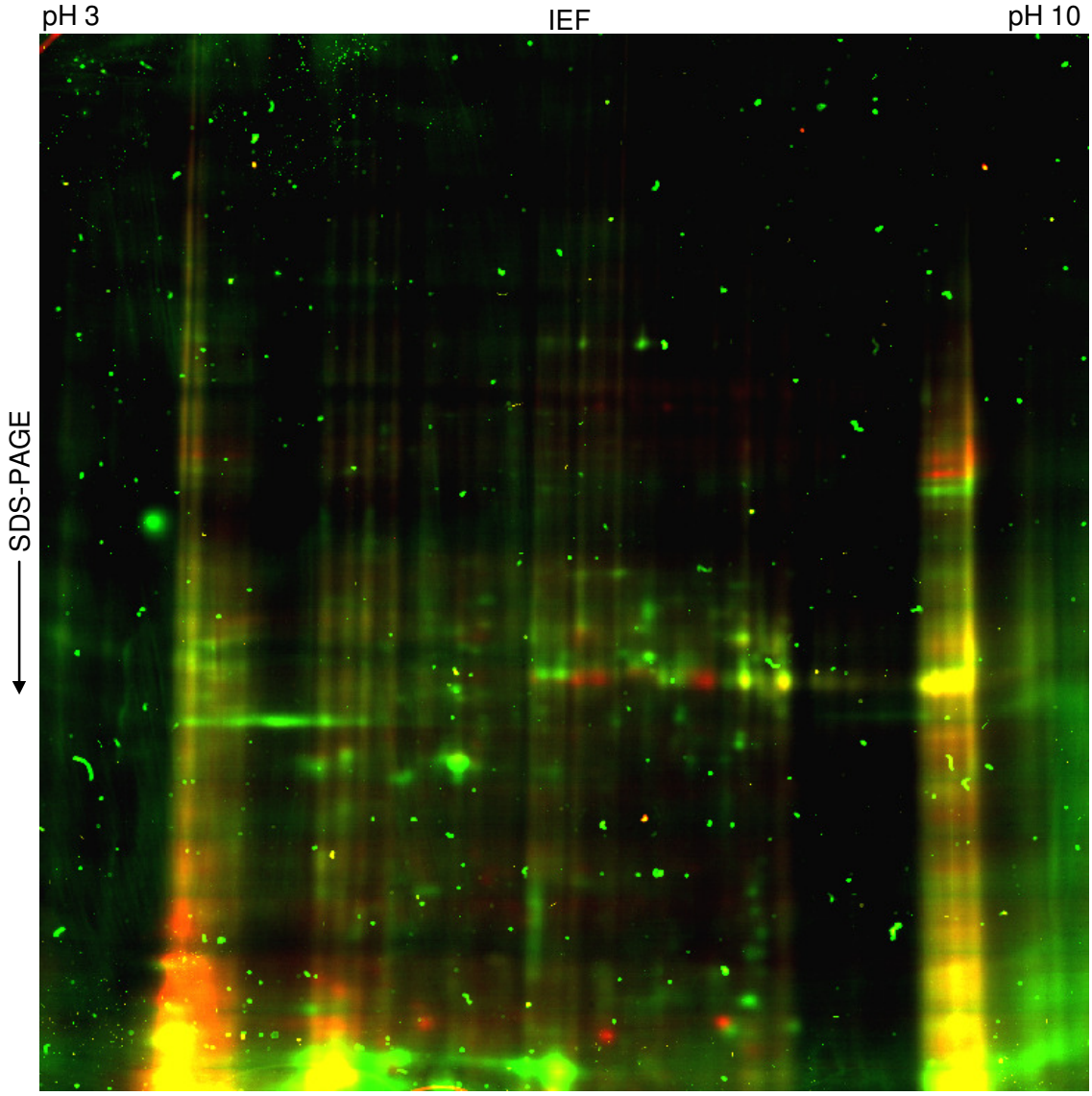

Figure 27: 2D-DIGE of indirubin-3-monoxime fished proteins from PBMC cell lysate. Red: Cy5 labelled IR3MO fished proteins, green: Cy3 labelled indole-3-carbinole fished proteins.

4.2.3 Myrtucommulone A

4.2.3.1 Immobilisation of Myrtucommulone A

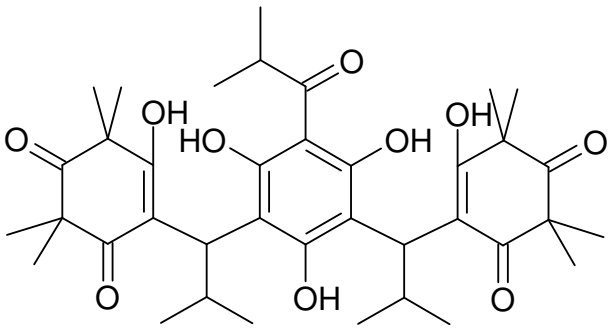

Figure 28: Molecular structure of Myrtucommulone A

For the immobilisation of Myrtucommulone [V] (MC) (Fig. 28), 10 mg MC were dissolved in 750 µl dioxane. After addition of an aqueous suspension of 140 mg Toyopearl® AF 650M Epoxy beads in 500 µl water, 10 µl of 10 N NaOH were added to adjust the pH value. Following steps were performed under standard conditions for epoxy activated beads (see 3.2.4.1.3).

4.2.3.2 Target-fishing experiments with Myrtucommulone

DIGE analysis of a fishing experiment using PMNL lysate showed identical spot patters for MC and n-propanol blocked beads (Fig. 29). Hence, no protein selectively binding to MC could be identified. Propanol was used to block remaining reactive epoxy-groups.

[V] Myrtucommulone was kindly provided by Prof. Dr. J. Jauch, Universität des Saarlandes, Organische Chemie II, Saarbruecken, Germany.

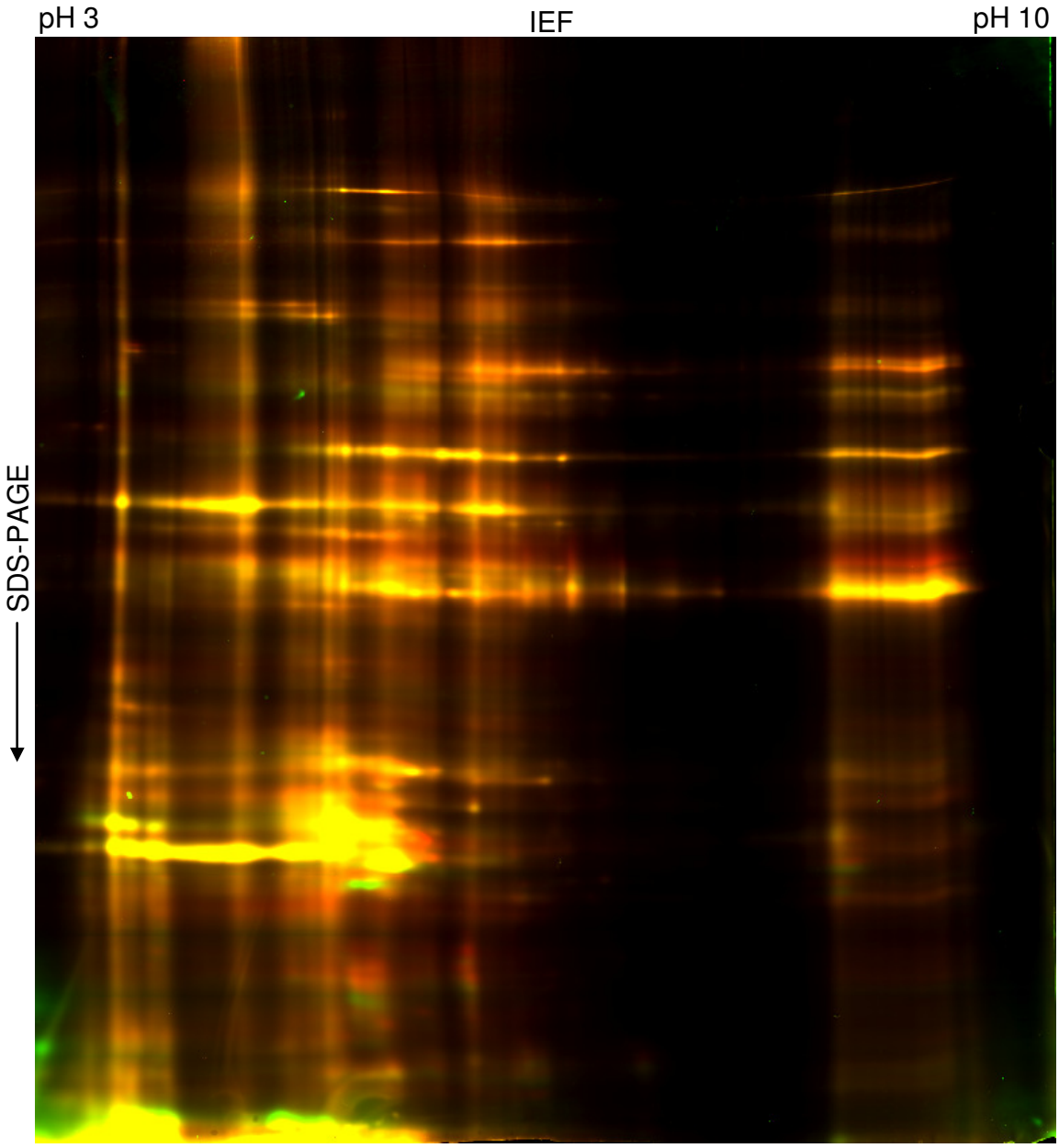

Figure 29: 2D-DIGE of proteins obtained from a fishing experiment using MC-Sepharose® and propranolol (control)-Sepharose® in lysates of PMNL. Red: Cy5 labelled MC fished proteins, green: Cy3 labelled control fished proteins, yellow: overlay of Cy5 and Cy3 labelled proteins.

4.2.4 Betulinic acid

4.2.4.1 Immobilisation of betulinic acid

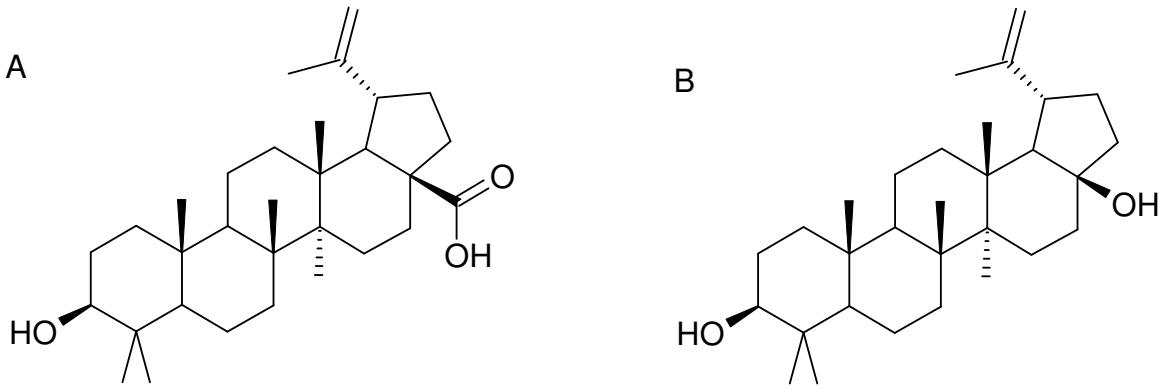

Figure 30: Molecular structure of betulinic acid (A) and lupeol (B)

Betulinic acid (BA) possesses one single hydroxy residue and a carboxylic acid group as possible sites for linking to solid matrices (Fig. 30, 31). Given that the carboxylic group is supposed to be essential for the pharmacological action of BA, the hydroxy residue was chosen for the immobilisation of BA. Since there are no interfering functional groups, BA could be immobilised without derivatisation steps directly to the Toyopearl® AF 650M Epoxy matrix. Knowing that the amount of a specifically bound protein varies in correlation to the amount of immobilised ligand (whereas unspecific bound proteins are always present in the same amount, independent from the amount of immobilised ligand), the binding specificity of a protein can be determined by comparing bead batches with different ligand amounts.

Thus, 1 µmol, 4 µmol and 40 µmol betulinic acid and 4 µmol lupeol (negative control) were dissolved in 100 µl THF respectively. This ligand solution was added to a suspension of 75 mg of epoxy-activated Toyopearl® AF 650M 500 µl THF. The coupling reaction was started by addition of 100 µl of 1 M NaOH solution. Additional details of the coupling reaction are described in 3.2.4.1.3.

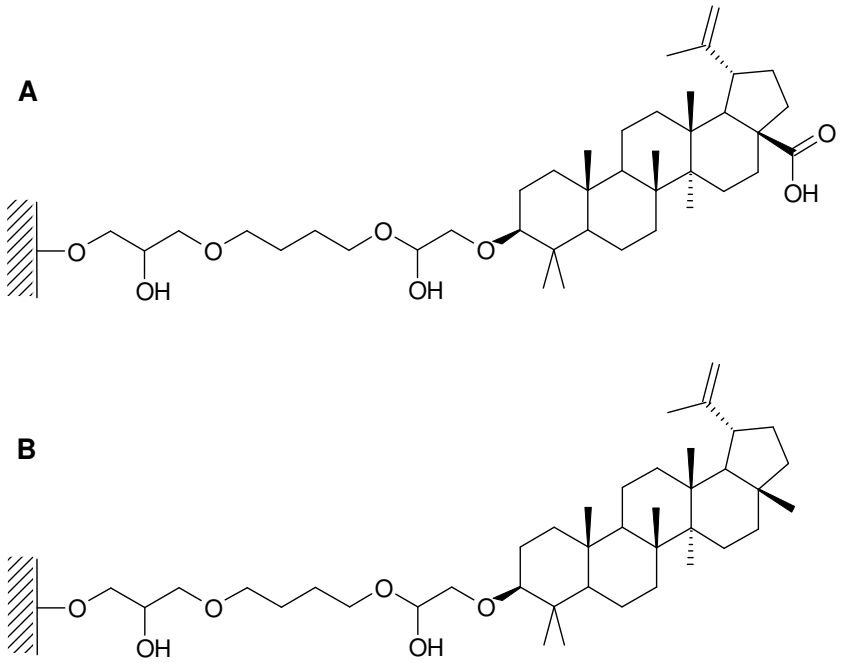

Figure 31: Structure of the BA and lupeol fishing constructs

4.2.4.2 Fishing experiments with BA

Fishing experiments with BA were performed in PMNL lysates in a semi-quantitative manner by relating eluates obtained from beads with different amounts of immobilised BA. Unspecific binding events resulted in bands with similar intensity independent of the amount of immobilised BA. Bands with increasing intensity at higher BA concentrations indicate a selective binding to BA. A double band with a size of about 25 kDa was specifically detected in the BA samples and not in the lupeol control and showed an increasing binding pattern in correlation to the increasing amounts of immobilised BA (Fig. 32). The lower, stronger band was identified via MS analytics as cathepsin G (CG) whereas the higher but weaker band as proteinase 3 (PR3) (Tab. 11).

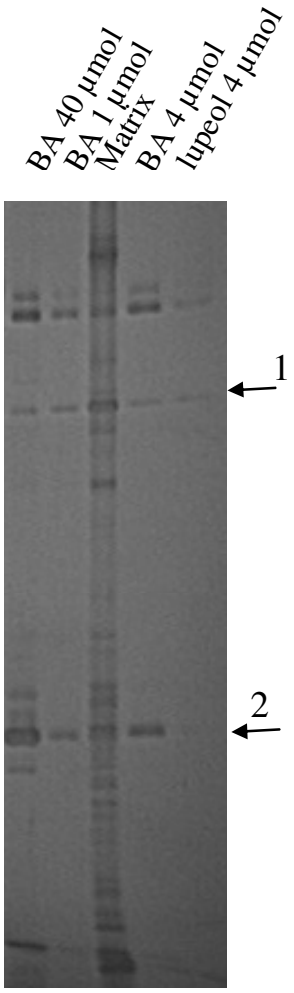

Figure 32: SDS-PAGE of proteins fished with a BA-affinity matrix from PMNL cell lysate and lupeol-matrix as control. Fishing was performed with beads coupled to different amounts of BA. Unspecific protein binding leads to bands with similar intensity (1) whereas the band intensity rises with higher amounts of immobilised BA for specific binding events (2).

	Protein origin	**Sequence**	**Score**
Spot 1	proteinase 3 (serine proteinase, neutrophil, Wegener granulomatosis autoantigen), isoform	-.MASLQMR.G	40
	proteinase 3 (serine proteinase, neutrophil, Wegener granulomatosis autoantigen), isoform	MASLQMR.G +Oxidation (M)	(40)
	proteinase 3 (serine proteinase, neutrophil, Wegener granulomatosis autoantigen), isoform	R.LVNVVLGAHN VR.T	94
Spot 2	Chain A, Human Cathepsin G	R.QICVGDR.R	14
	Chain A, Human Cathepsin G	R.NVNPVALPR.A	33

Table 11: Mass spectrometric identification of proteins fished with a BA-affinity matrix: Mascot score significance level was 44, spot 1 was identified as proteinase 3 with a mascot score of 134, spot 2 was identified as cathepsin G with a mascot score of 47.

4.2.4.3 Western blot confirmation

Western blot analysis of the eluates confirmed the mass spectrometric results and showed the presence of both proteins, PR3 and CG in the eluates of BA-affinity matrix but not for proteins fished in lupeol-affinity matrix (Fig. 33).

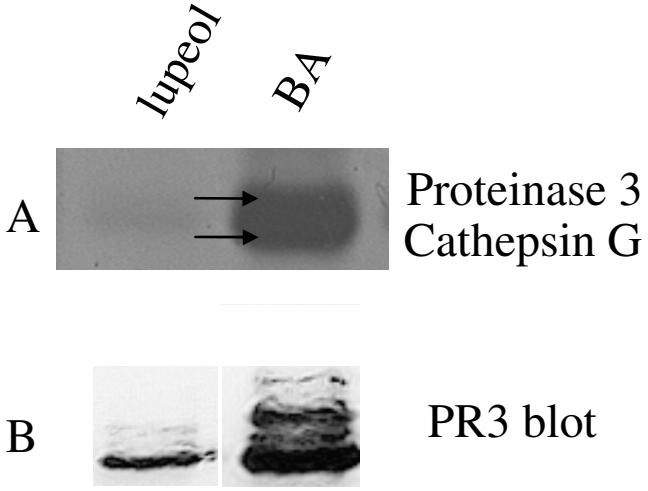

Figure 33: (A): Silver staining of a SDS-PAGE performed with eluates of BA-fished proteins. Arrows indicate spots that were cut out for protein analysis via MS. (B): Western blot experiment for PR3. Western blot data shown are representative of at least three independent experiments.

4.2.4.4 CG and PR3 enzyme activity assay

To investigate the functional effects of the interaction of BA with CG and PR3, enzyme activity assays for CG and PR3 were performed. In these enzyme assays, neither BA nor lupeol showed any functional effect on the enzymatic activity of CG (Fig. 34). For PR3, an inhibitory effect of BA was observed at concentrations ≥ 10 µM, whereas lupeol did not show a significant effect up to 30 µM (Fig. 35).

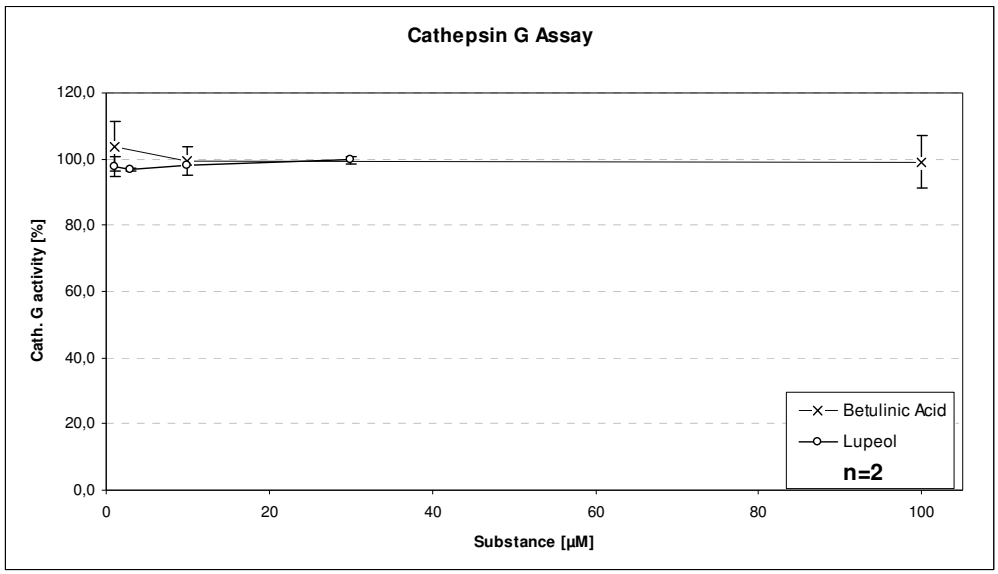

Figure 34: Activity assay for CG activity after BA and lupeol treatment.

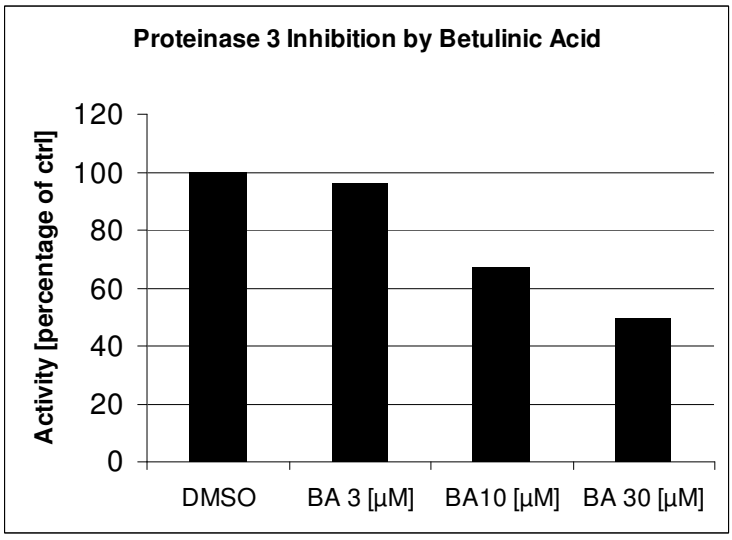

Figure 35: Activity of PR3 after treatment with BA. Data shown are representative of at least three independent experiments.

4.2.5 Resveratrol

4.2.5.1 Derivatisation and immobilisation of Resveratrol

Resveratrol possesses three phenolic hydroxylic residues. Each of them could be used for immobilisation but their similar pKs values and reactivities exclude a selective immobilisation on only one of these three positions. Thus an appropriate derivative had to be synthesised. Since a derivatization on the 4´ position was found to not hinder RV activity on AKT phosphorylation (unpublished data), a carboxy-functionalised butyl linker was inserted at the C4 position (Fig.36B) [VI]. As negative control, phenoxybutyric acid (PBA) was immobilised to partially mimic the synthetic RV derivative (Fig.36C).

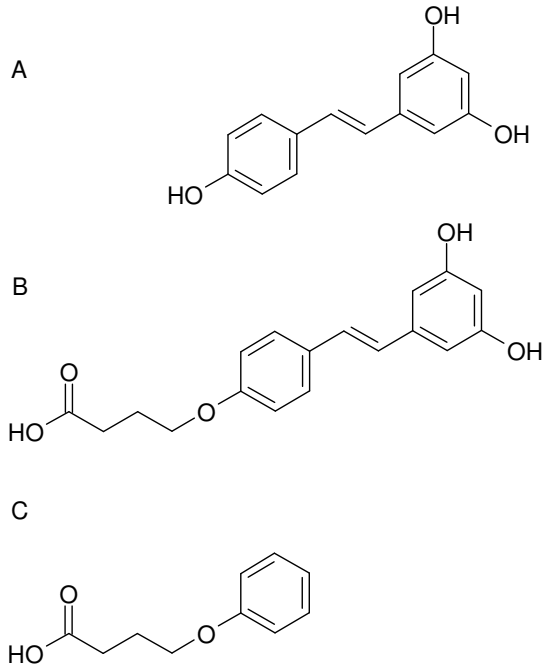

Figure 36: Resveratrol, B: carboxybutyl resveratrol for immobilisation, C: phenoxybutyric acid als control for 4´-*O*-carboxybutyl-resveratrol.

For immobilisation of Resveratrol and PBA (Fig. 37), 16.7 mg Resveratrol and 9.58 mg PBA were dissolved in 1 ml dioxane. 200 µl Toyopearl® AF 650 Amino respectively were washed 2 times with 1 ml water, once with 1 ml dioxane 50% (v/v) and finally two times with 1 ml pure dioxane on a G4 glass filter crucible. The ligand solution, 10 µl 1 N HCl and 20 µl DIC were added to the beads. The reaction was performed for 72 h at

[VI] Synthesis of the Resveratrol derivative (Fig. 36 B) was done by the group of Prof. Dr. T. Erker, Department of Medicinal Chemistry, University of Vienna, Austria

RT on a rotator. Subsequent washing steps were performed as described in 3.2.4 after completed reaction.

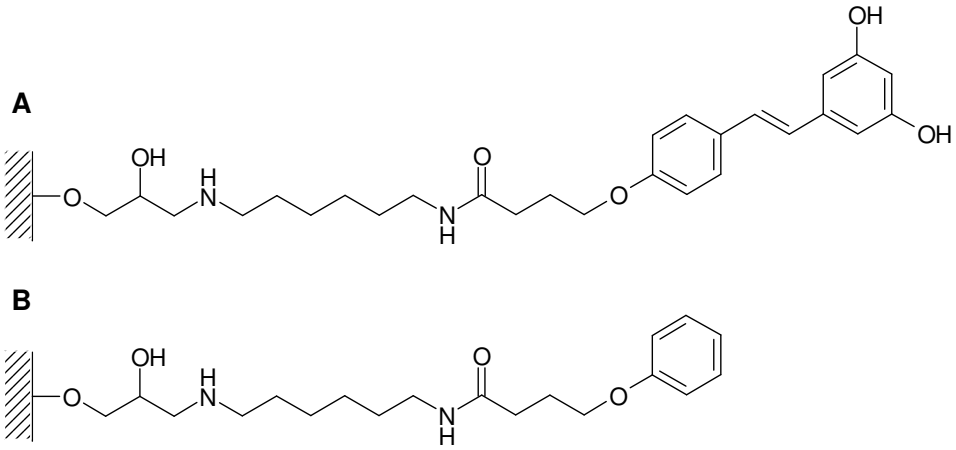

Figure 37: Immobilised resveratrol (A) and phenoxybutyric acid (B) as negative control

4.2.5.2 Target-fishing experiments with RV

Proteins were fished from PBMC lysates with resveratrol and PBA as negative control. After elution with 4 M urea, the released proteins were labelled with Cy3 and Cy5 dye, respectively (see 3.2.6.4). Proteins were separated via isoelectric focussing in the first dimension followed by SDS-PAGE in the second dimension. Spots were detected by scanning the gel with an ETTAN^{TM} DIGE imager with a resolution of 100 µm and an exposure time of 2 sec (Fig. 38).

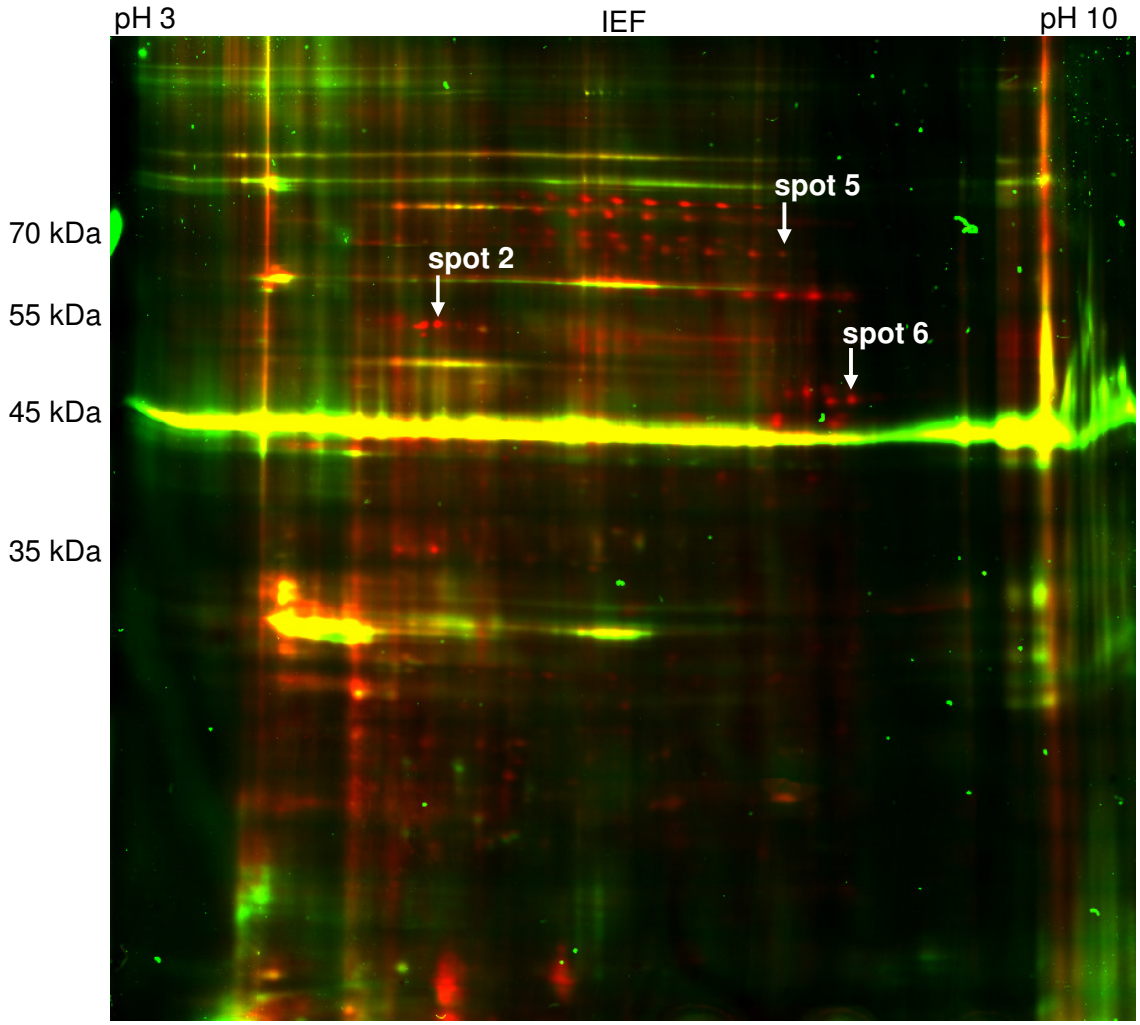

Figure 38: 2D-DIGE of resveratrol-fished proteins from PBMC lysates. Red: Cy5 labelled proteins fished by resveratrol, green: Cy3 labelled proteins fished by PBA, yellow: overlay of Cy5 and Cy3 labelled proteins. Marked spots were picked for identification via MS analytics.

The gel image was analysed with DeCyder™ 7 software to selectively detect RV-fished proteins (Fig. 39).

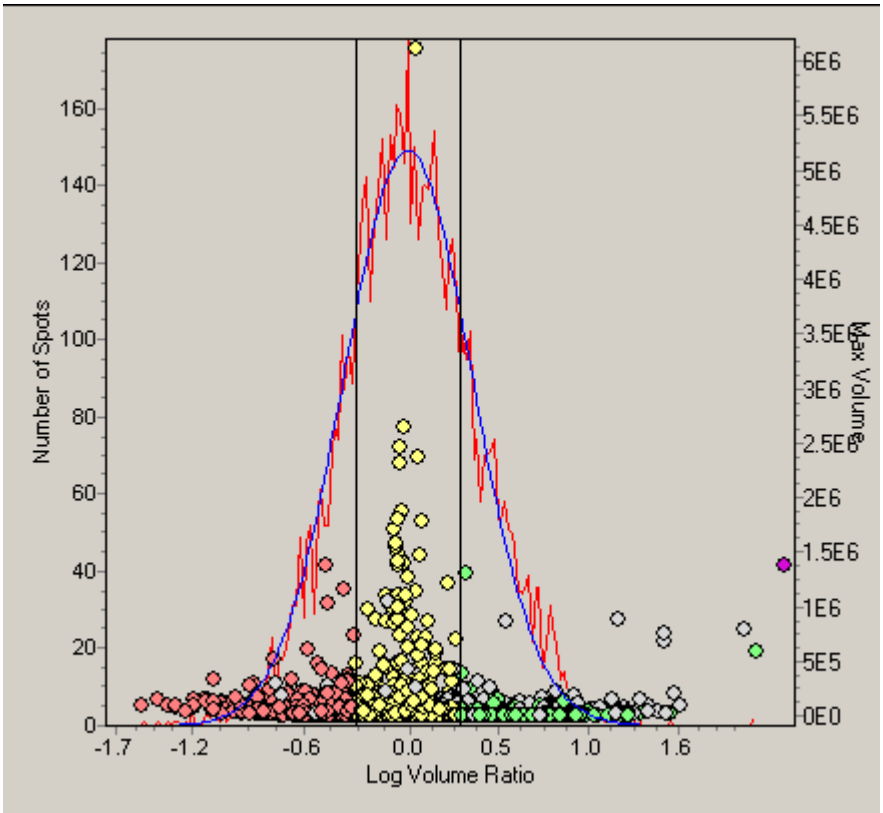

Figure 39: Evaluation of the protein distribution of RV fished proteins. 7473 spots could be detected on the gel. 454 spots were excluded due to their high slope indicating artificial spots (colourless). 4087 spots were detected in the same amount in the RV fishing eluate and the control eluate (yellow). 1589 spots were detected as selectively fished with RV (red) and 1343 proteins were present in the control but not in the RV sample (green).

For picking differentially fished proteins, the proteins were visualised by silver staining. In the DIGE gel, the differential pattern of selectively fished proteins showed protein sets with the same size differing in their IEP. Since this indicates that these sets consist of the same protein but different ionic forms (e.g., due to differential phosphorylation), only one spot out of each set was picked for MS analysis.

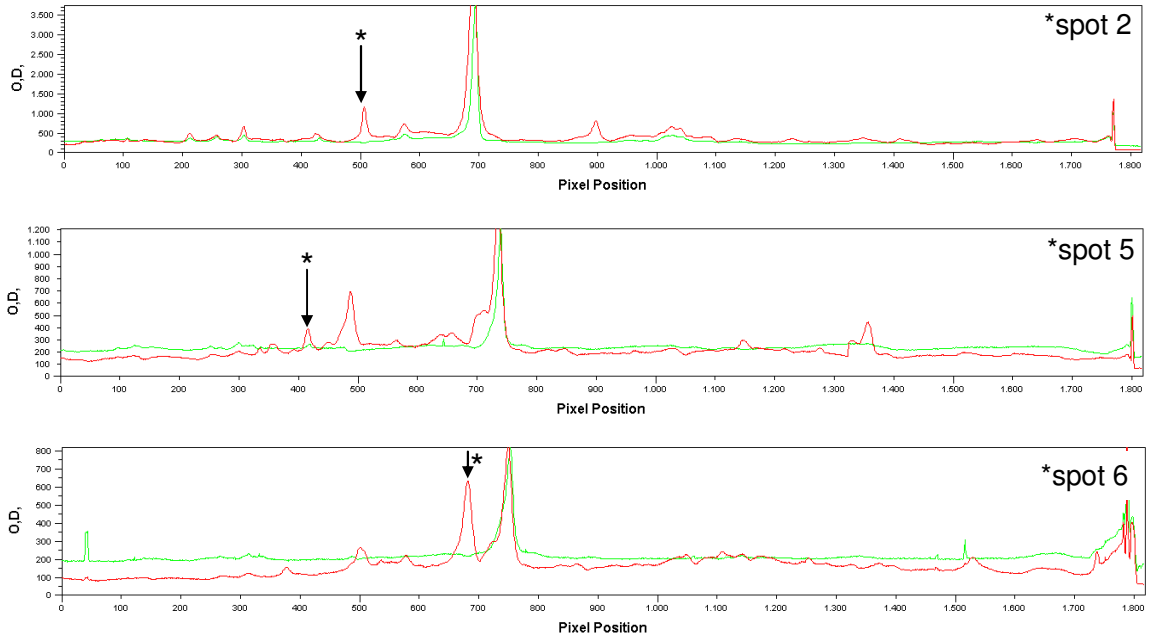

Figure 40: Intensity profile of the DIGE experiment with PBMC cell lysate. Indicated spots are marked with an arrow.

The fluorometric comparison of RV- and PBA-fished proteins from the DIGE gel clearly showed a higher presence of proteins fished by RV at spot number 2, 5 and 6 as compared to respective proteins fished by PBA (Fig. 40).

	Resveratrol fished	**PBA (control) fished**
Spot 2 Volume ratio: 1226% RV. Vol.: 132843 Ctrl. Vol.: 7695	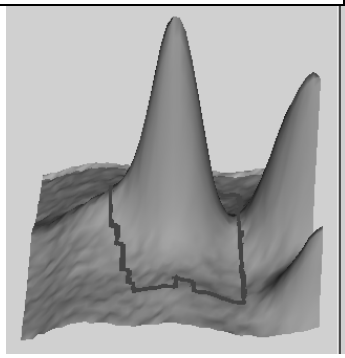	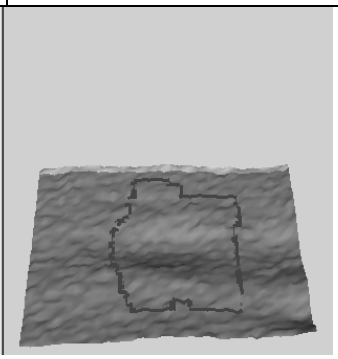
Spot 5 Volume ratio: 366% RV. Vol.: 49067 Ctrl. Vol.: 9534	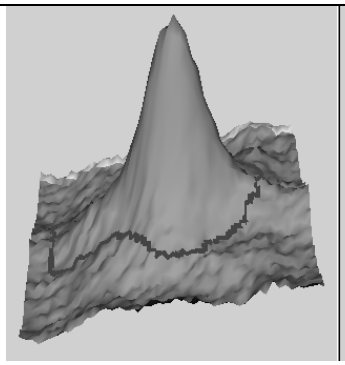	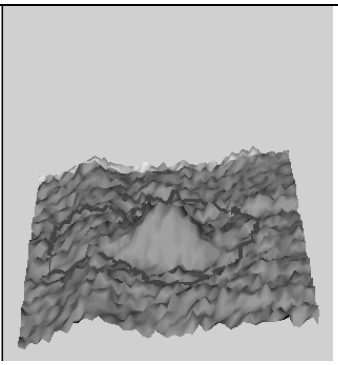
Spot 6 Volume ratio: 1459% RV. Vol.: 149962 Ctrl. Vol.: 7301	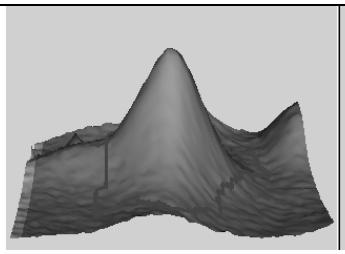	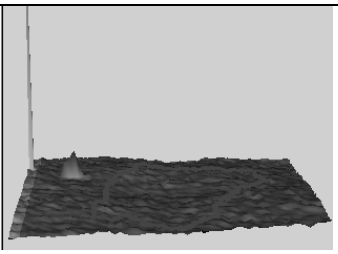

Table 12: 3D single spot evaluation and spot volume calculation of the DIGE experiment.

Exact determination of the spot volumes show that the protein at the analysed spots are present in a RV/control volume ration of 1226 in spot 2, 366 in spot 5 and 1459 in spot 6. The 3 dimensional visualisation of the spot volume clearly shows the presence of these proteins in the RV fishing as well as the absence in the appropriate negative control (Tab. 12).

	Protein origin	Sequence	Score
Spot 2	KHSRP KH-type splicing regulatory protein	IINDLLQSLR	63
	KHSRP KH-type splicing regulatory protein	AWEEYYK	46
	KHSRP KH-type splicing regulatory protein	IGGGIDVPVPR	45
	FUBP1 Isoform 1 of Far upstream element-binding protein 1	IGGNEGIDVPIPR	67
	FUBP1 Isoform 1 of Far upstream element-binding protein 1	IQIAPDSGGLPER	68
	FUBP1 Isoform 1 of Far upstream element-binding protein 1	LLDQIVEK	55
	FUBP1 Isoform 1 of Far upstream element-binding protein 1	GTPQQIDYAR	46
	FUBP1 Isoform 1 of Far upstream element-binding protein 1	IAQITGPPDR	44
Spot 5	KHSRP KH-type splicing regulatory protein	IGGGIDVPVPR	71
	KHSRP KH-type splicing regulatory protein	IIGDPYK	55
	KHSRP KH-type splicing regulatory protein	IINDLLQSLR	58
	KHSRP KH-type splicing regulatory protein	VQISPDSGGLPER	65
	KHSRP KH-type splicing regulatory protein	AWEEYYK	43
	KHSRP KH-type splicing regulatory protein	DAFADAVQR	47
Spot 6	KHSRP KH-type splicing regulatory protein	IGGGIDVPVPR	71
	KHSRP KH-type splicing regulatory protein	IINDLLQSLR	68
	KHSRP KH-type splicing regulatory protein	MMLDDIVSR	61
	KHSRP KH-type splicing regulatory protein	VQISPDSGGLPER	63
	KHSRP KH-type splicing regulatory protein	DAFADAVQR	47

Table 13: Peptides detected via MS analytics and corresponding mascot search results

For all three spots the KH-type splicing regulatory protein (KHSRP) was identified via mass spectroscopy (Tab. 13).

4.2.5.3 Western blot confirmation

The fishing experiment was repeated under the same conditions as for the DIGE gel analysis to confirm the MS results by immunological methods. Thus, a Western blot analysis was performed with the fishing eluates of RV and the corresponding PBA control.

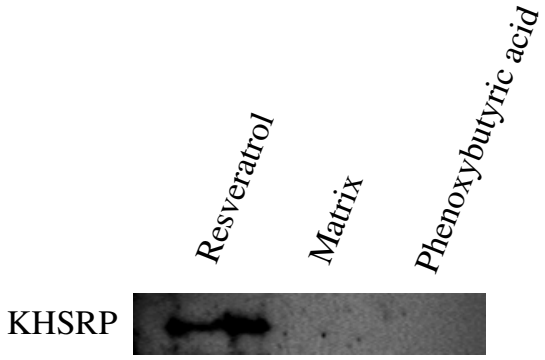

Figure 41: Western blot analysis of KHSRP in eluates from RV-fished proteins, PBA-fished proteins and the matrix-fished proteins. Data shown are representative of at least three independent experiments.

The detection of KHSRP by Western blot analysis clearly shows the presence of KHSRP in the fishing eluate of the RV fishing construct, but neither in eluates of the PBA construct nor the matrix itself (Fig. 41).

4.2.6 Testosterone / Progesterone

4.2.6.1 Immobilisation of Testosterone and Progesterone

For a successful immobilisation, testosterone and progesterone had to be derivatised. Altogether, three different derivatives were synthesised[VII] and subsequently immobilised. These derivatives are: i) progesterone and testosterone with a carboxymethoxylamine function on the C3 position; ii) progesterone and testosterone with a pentanoic acid function on the C7 position; iii) testosterone derivative with a hydroxyl activated polyethylenglycol linker on the C17 position (see Fig. 43).

[VII] Synthesis of all steroid derivatives was done in cooperation by dipl. chem. M. Golkowski and the group of Prof. Dr. T. Ziegler, Institute of Organic Chemistry, University Tübingen

4.2.6.2 Immobilisation of the C3 derivatised testosterone and progesterone

2 × 3.3 ml Toyopearl® AF 650M Amino were washed as described in 3.2.4. 375 mg progesterone carboxymethoxylamine and 360 mg testosterone carboxymethoxylamine were dissolved in 2 ml dioxane. After addition of 350 µl DIC and 10 µl HCl (1 N) the reaction was performed for 72 h at RT on a rotator. After the reaction was completed, washing steps were performed according to 3.2.4.
Carboxymethoxylamin derivatised testosterone and progesterone were coupled to EAH Sepharose® 4B under the same conditions using only a tenth of ligand as for immobilisation on Toyopearl® AF 650M Amino.

4.2.6.3 Immobilisation of the C17 derivatised testosterone and progesterone

The testosterone and progesterone derivatives with a hydroxyl-activated polyethylenglycol linker on C7 were immobilised on Epoxy-activated Sepharose® 6B beads using standard conditions (see 3.2.4.1.3).

4.2.6.4 C7 derivatised testosterone and progesterone

The testosterone and progesterone derivatives with a pentanoic acid function on C7 were immobilised on Toyopearl® AF 650M Amino beads using standard conditions (see 3.2.4).

Steroids with a partially unsaturated A-ring show fluorescence at 366 nm after treatment with ethanolic sulfuric acid which was used to detect successful immobilisation of steroid derivatives (see Fig. 42).

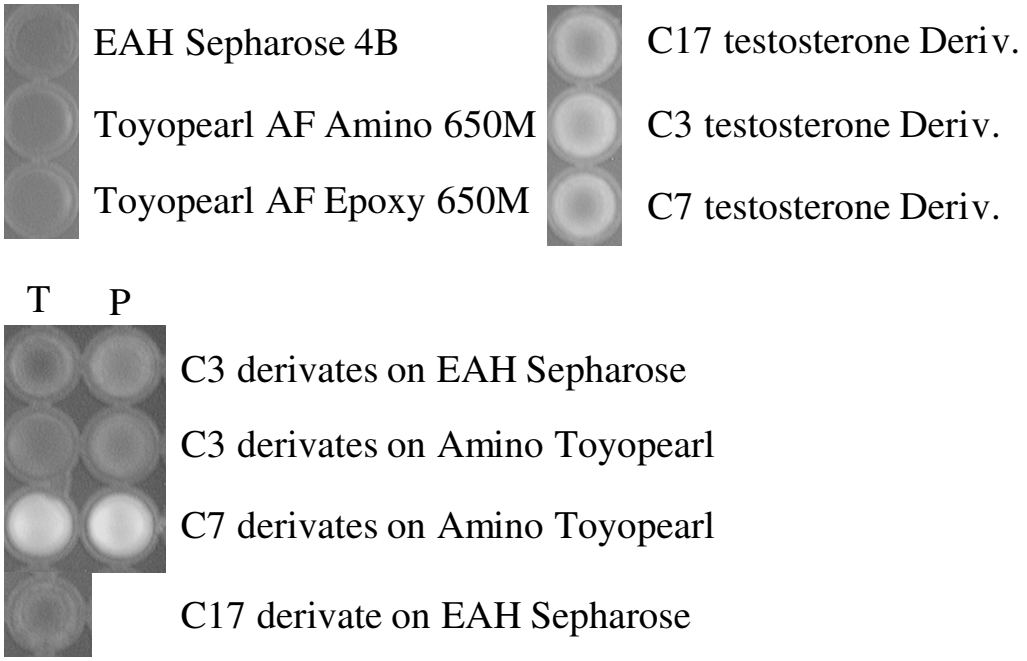

Figure 42: Fluorescence analytics of immobilised testosterone derivatives

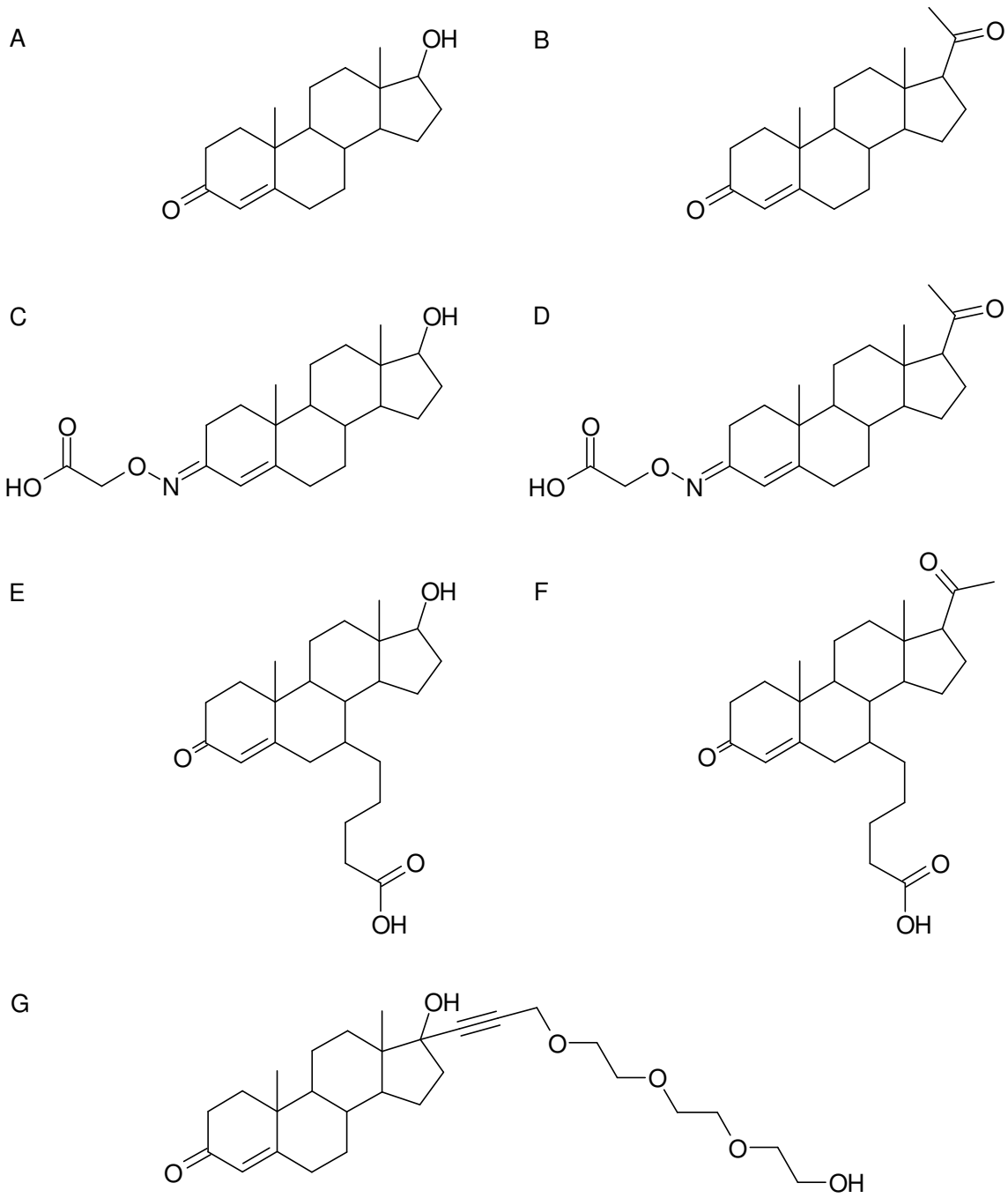

Figure 43: Testosterone (A), progesterone (B) and their derivatised forms used for immobilisation: testosterone carboxymethoxylamin (C), progesterone carboxymethoxylamine (D), C7 pentanoic acid testosterone (E), C7 pentanoic acid progesterone (F) and C17 ethinyl-polyglycol derivatised testosterone.

4.2.6.5 Target-fishing in PMNL cell lysates using C3- and C17-derivatised testosterone

The fishing experiment was performed as described in chapter 3.2 using PMNL cell lysate as protein source. To avoid problems regarding different protein amounts due to experimental inaccuracies, the fishing experiment with testosterone beads was performed with only 60% and 30% of the protein concentration of the control samples. Since these experimental inaccuracies are by far smaller than 30% or 60%, differences in the band intensity are caused by different affinities to the ligands.

The samples were eluted with SDS buffer (see 3.2.5.3) and separated via SDS-PAGE. Detection by silver staining showed one band with 69 kDa and one with approximately 95 kDa, both present in the eluate of C3-testosterone but missing in both, the C17 and the EAH-Sepharose® eluates. Since these bands were visible also in eluates from fishing approaches conducted only with 60% and 30% protein amount, they were a clear result for proteins with a higher affinity to C3 testosterone than to C17 testosterone (Fig. 44). Indicated bands were picked out and analysed by MS as described (3.2.6.6).

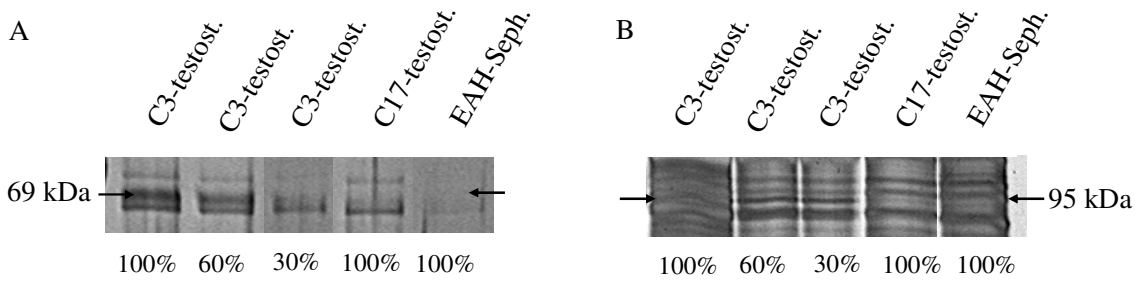

Figure 44: (A) SDS-PAGE of proteins fished with C3- and C17-derivatised testosterone in PMNL cell lysates visualised by silver staining. (B): SDS-PAGE of carboxymethoxylamine fished proteins from PMNL cell lysates visualised via silver staining

Protein name	**Serum albumin** [***homo sapiens***]	**Karyopherin beta 1** [***homo sapiens***]
MW [kDa]	69.3	97.1
Sequence coverage [%]	19	5
Mascot score	670	165
No. of matched peptides	15	5
Significance threshold mascot score >39		

Table 14: Peptide sequences derived from the indicated spots after tryptic digest and MS analytics and corresponding mascot search results

The sequenced protein at 69 kDa was identified as human serum albumin (Tab. 14). Since this is a protein that is known to bind steroids [143], it implies that the testosterone derivative immobilised via C3 exhibits the structural properties required for binding to/fishing of known interacting proteins. Instead, it was not possible to fish a known interacting protein with the testosterone derivative linked on C17, indicating that this derivative might not exhibit the biochemical functionality of testosterone.

The 95 kDa protein was identified as karyopherin β (KPN-β) (Tab. 14) by MS analytics. Since this protein is an interesting target candidate, Western blot analysis using a KPN-β antibody was performed to validate the results of the MS analytics. In addition to the upper experiment immobilised progesterone was used as control.

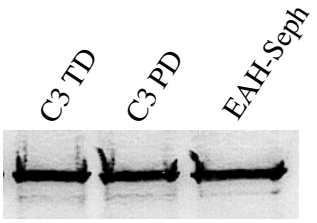

Figure 45: KPN-β Western blot analysis of testosterone (C3 TD) and progesterone (C3 PD) fished proteins. Data shown are representative of at least three independent experiments.

In contrast to the SDS-PAGE developed with silver staining, Western blot analysis of the fishing eluates showed same intensities of the bands for testosterone and the matrix without any derivatisation (Fig. 45). In addition, in a sample of progesterone-fished proteins, where progesterone was immobilised in the same way as testosterone, the same intensity of the KPN-β band was detected. Since KPN-β turned out to bind to the Sepha-

rose® surface itself, a selective testosterone-KPN-β interaction could not be confirmed and is conseqently excluded.

4.2.6.6 2D-DIGE analysis of testosterone and progesterone fished proteins

Fishing experiments for subsequent DIGE analysis were performed with C3-derivatised testosterone and progesterone coupled to Toyopearl® AF 650M Amino. For comprehensive fishing results, the fishing- and DIGE experiments were performed separately with lysates of PMNL, PBMC and platelets.

4.2.6.7 Testosterone and progesterone fishing in PMNL cell lysates

Fishing experiments were performed as described in 3.2.5. Proteins were eluted using 4 M urea and subsequently labelled with appropriate fluorophoric groups (CyDye™-fluor labelling, see 3.2.6). 2D electrophoresis was performed and proteins on the 2D gel were visualised by scanning the gel with the ETTAN™ DIGE scanner (see 3.2.6) (Fig. 46). The spot pattern of the gel was evaluated using the ImageQuant™ TL software to identify differentially fished proteins. Detailed evaluation of the differentially fished protein spots was executed with the DeCyder™ software.

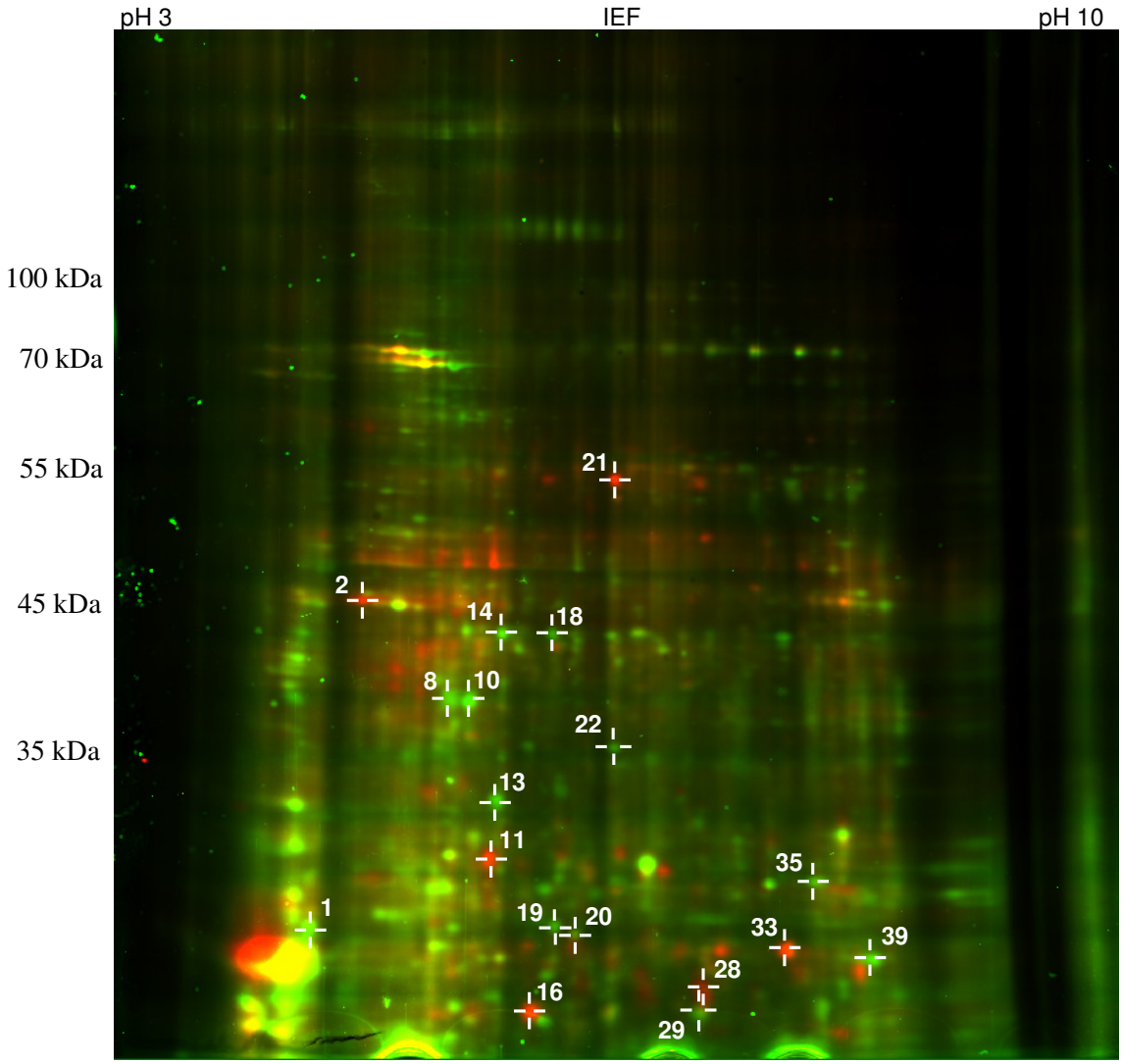

Figure 46: 2D-DIGE of testosterone and progesterone fished proteins from PMNL cell lysate. Red: Cy5 labelled proteins fished by testosterone, green: Cy3 labelled proteins fished by progesterone, yellow: overlay of Cy5 and Cy3 labelled proteins. Marked spots showed a prominent difference of protein amount in the compared samples.

The 39 spots with the most prominent difference between the testosterone and progesterone sample were analysed in detail (Fig. 48, 49). Due to the fact that the detection via CyDye™ labelling is up to 500 fold more sensitive than silver staining, only 18 of these 39 spots could be recovered in the silver stained 2D gel. Since spots that are not visible after a silver staining can not be picked for MS analytics, spot selection and evaluation focussed on the 18 spots that were visualised by silver staining (Fig. 47).

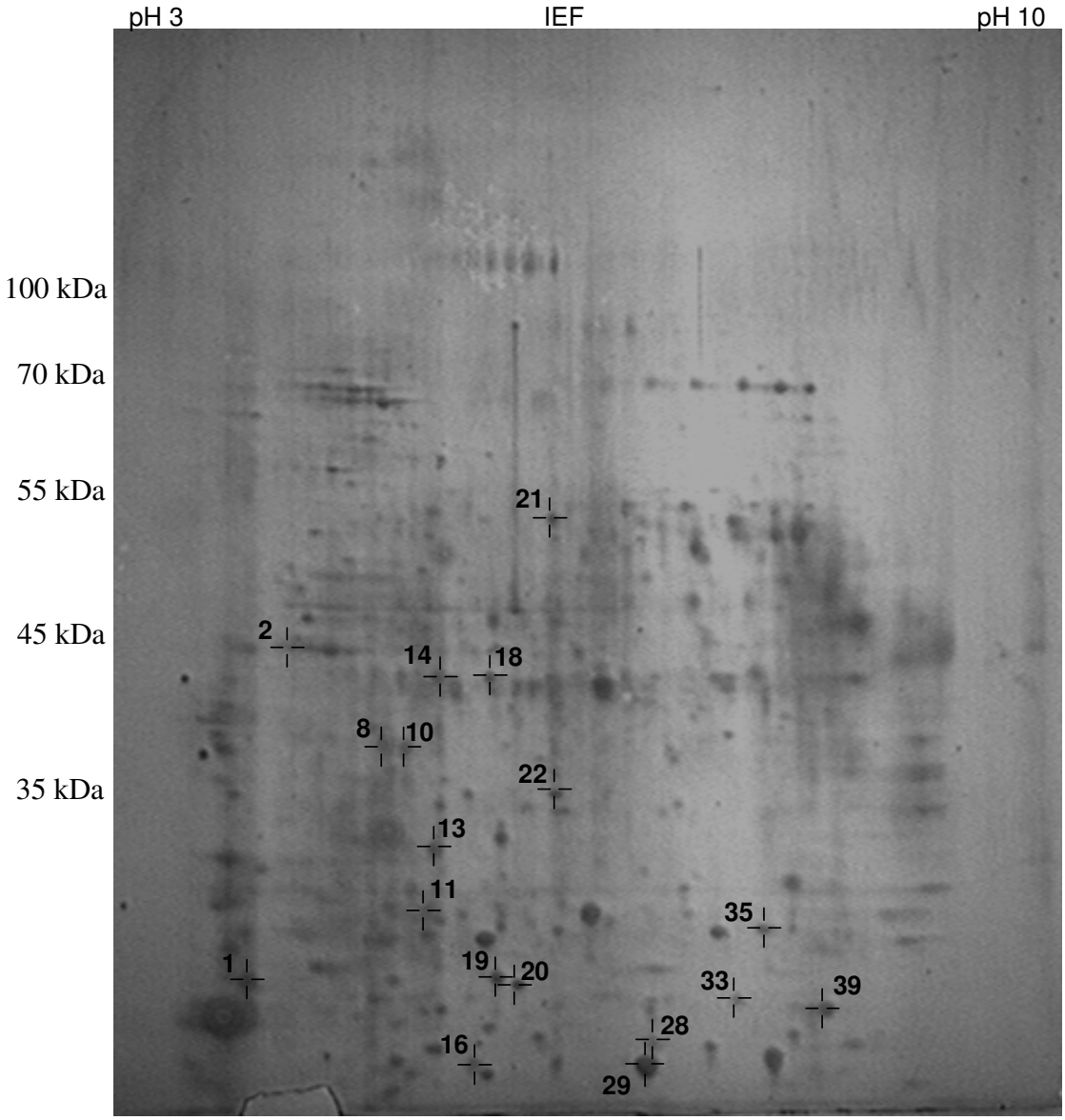

Figure 47: Silver staining of the 2D-DIGE gel of figure 46; testosterone and progesterone fished proteins from PMNL cell lysate. Marked spots were picked for identification via MS analytics.

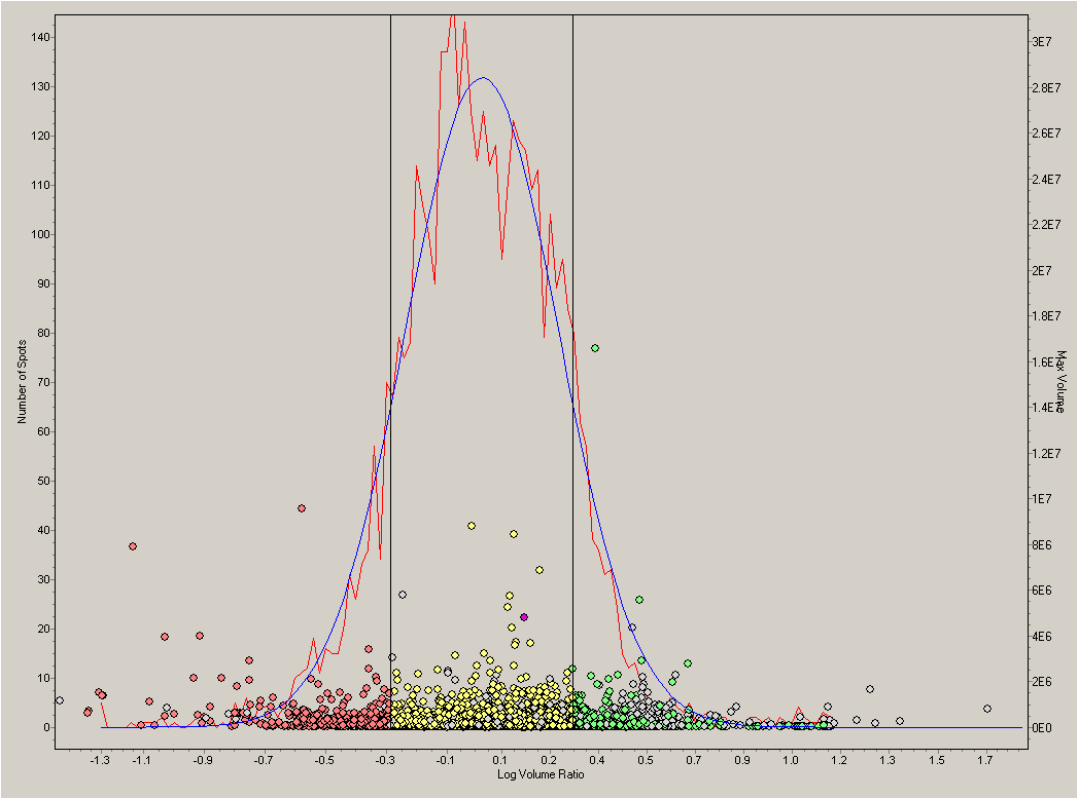

Figure 48: Spot distribution histogram of the testosterone DIGE experiment with PMNL cells. 4767 spots were detected on the gel whereas 576 spots (colourless) were recognised as artificial spots due to their high slope and therefore are not included in following calculation steps. From the remaining 4191 spots 3245 (77.4%) spots were recognised to show no differences within a threshold of 200% (yellow). 455 (10.9%) spots were recognised to be present in at least two fold amount in the progesterone eluate (green) whereas 491 (11.7%) spots showed this in the testosterone sample (red).

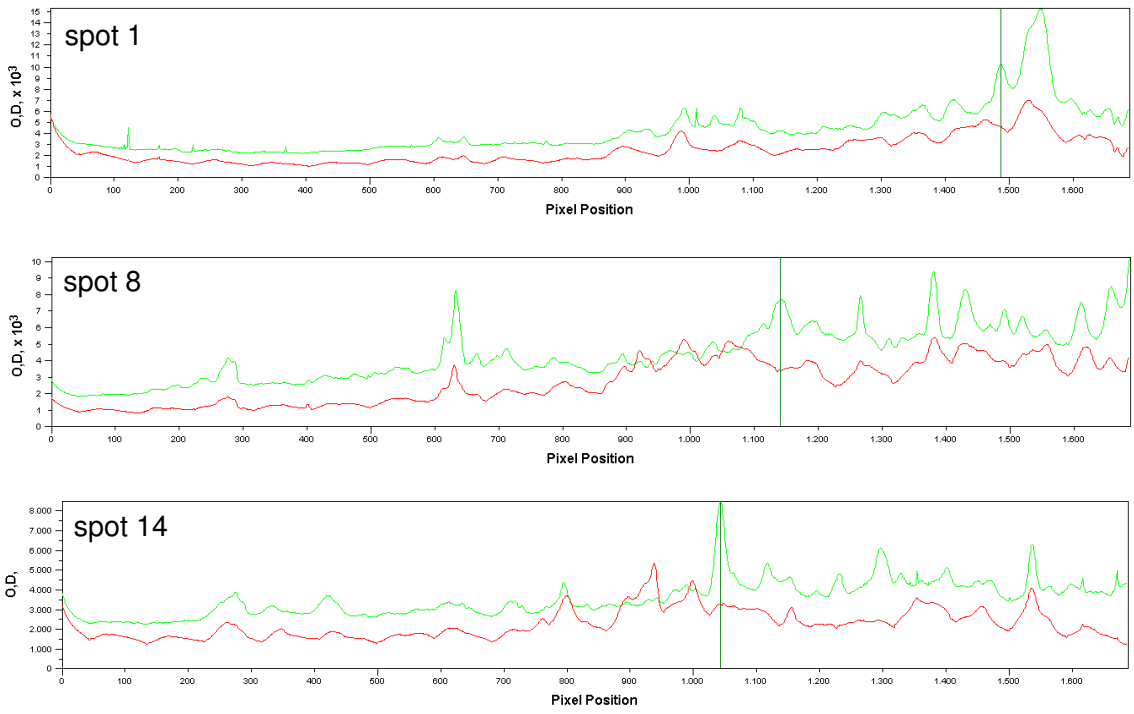

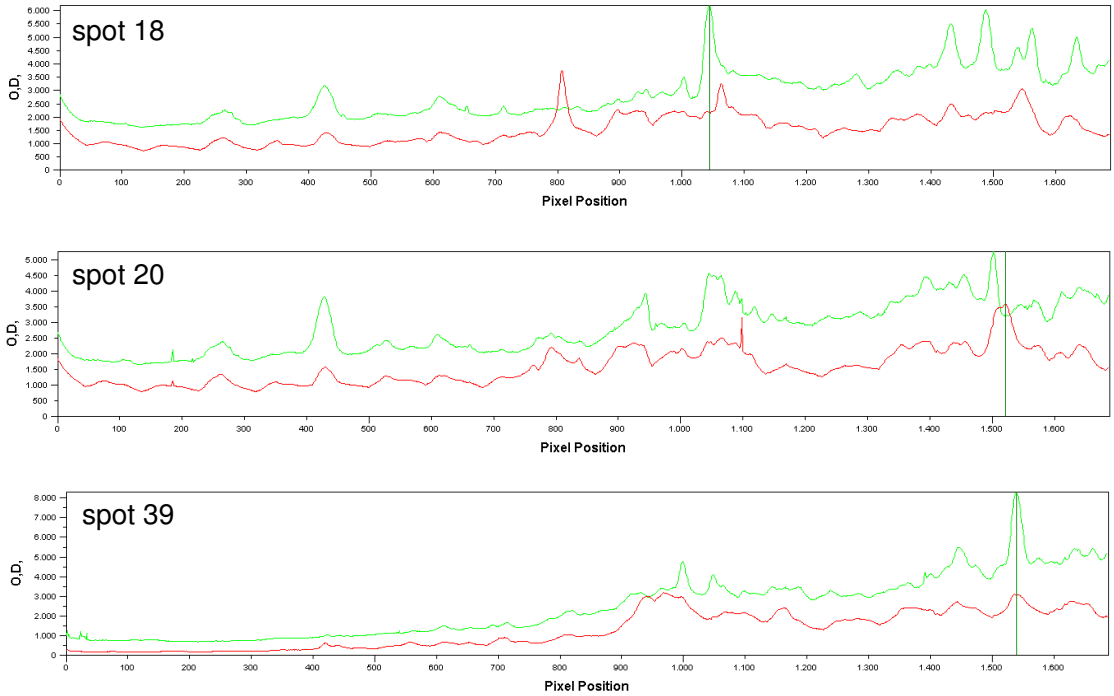

Figure 49: Intensity profile of the DIGE experiment in PMNL. Green profile: Cy3 labelled, progesterone fished proteins. Red profile: Cy5 labelled, testosterone fished proteins. Indicated spots are marked with a vertical green line.

For detailed quantitative analytics of the single spots, the peak volumes as well as the volume ratio of corresponding spots were calculated (Tab. 15).

Spot values	**Testosterone fished**	**Progesterone fished**
Spot No.1: Volume ratio: 102% Test. Vol.: 2365867 Prog. Vol.: 3217799	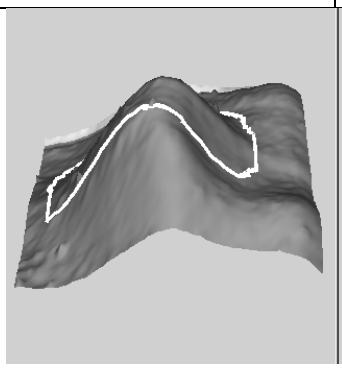	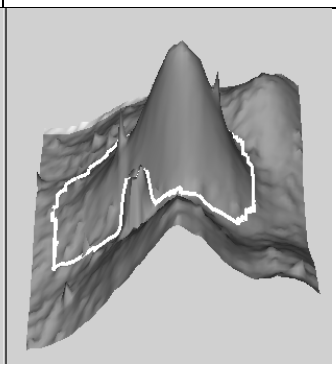
Spot No.8: Volume ratio: 338% Test. Vol.: 636806 Prog. Vol.: 2881478	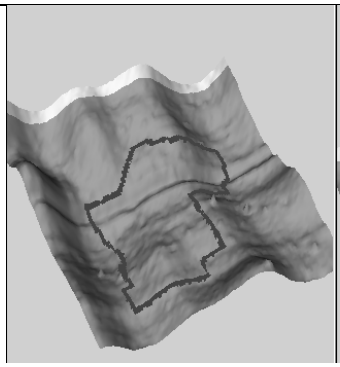	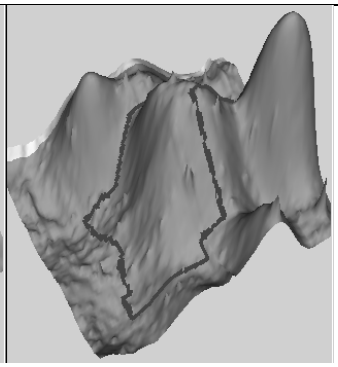
Spot No.14: Volume ratio: 241% Test. Vol.: 579498 Prog. Vol.: 187057	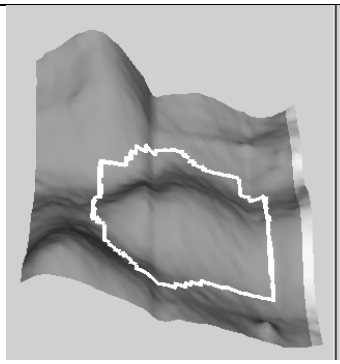	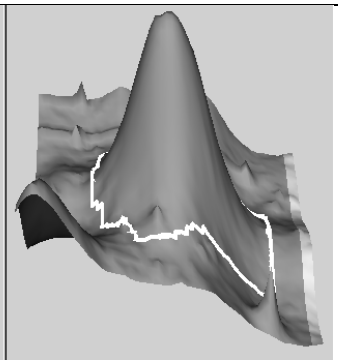

	Testosterone fished	**Progesterone fished**
Spot No.18: Volume ratio: 324% Test. Vol.: 312803 Prog. Vol.: 1356441	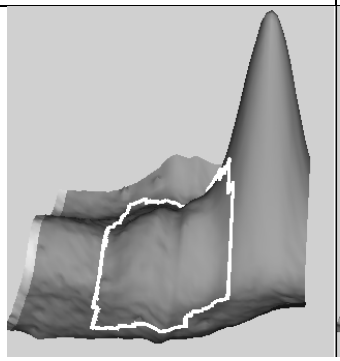	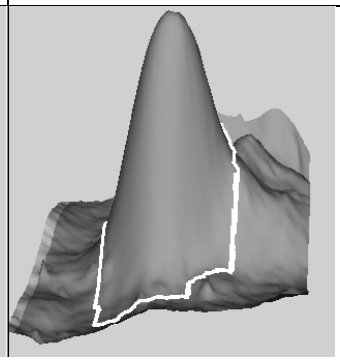
Spot No.20: Volume ratio: 655% Test. Vol.: 601186 Prog. Vol.: 122700	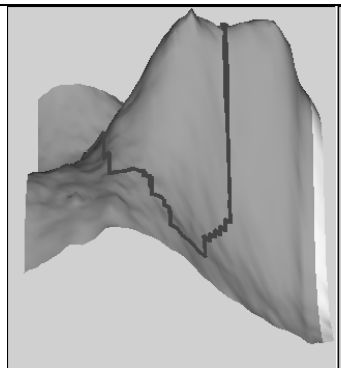	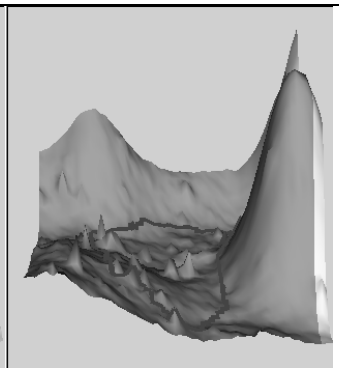
Spot No.39: Volume ratio: 264% Test. Vol.: 437713 Prog. Vol.: 1547362	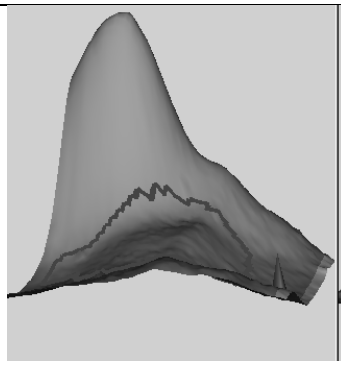	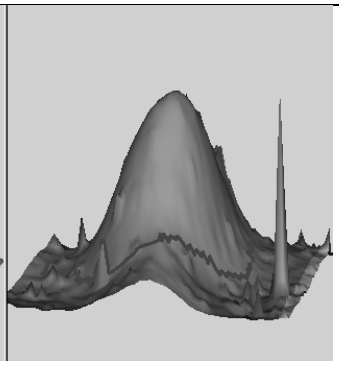

Table 15: 3D single spot evaluation and spot volume calculation of the DIGE experiment.

MS analytics of the indicated spots and following mascot evaluation of the measured peptides led to following results (Tab. 16).

Vimentin was identified in spot 1 with a low mascot score and in spot 8 and 10 with high mascot scores. ***Serpin B1*** was identified for spots14 and 18, ***HSP B1*** for spot 20 and ***NAMPT*** for spot 39. The remaining spots had low scores or contradictory results for single peptide sequences. Spots detected as keratin were not considered since the protein amount was to low to detect the actual protein besides keratin contaminations.

	Protein origin	**sequence**	**score**
Spot 1	VIM Vimentin	FADLSEAANR	54
	VIM Vimentin	QDVDNASLAR	48
	ACTB Actin, cytoplasmic 1	DLTDYLMK	46
	ACTB Actin, cytoplasmic 1	DSYVGDEAQSK	61
	ACTB Actin, cytoplasmic 1	GYSFTTTAER	46
	PML Isoform PML-1 of Probable transcription factor PML	CDISAEIQQR	48
	PML Isoform PML-1 of Probable transcription factor PML	TGSALVQR	52
	PML Isoform PML-1 of Probable transcription factor PML	LDAVLQR	41
Spot 8	VIM Vimentin	QDVDNASLAR	85
	VIM Vimentin	QVDQLTNDK	57
	VIM Vimentin	FADLSEAANR	40
	VIM Vimentin	QQYESVAAK	37
Spot 10	VIM Vimentin	FADLSEAANR	54
	VIM Vimentin	QDVDNASLAR	68
	VIM Vimentin	QQYESVAAK	40
	VIM Vimentin	QVDQLTNDK	38
Spot 14	SERPINB1 Leukocyte elastase inhibitor	IEEQLTLEK	66
	SERPINB1 Leukocyte elastase inhibitor	LGVQDLFNSSK	46
	SERPINB1 Leukocyte elastase inhibitor	ADLSGMSGAR	41
	SERPINB1 Leukocyte elastase inhibitor	KIEEQLTLEK	43
	SERPINB1 Leukocyte elastase inhibitor	TINQWVK	35
Spot 18	SERPINB1 Leukocyte elastase inhibitor	FQSLNADINK	48
	SERPINB1 Leukocyte elastase inhibitor	IEEQLTLEK	62
	SERPINB1 Leukocyte elastase inhibitor	KIEEQLTLEK	75
	SERPINB1 Leukocyte elastase inhibitor	LGVQDLFNSSK	47
	SERPINB1 Leukocyte elastase inhibitor	ADLSGMSGAR	36
Spot 20	HSPB1 Heat shock protein beta-1	AQLGGPEAAK	57
	HSPB1 Heat shock protein beta-1	DGVVEITGK	47
	HSPB1 Heat shock protein beta-1	QDEHGYISR	60
	HSPB1 Heat shock protein beta-1	QLSSGVSEIR	59
	HSPB1 Heat shock protein beta-1	TKDGVVEITGK	70
Spot 39	NAMPT Isoform 1 of Nicotinamide phospho-ribosyltransferase	DLLNCSFK	46
	NAMPT Isoform 1 of Nicotinamide phospho-ribosyltransferase	KFPVTENSK	56
	NAMPT Isoform 1 of Nicotinamide phospho-ribosyltransferase	TPAGNFVTLEEGK	69
	NAMPT Isoform 1 of Nicotinamide phospho-ribosyltransferase	NAQLNIELEAAHH	39
	NAMPT Isoform 1 of Nicotinamide phospho-ribosyltransferase	SYSFDEIR	39

Table 16: Peptide sequences derived from the indicated spots after tryptic digest and MS analytics and corresponding mascot search results.

Spots that are not described in table 16 either (i) could not be referred to a certain protein with an adequate score value, (ii) resulted in a identification of a unknown or hypothetical protein or (iii) were identified as keratin or actin which are known to be possible contaminations in 2D-DIGE or MS approaches.

4.2.6.8 Testosterone and progesterone fishing in PBMC cell lysates

Fishing experiments and 2D-DIGE analysis were performed as described above (3.2.5 and 3.2.6) using PBMC cell lysate as protein source. The high concentration of actin on a 2D-gel analysed by ETTAN^{TM} DIGE led to a smeary band at 45 kDa (Fig. 58). This high actin concentration caused an insufficient focussing in the first dimension and poor resolution of proteins with a higher molecular weight than actin in the second dimension. Thus, no clearly separated spots could be seen in the upper part of the gel. The poor resolution in combination with the lower sensitivity of the subsequent silver staining finally resulted in only five differentially fished spots with suitable protein amounts for subsequent MS analytics (Tbl. 20, Fig. 59, 60).

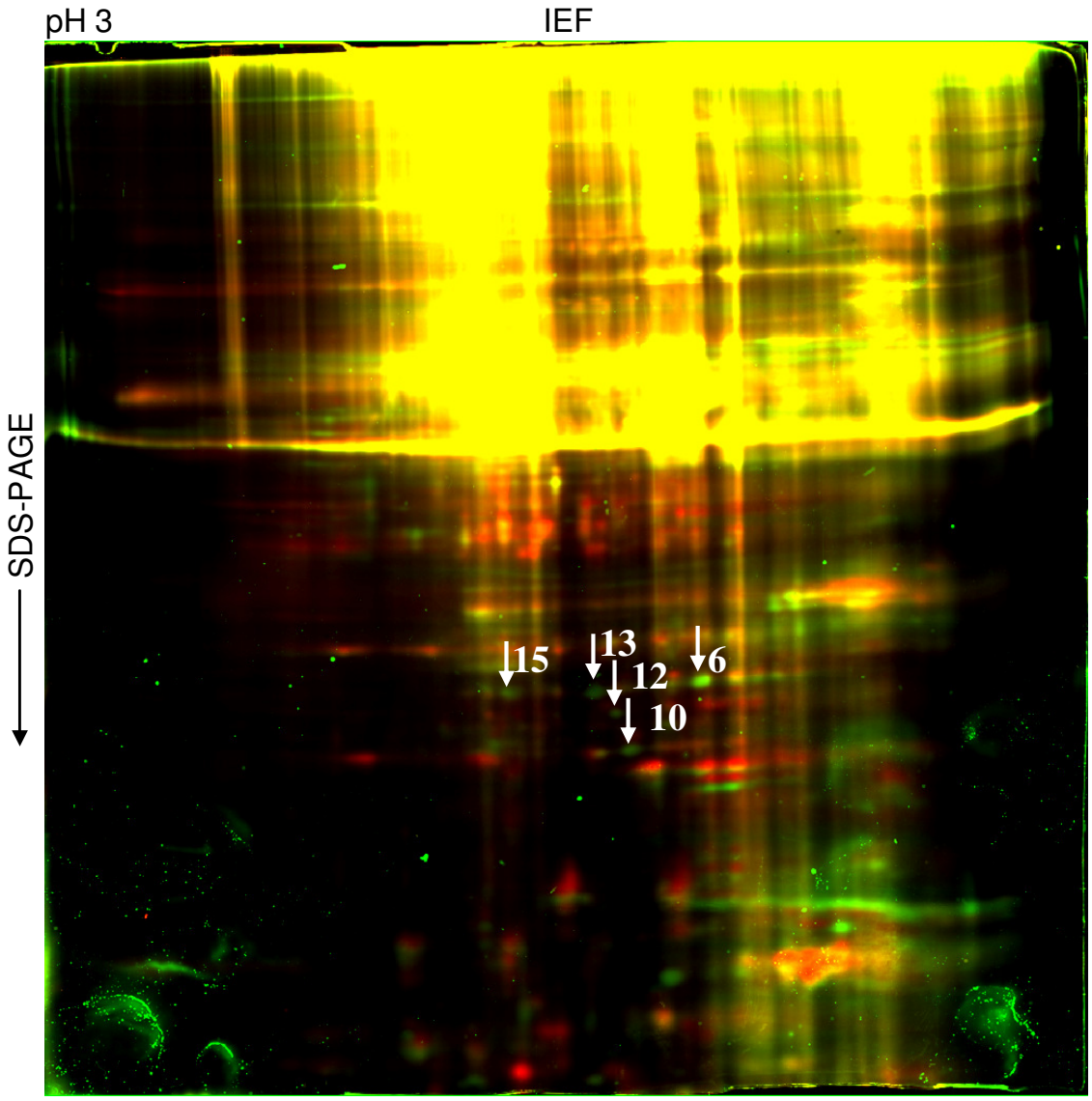

Figure 50: 2D-DIGE of proteins fished with testosterone and progesterone in PBMC cell lysates. Green: Cy5 labelled testosterone fished proteins, red: Cy3 labelled progesterone fished proteins, yellow: overlay of Cy3 and Cy5 labelled proteins. Marked spots were picked for identifikation via MS analytics.

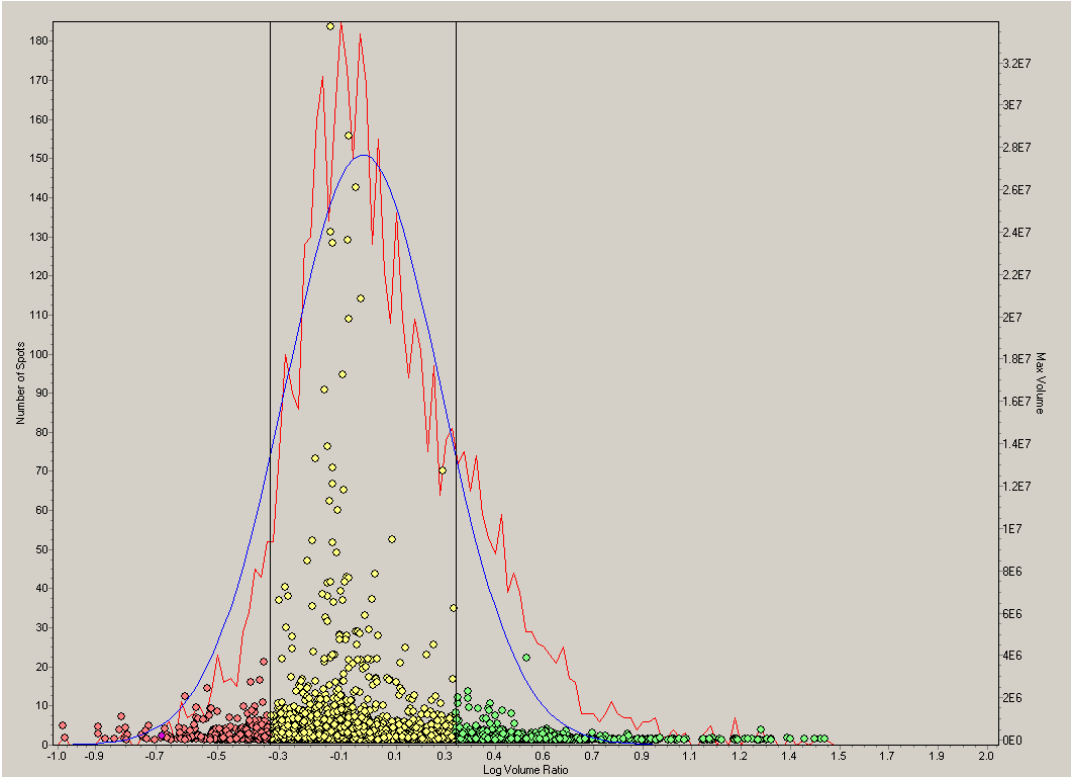

Figure 51: Spot distribution of the DIGE experiment with testosterone and progesterone in PBMC cell lysate. Evaluation via the DeCyder7 algorithm showed a total number of 6072 spots. 1129 spots were excluded since a high slope indicated an artificial origin (excluded spots are not shown). From the remaining 4943 spots 3609 were recognised with similar intensities in both, the testosterone and progesterone, fishing eluates (yellow). Finally, 360 spots were detected with higher intensity for progesterone (green) and 974 spots with a higher presence in the testosterone sample (red).

	Testosterone fished	**Progesterone fished**
Spot 10 Volume ratio: 231% Test. Vol.: 196016 Prog. Vol.: 597040	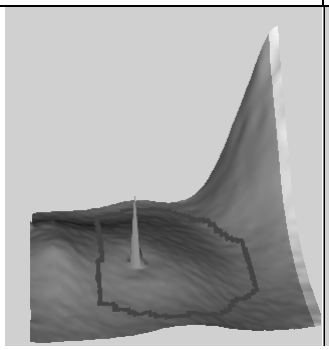	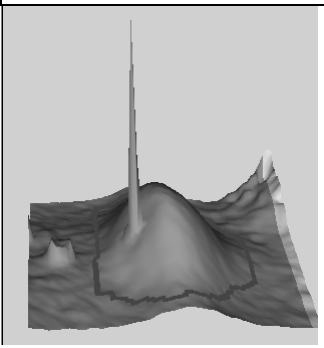
Spot 13 Volume ratio: 310% Test. Vol.: 182794 Prog. Vol.: 746862	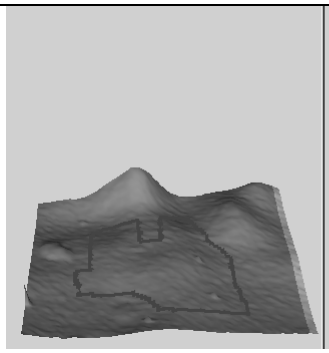	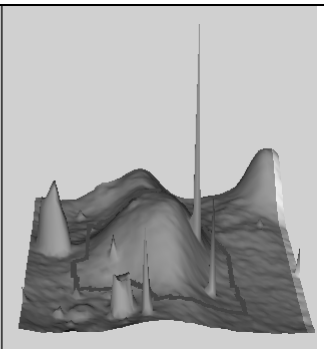
Spot 15 Volume ratio: 252% Test. Vol.: 301130 Prog. Vol.: 999260	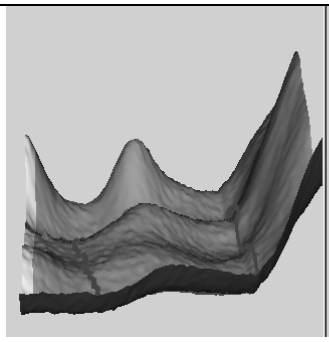	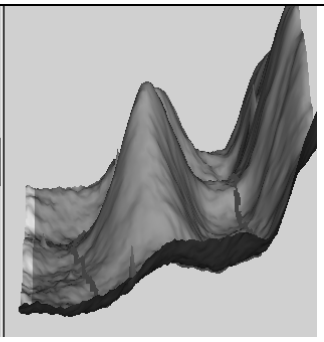

Table 17: 3D single spot evaluation and spot volume calculation of the DIGE experiment.

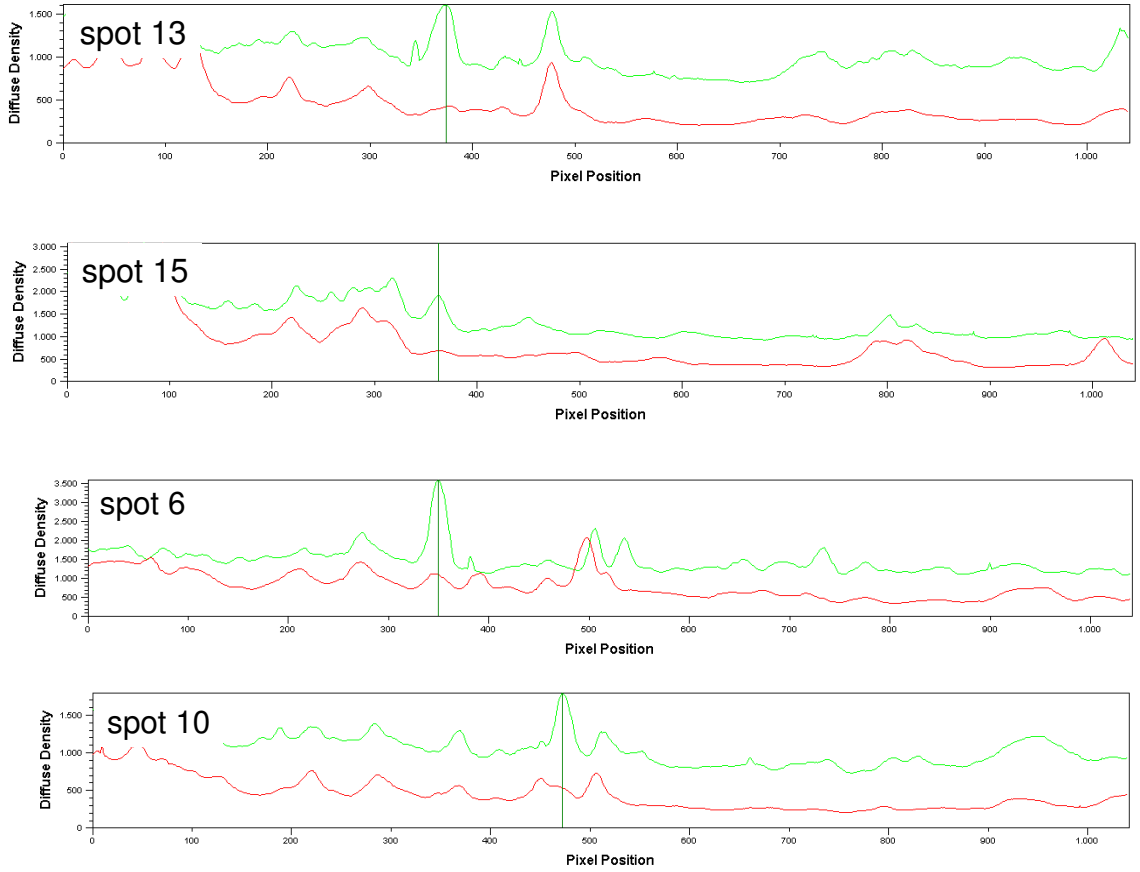

Figure 52: Intensity profile of the DIGE experiment in PBMC. Green profile: Cy3 labelled, progesterone fished proteins. Red profile: Cy5 labelled, testosterone fished proteins. Indicated spots are marked with a green line.

	Protein origin	**sequence**	**score**
Spot 6	HSPB1 Heat shock protein beta-1	DGVVEITGK	62
	HSPB1 Heat shock protein beta-1	GPSWDPFR	54
	HSPB1 Heat shock protein beta-1	LATQSNEITIPVTFESR	109
	HSPB1 Heat shock protein beta-1	PLPPAAIESPAVAAPAYSR	68
	HSPB1 Heat shock protein beta-1	QLSSGVSEIR	52
	HSPB1 Heat shock protein beta-1	TKDGVVEITGK	44
	HSPB1 Heat shock protein beta-1	VPFSLLR	40

	Protein origin	sequence	score
Spot 13	HSPB1 Heat shock protein beta-1	DGVVEITGK	54
	HSPB1 Heat shock protein beta-1	LATQSNEITIPVTFESR	66
	HSPB1 Heat shock protein beta-1	LFDQAFGLPR	70
	HSPB1 Heat shock protein beta-1	PLPPAAIESPAVAAPAYSR	68
	HSPB1 Heat shock protein beta-1	QDEHGYISR	52
	HSPB1 Heat shock protein beta-1	QLSSGVSEIR	79
	HSPB1 Heat shock protein beta-1	TKDGVVEITGK	72
	HSPB1 Heat shock protein beta-1	VSLDVNHFAPDELTVK	63
	HSPB1 Heat shock protein beta-1	HEERQDEHGYISR	46
	HSPB1 Heat shock protein beta-1	VPFSLLR	43
Spot 15	HSPB1 Heat shock protein beta-1	LFDQAFGLPR	61
	HSPB1 Heat shock protein beta-1	QLSSGVSEIR	79
	HSPB1 Heat shock protein beta-1	LATQSNEITIPVTFESR	46
	HSPB1 Heat shock protein beta-1	GPSWDPFR	41
	PRDX6 Peroxiredoxin-6	DFTPVCTTELGR	57
	PRDX6 Peroxiredoxin-6	LPFPIIDDR	75
	PRDX6 Peroxiredoxin-6	VVFVFGPDK	66
	PRDX6 Peroxiredoxin-6	LSILYPATTGR	46
	PRDX6 Peroxiredoxin-6	VVFVFGPDKK	39

Table 18: Peptide sequences derived from the indicated spots after tryptic digest and MS analytics and corresponding mascot search results.

The spots number 6 and 13 were both identified as Heat shock protein beta-1 (= Heat shock protein 27). For spot number 15, peptides of Heat shock protein beta-1 as well as of Peroxiredoxin-6 were identified.

Spot 10 was identified as isoform 1 of Abhydrolase domain-containing protein 14B (ABHD14B) which is not known in literature. Thus, subsequent validation and characterisation of ABHD14B is not possible and ABHD14B was not considered further on (Tbl. 21).

4.2.6.9 Testosterone and progesterone fishing in platelet lysates

For target-fishing in platelet cell lysates, experiments were performed as described in 3.2.5. 2D DIGE was performed under standard conditions as described in 3.2.6[144-148]. However, only two spots could be picked out of the silver stained gel for subsequent MS analytics (Fig. 61). Interestingly, both spots were identified as HSP B1 although they were clearly separated.

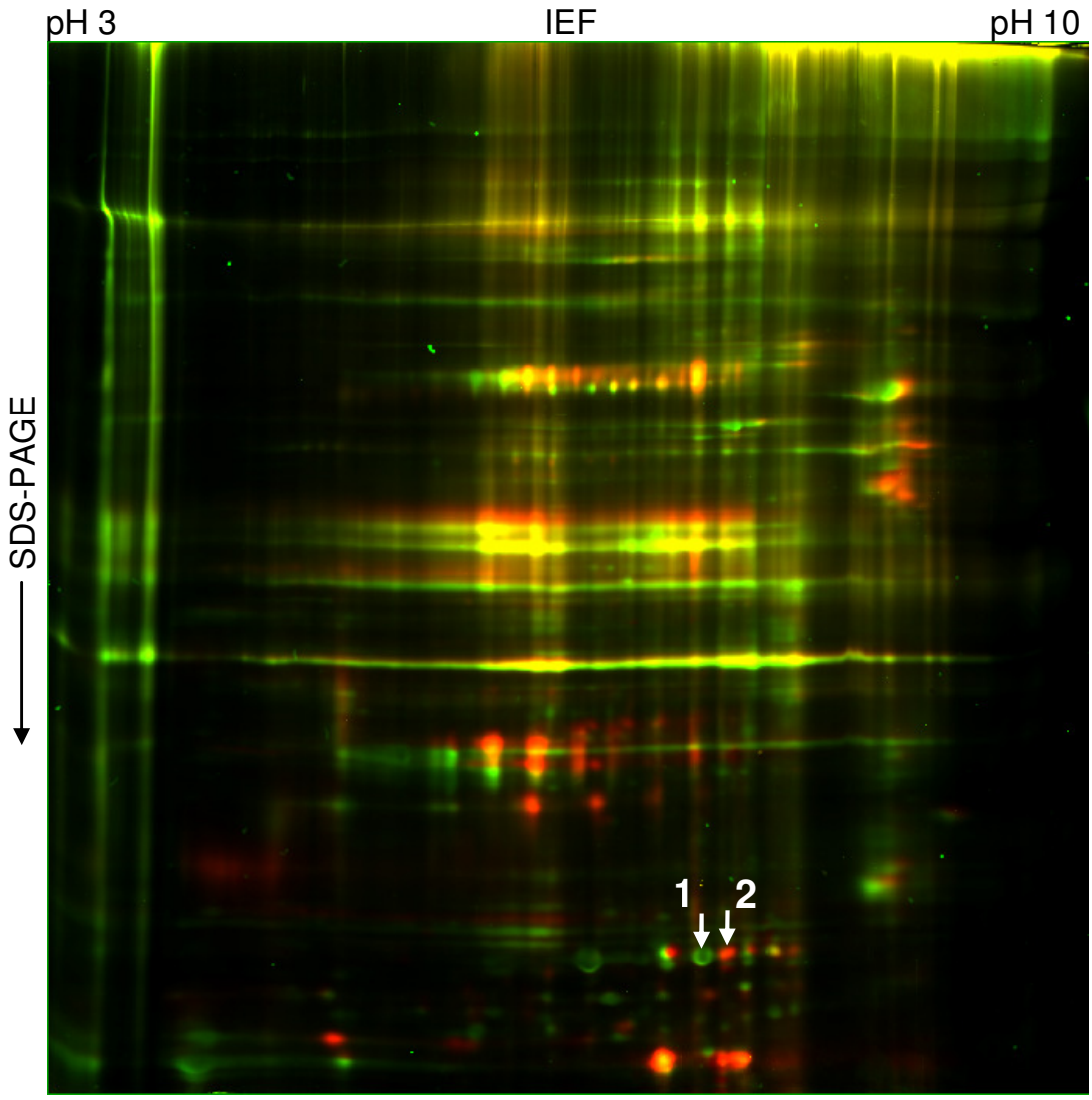

Figure 53: 2D-DIGE of proteins fished with testosterone and progesterone in platelet cell lysates. red: Cy5 labelled testosterone fished proteins, green: Cy3 labelled progesterone fished proteins, yellow: overlay of Cy3 and Cy5 labelled proteins. Marked spots were picked for identification via MS analytics.

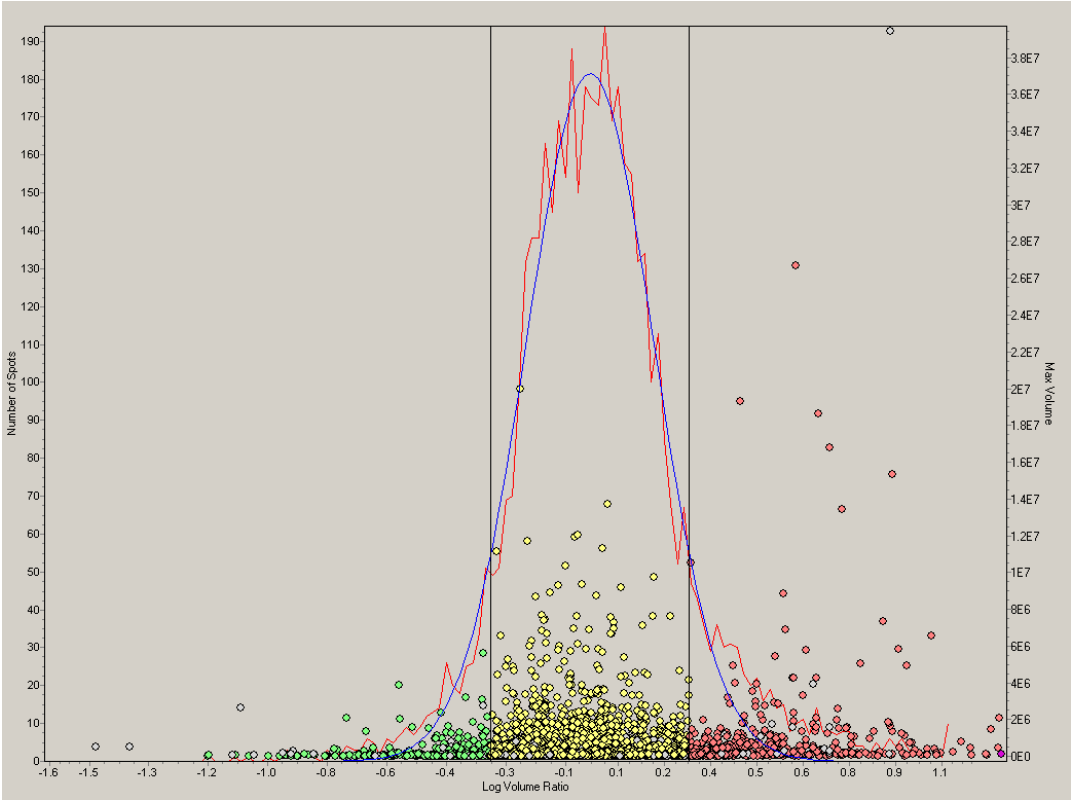

Figure 54: Spot distribution of the DIGE experiment with testosterone and progesterone in platelet cell lysate. DeCyder analysis detected 5068 spots including 335 spots with artificial origin (colourless). Non artificial spots consisted of 3851 spots with no difference (yellow), 338 spots of proteins fished selectively with progesterone (green) and 544 spots of proteins with a higher amount in the testosterone eluates (red).

	Testosterone fished	**Progesterone fished**
Spot 2 Volume ratio: 659% Test. Vol.: 1082553 Prog. Vol.: 5047068	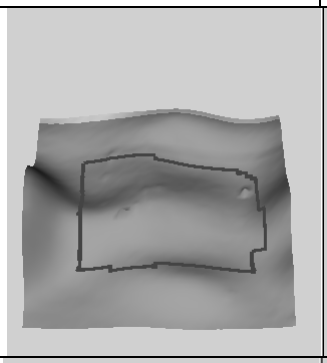	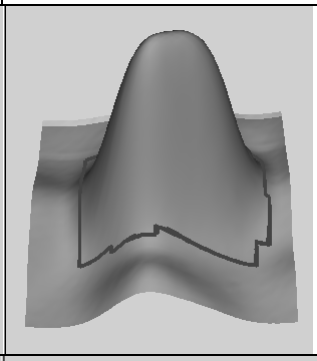
Spot 1 Volume ratio: 179% Test. Vol.: 3700332 Prog. Vol.: 1465368	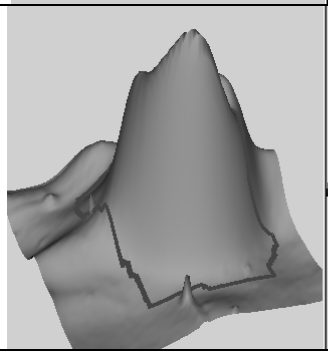	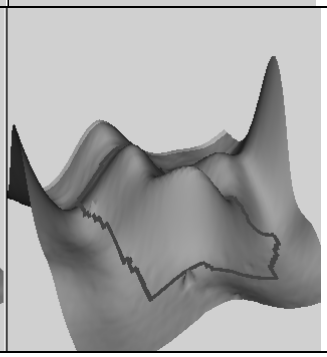

Table 19: 3D single spot evaluation and spot volume calculation of the DIGE experiment.

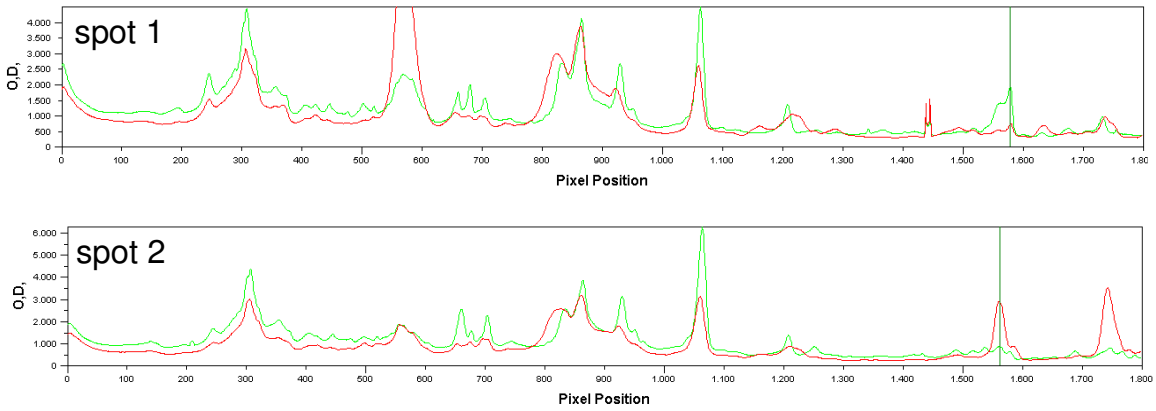

Figure 55: Intensity profile of the DIGE experiment in platelet cell lysate. Green profile: Cy3 labelled, progesterone fished proteins. Red profile: Cy5 labelled, testosterone fished proteins. Indicated spots are marked with a green line.

	Protein origin	sequence	score
Spot 1	HSPB1 Heat shock protein beta-1	DGVVEITGK	49
	HSPB1 Heat shock protein beta-1	QDEHGYISR	53
	HSPB1 Heat shock protein beta-1	QLSSGVSEIR	55
	HSPB1 Heat shock protein beta-1	AQLGGPEAAK	43
	HSPB1 Heat shock protein beta-1	TKDGVVEITGK	36
Spot 2	HSPB1 Heat shock protein beta-1	AQLGGPEAAK	49
	HSPB1 Heat shock protein beta-1	DGVVEITGK	48
	HSPB1 Heat shock protein beta-1	QDEHGYISR	54
	HSPB1 Heat shock protein beta-1	QLSSGVSEIR	60
	HSPB1 Heat shock protein beta-1	TKDGVVEITGK	69
	HSPB1 Heat shock protein beta-1	VPFSLLR	53

Table 20: Peptide sequences derived from the indicated spots after tryptic digest and MS analytics and corresponding mascot search results

Both, the protein contained in spot 1 and 2 were identified as Heat shock protein beta 1 (HSP B1) (Fig. 62, 63; Tab. 22, 23).

4.2.6.10 Confirmation via Western blot analysis

Western blot analysis of fishing eluates was performed in order to confirm the results of the MS analytics (Fig. 64).

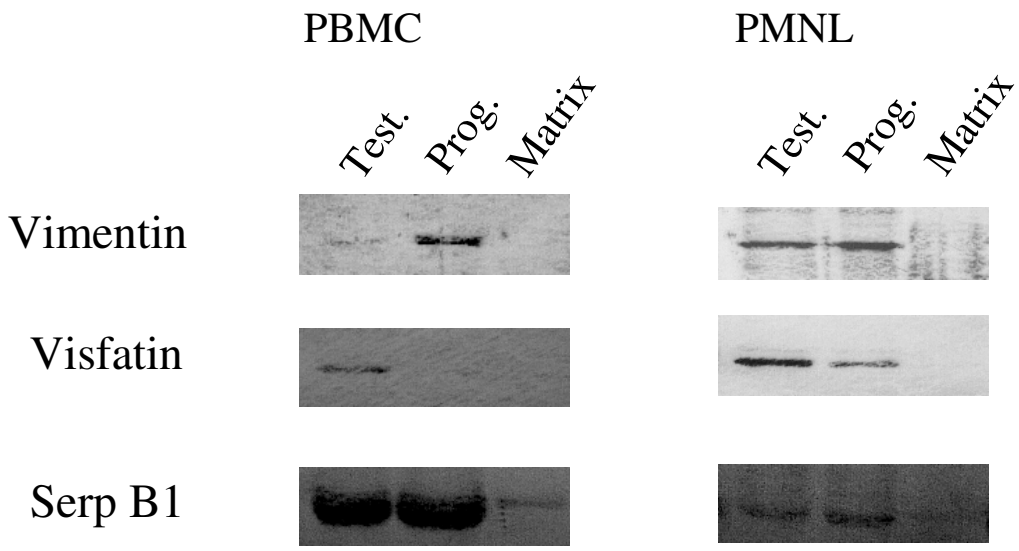

Figure 56: Western blot analysis of proteins fished with testosterone and progesterone in PMNL and PBMC cell lysates. Data shown are representative of at least three independent experiments.

Next, Western blot analysis was performed with eluates obtained from fishing experiments with PMNL and PBMC cell lysates. Vimentin (Vim) could be fished selectively with progesterone in PBMC cell lysates. In eluates from fishing experiments in PMNL cell lysates, only a slight difference with more Vim in the fishing experiment using progesterone as bait could be seen. For visfatin (Vis) a clear band could be identified in the testosterone fishing experiments in PBMC cell lysates, whereas no band was visible in the corresponding progesterone sample. For Vis blots from the PMNL lysate fishing, a stronger band for testosterone eluates than for progesterone eluates was detected. Regarding Serpin B1, Western blot analysis results from the fishing experiments in both, PBMC and PMNL cell lysates showed no clear difference between testosterone and progesterone. For all Western blots the matrix alone turned out to bind no or very low of the analysed protein.

4.2.6.11 Evaluation of Vimentin as target structure

The protein Vimentin (Vim) is an intermediate filament and thereby part of the cytoskeleton. Although scientists recognised that Vim is not a classical part of the cytoskeleton but a regulatory protein (see [144-147]) its function is only poorly understood and no assay systems for testing regulatory effects of Vim exist so far. Thus, no further experiments could be performed to characterise the functionality of the progesterone – Vim interaction.

4.2.6.12 Evaluation of Serpin B1 as target structure

Since the specificity of the Serpin B1 – progesterone interaction could not be confirmed in Western blot experiments, no further experiments were performed to validate the Serpin B1 – progesterone interaction.

4.2.6.13 Evaluation of HSP27 as target structure

In PBMC and PMNL, HSP27 binds to both: testosterone and progesterone with a slightly higher affinity to testosterone. In contrast, fishing experiments performed in platelets resulted in a prominent band in the Western blot experiment for HSP27 for the testosterone sample, whereas almost no band was visible for the progesterone sample (Fig. 65).

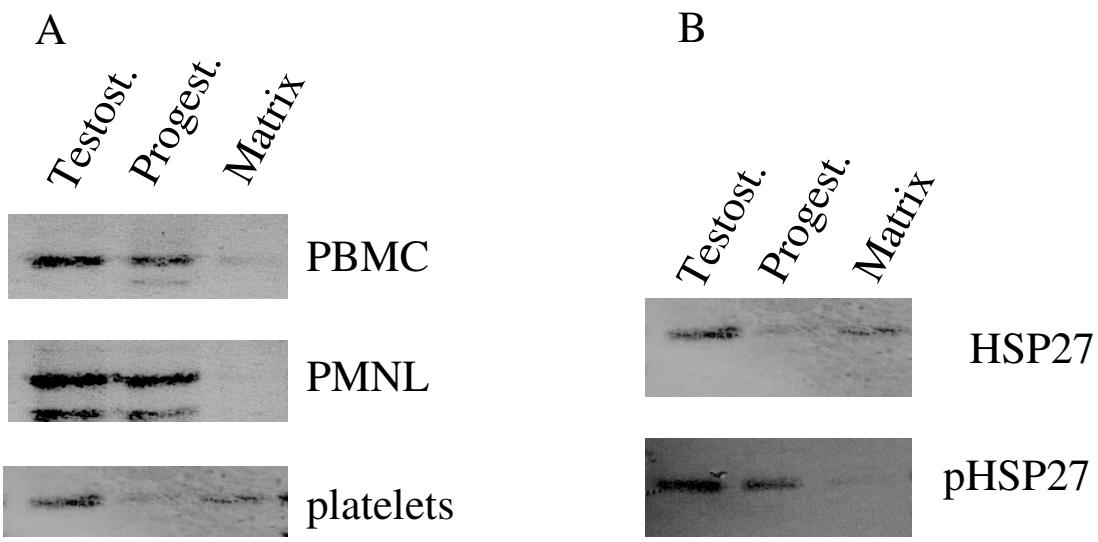

Figure 57: (A) Western blot analysis of HSP27 fished by testosterone and progesterone in PBMC-, PMNL- and platelet lysates. (B) Western blot analysis of HSP27 and p(Ser82)HSP27 fished by testosterone and progesterone in platelet lysates. Data shown are representative of at least three independent experiments.

To determine whether the binding of HSP27 to testosterone is a direct interaction or mediated via adaptor proteins a fishing experiment with isolated recombinant HSP27 was performed. Western blot analysis showed that only testosterone but not progesterone is able to bind isolated HSP27 and thereby causes a reduction of the protein in the supernatant (Fig. 66).

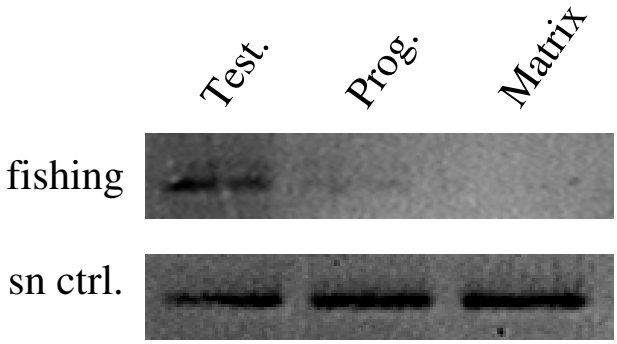

Figure 58: Western blot analysis of a testosterone fishing with isolated recombinant HSP27 and its supernatant. Data shown are representative of at least three independent experiments.

In the DIGE experiment performed with platelet lysates, two separated spots (one fished with testosterone and one with progesterone) were both identified as HSP27 (see Fig. 61). The result of the Western blot analysis might explain the second spot corresponding to HSP27 in the testosterone sample. In contrast, progesterone was able to pull down HSP27 in the DIGE experiment but not in the Western blot analysis. Since both spots of HSP27 differed in their isoelectric point but not in their size, we considered that different phosphorylation states could differentially influence the binding affinity to

progesterone. In fact, protein phosphorylation may cause a shift of the isoelectric point. Thus, further Western blot analysis with antibodies against p(Ser82)HSP27 were performed (Fig. 65B). These results showed that the phosphorylated HSP27 binds clearly to progesterone, whereas unphosphorylated HSP27 does barely bind to progesterone.

The levels of HSP27 and pHSP27 in platelets from male and female donors were analysed by Western blot analysis. The levels of both HSP27 and pHSP27 were distinctly higher in platelets from female donors compared with platelets from male donors. Knowing that the binding affinity of progesterone to HSP27 is lower than to testosterone, these results suggest that the levels of HSP27 in platelets from female donors compensates the lower binding affinity of HSP27 to progesterone (Fig. 67).

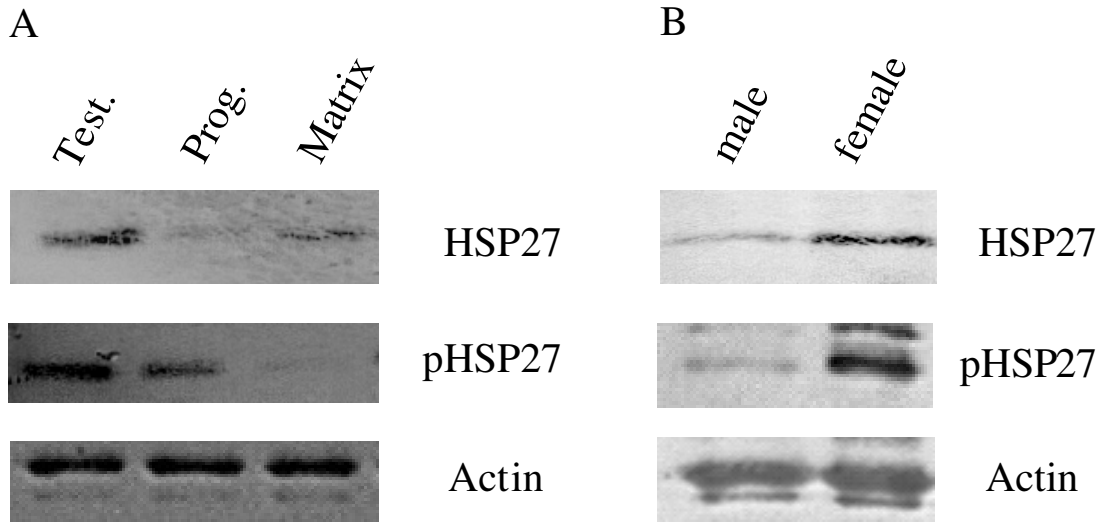

Figure 59: (A): Western blot analysis of HSP27 and p(Ser82)HSP27 fished in platelets; (B): Western blot analysis of the HSP27 and p(Ser82)HSP27 amount in platelets from male- and female donors and Actin as loading control. Data shown are representative of at least three independent experiments.

4.2.6.14 Evaluation of visfatin as target structure

To investigate whether the visfatin (Vis) interacts directly or via an adaptor protein to testosterone, fishing experiments with isolated Vis were performed. In the Western blot analysis of this fishing experiment, a specific interaction between testosterone and Vis was seen. In addition, a decrease of the Vis amount in the supernatant indicated that Vis can be selectively fished out of solution (Fig. 68).

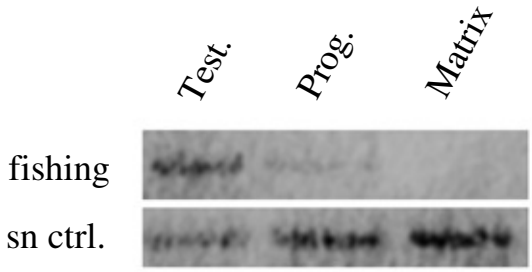

Figure 60: Western blot analysis of a testosterone fishing with isolated recombinant visfatin. After the fishing experiment visfatin levels are decreased in the supernatant (sn ctrl.) of the testosterone fishing, whereas elution of the beads (fishing) shows the presence of visfatin specifically in the testosterone sample. Data shown are representative of at least three independent experiments.

Since both, testosterone and Vis are known to influence ERK phosphorylation [96, 149], experiments on combined effects of both compounds have been performed as described in 3.2.7.1 (Fig. 69).

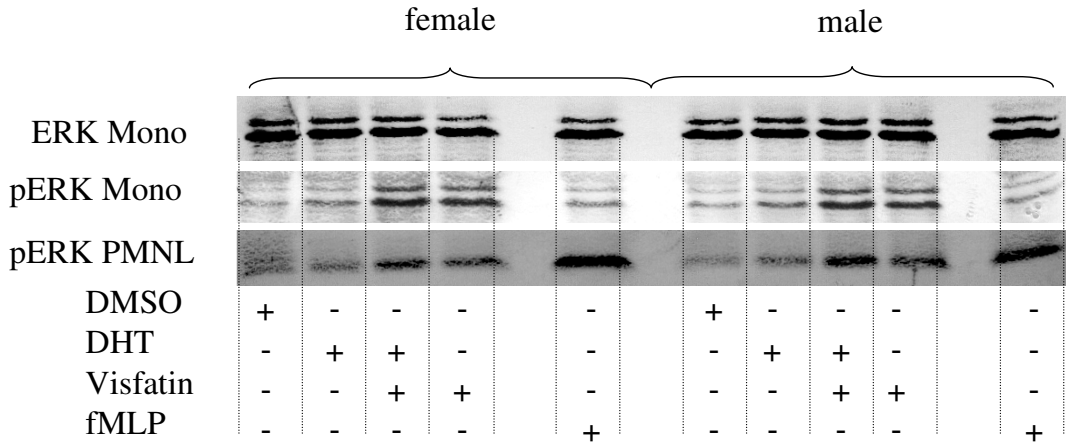

Figure 61: Western blot analysis of the ERK phosphorylation assay. DMSO was used as vehicle control. Monocytes (Mono) and neutrophils (PMNL) were incubated 90 sec with DHT (30 nM), Visfatin (100 nM) or fMLP (100 nM). Data shown are representative of at least three independent experiments.

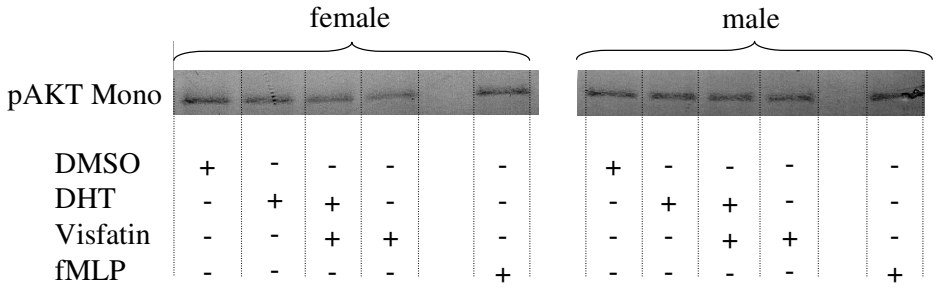

Figure 62: Western blot analysis of the AKT phosphorylation assay. DMSO was used as vehicle control. Monocytes (Mono) were incubated 90 sec with DHT (30 nM), Visfatin (100 nM) or fMLP 100 nM. Data shown are representative of at least three independent experiments.

DHT enhances the basal phosphorylation state of ERK as well as Vis. The combination of DHT and Vis resulted in the highest phosphorylation state of ERK. These effects

could be shown in monocytes and PMNL. No difference of the effects between genders could be observed. Although it has been described, that AKT can, like ERK, be phosphorylated by addition of Vis [149-150], this effect was not observed in our experiments (Fig. 70).

4.2.6.15 Comparison of different testosterone and progesterone derivatives

Since the possibilities to immobilise a compound is limited to its chemical structure, derivatives have to be synthesised to obtain new possibilities for successful target-fishing experiments. Thus, in the course of this study, several derivatives have been synthesised by collaborators[VIII]. To find out which derivatives of a certain compound are most convenient for target-fishing experiments, multiplexed DIGE experiments were performed.

To compare C3 carboxymethoxylamine derivatives of testosterone and progesterone with corresponding C7 pentanoic acid derivatives, fishing experiments were performed with both derivatives as well as with the uncoupled matrix. Both progesterone derivative eluates were labelled with the Cy3 dye whereas both testosterone eluates were Cy5 labelled. In addition, a sample consisting of an aliquot of each eluate was labelled with the Cy2 dye. Thus, two corresponding testosterone and progesterone eluates as well as the Cy2 labelled sample could be separated on one 2D gel. The Cy2 labelled sample as internal standard allows the comparison of different 2D DIGE gels with the same internal standard (Fig. 73).

[VIII] Synthesis of all steroid derivatives was done in cooperation by dipl. chem. M. Golkowski and the group of Prof. Dr. T. Ziegler, Institute of Organic Chemistry, University Tübingen

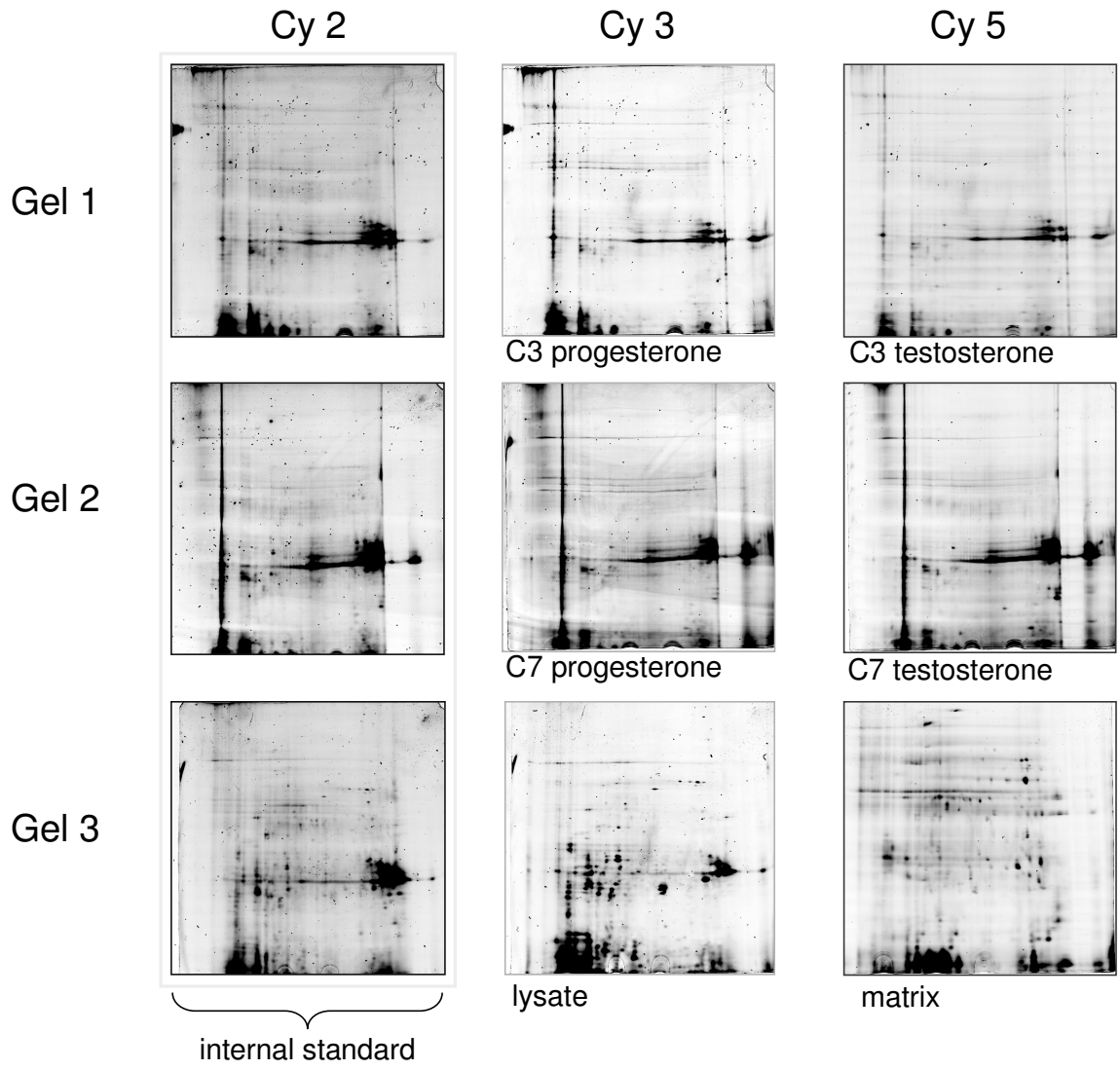

Figure 63: Scheme of the multiplexed DIGE experiment. Samples were labelled with Cy3 or Cy5 dyes respectively. A mixture of all 6 samples was labelled with the Cy2 dye to obtain a multiplexed standard. 3 different gels were loaded with a Cy3 labelled and a Cy5 labbelded sample as well as with the Cy2 labelled standard.

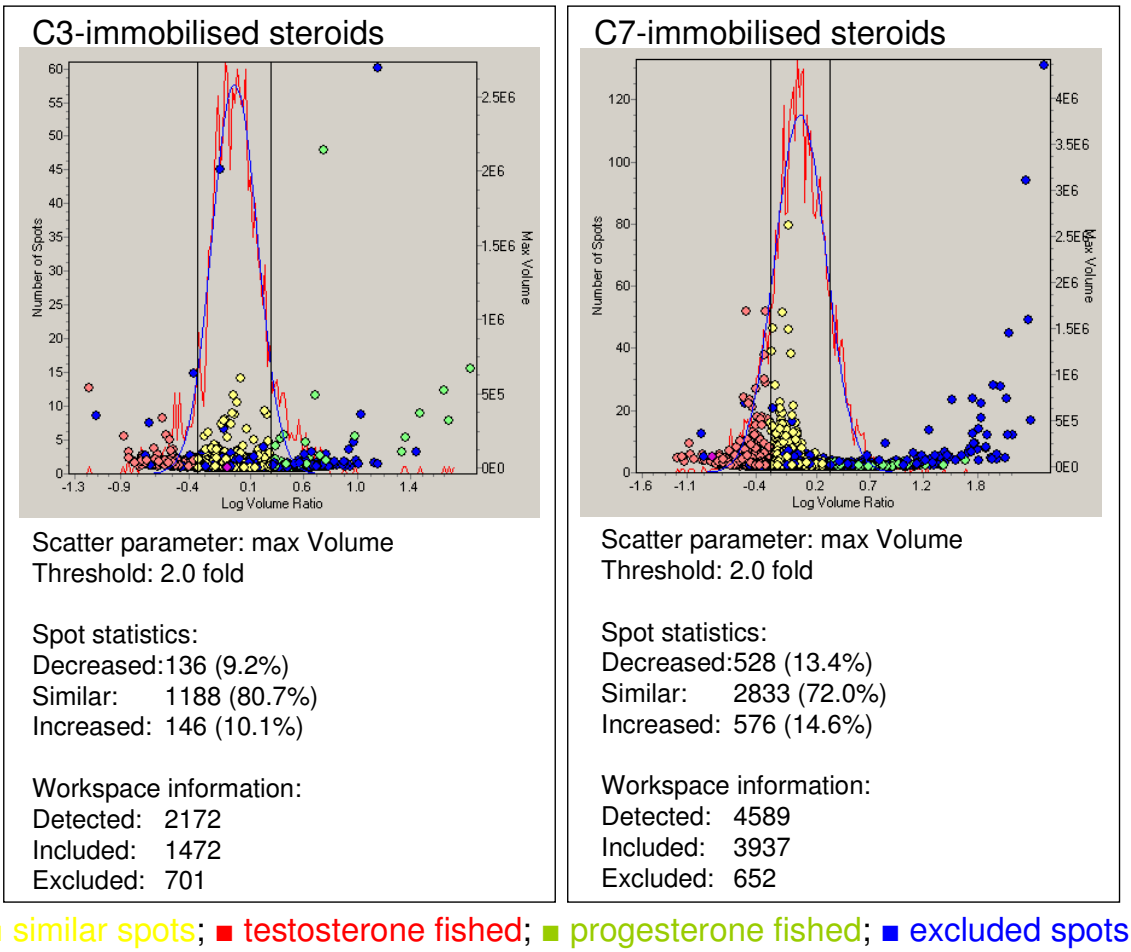

Figure 64: Comparison of proteins fished by differentially immobilised steroid. Blue: artificial spots, yellow spots: proteins with no difference in their affinity for progesterone and testosterone, red spots: proteins fished with a higher selectivity for testosterone, green spots: proteins fished with a higher selectivity for progesterone.

The entire evaluation of fished proteins showed that more proteins are fished with the C7 derivatives of testosterone and progesterone in comparison to the C3 derivatives. The fishing experiment with C3 derivatives led to the detection of 1472 spots whereas 3937 spots could be detected in the eluates of the C7 derivative fishing experiment. In addition, fishing with C7 derivatives led to less unspecific fished proteins. While 80.7% of all spots in the C3 fishing eluates were detected with similar concentrations for progesterone and testosterone only 72.0% of the proteins in the C7 derivative eluates were present in similar amounts (Fig. 74).

5 Discussion

State of the art pharmacotherapy requires a comprehensive understanding of the molecular action of a drug. Therefore, durg-target research is one of the major disciplines of modern medical and pharmaceutical science.
As mentioned above, today´s drug-target research focusses on the development of new drugs for known targets. In addition, the effectiveness of many natural compounds that were traditionally used for the treatment of several diseases is rediscovered by today´s medical scientists. These findings are often limited to clinical observations and the molecular base for the effects of these compounds often remains unclear. Thus, the identification of new targets for known compounds offers an important possibility of a rational pharmacotherapy for compounds that are known to be effective and safe in use for a long time.
Up to date, there is a lack of knowledge for molecular drug actions as well as a lack of suitable methods for the investigation of these drug actions.

5.1 Methodological improvements of the target-fishing approach

The target-fishing approach was successfully used in the past for the identification of new targets for known compounds [18-19]. Although the results of Harding et. al. and Taunton et. al. impressively showed the potency of the target-fishing approach it was barely regarded by scientists and no efforts were made to improve the target-fishing approach. Comprehensive investigations on matrix types, fishing and elution conditions as well as the establishment of modern proteomic methods are needed to develop the target-fishing approach to a reliable and versatile method.

5.1.1 Matrix types for target-fishing experiments

The chemical composition of a fishing-matrix plays an essential role for the success of target-fishing experiments. It has to provide an appropriate type and amount of functional groups, it has to possess sufficient chemical resistance and it should show low unspecific protein interaction.

As mentioned in 4.1.1, matrices consisting of polymethacrylic acid turned out to possess extended chemical resistance and thereby offer a wide range of possibilities for subsequent chemical modifications. In addition, matrices based on methacrylic acid are available with a distinct higher immobilisation capacity. Amino functionalised methacrylic matrices such as Toyopearl AF Amino-650M, for example, possess tenfold higher amounts of functional groups compared to the commonly used EAH Sepharose® 4B. Thus, methacrylic acid matrices combine both the possibility to immobilise a higher amount of ligand and more options of chemical reactions to immobilise ligands.

5.1.2 Generation of carboxymethoxylamine beads for immobilisation of ligands via keto- or aldehyde groups

Carboxymethoxylamine residue allows the immobilisation of both ketones and aldehydes under mild reaction conditions, which are both compatible with beads and harmless to a wide range of possible ligands. Up to date, carboxymethoxylamine activated beads are neither commercial available, nor are they described in literature.

For a successful immobilisation of ligands containing a keto or an aldehyde group via carboxymethoxylamine residues, suitable beads had to be developed. To this aim, an appropriate functionalisation of commercially available beads was performed. To achieve a carboxymethoxylamine surface functionalisation, N-boc-carboxymethoxylamine was chosen as derivatisation agent for commercially available amino-functionalised beads.

Testosterone was used as model compound to prove the applicability of this procedure. As shown in 4.1.2 (Fig. 15), the derivatisation of amino functionalised matrices using N-boc carboxymethoxylamine allows subsequent immobilisation of testosterone. Since keto groups are seldom present in natural compounds or drugs, the application of this procedure might be limited to a small number of potential ligands. Nevertheless, major benefits of this procedure are: (i) the reaction conditions are moderate, thus side reactions or harmful effects to the ligand are improbable; (ii) the derivatisation of the beads is easy to be performed with common equipments of a biochemical laboratory; (iii) most of the molecules containing a keto group present not more than one keto moiety, which allows a specific immobilisation on one defined position without further derivati-

sation of the molecule. Certainly, this procedure is limited to those molecules where the keto group is not essential for the pharmacological activity.
Establishing this immobilisation strategy offers extended possibilities for ligand immobilisation and target-fishing experiments.

5.1.3 Evaluation of fishing conditions

Aside from the chemical composition of the matrix, the fishing conditions play an essential role for a successful target-fishing experiment.
Since the type of protein fished with a certain ligand is not predictable, an extensive and unique development of fishing conditions is not possible. However, several improvements of the fishing conditions could be made in consideration of the general processes that are involved in affinity based approaches.
(i) Only fresh prepared cell lysates were used. Although proteins can be stored for a certain time at -80°C, freezing of proteins without appropriate kryoprotecting agents can lead to a conformational change of the protein. This could lead to both an alteration of 3-dimensional structure of the ligand binding side and precipitation of the protein. In both cases, the affected protein will not be suitable for a subsequent target-fishing approach. (ii) 1% of triton® X-100 was used in cell lysis buffers. This enhances the solubilisation of lipophilic proteins. In order to keep solubilised proteins in solution, the same concentration of triton® X-100 was used in all following experimental steps. In addition, the use of detergent during the fishing-experiment leads to a decreased amount of unspecifically bound proteins. (iii) Cell lysates were cleared by ultracentrifugation at 100,000 × g. Thus, a better separation of cell lysate and cell debris is possible. In addition, ultracentrifugation steps at 4°C allow a separation of lipid components from the cell lysate. Since lipids negatively influence subsequent electrophoretical and massspectrometric methods, clearing lysates from lipids facilitates subsequent analysis.
Although individual conditions may be needed for certain experiments, the sum of all these improvements led to a reliable procedure that is applicable to a broad range of fishing-constructs.

5.1.4 Evaluation of elution condition for target-fishing experiments

Needless to say, that fishing a protein is the primary aim of the target-fishing approach. Appropriate elution of this protein is as important as the fishing itself. Thus, proteins have to be eluted in a purity and amount that allows reliable separation and identification later on.

Standard elution protocols use SDS buffer for protein elution [11]. Since protein denaturation using SDS is needed for subsequent electrophoretic separation by SDS-PAGE, SDS buffers combine simple elution and sample preparation for subsequent analysis in one step. However, elution by SDS is a rough and highly unselective procedure. However, other elution agents such as high salt concentrations turned out to be less efficient than SDS without improvement of elution selectivity.

For a more selective elution, proteins were eluted in a competitive manner by addition of the ligand itself. For ACAP, ligand concentrations up to 50 mM were used for protein elution. Figure 17 shows that a competitive elution results in insufficient protein amounts also at these high concentrations. In view of the fact that aqueous buffers are needed in proteomic and affinity based approaches, but lipophilic ligands such as steroids or terpenes show poor solubility in aqueous buffers, a competitive strategy of elution must be considered as an exceptional rather than a general option.

Since the lack of selectivity was the major disadvantage of common elution procedures, we focussed also on the improvement of separation capacities. Using a separation method with a high resolution allows the analysis of a large number of proteins. Thus, specific bound proteins can be detected in the presence of a high number of unspecific bound proteins.

The gel based method with the highest resolution is the 2-dimensional gel electrophoresis (2D-EL). Since urea buffers are needed for the development of the first dimension in 2D-EL approaches, urea offers the possibility to perform elution and sample preparation in one step.

5.1.5 Development of a photoreactive linker system

As mentioned above, it is not possible to develop a general method for selective elution, independently from the ligand used or the protein fished. Nevertheless, the possibility to cleave off the ligand together with the specific bound protein from the matrix would

offer an alternative, high selective elution. Thus, we developed a photoreactive linker system that could be cleaved by UV light exposure.

The use of the UV light cleavable linker system allows a highly specific elution of ligand bound proteins. UV light exposure of photoreactive beads after a fishing experiment leads to the release of ligand bound proteins. The beads themselves together with unspecific bound proteins can be easily removed by centrifugation. Thus, the supernatant contains only specific bound proteins.

Although UV reactive molecules and their application in biochemical approaches are known [21-23, 141], cleavage of these molecules was not possible without degrading proteins. Thus, chemical modifications of the o-nitrobenzylic core as well as modifications of the irradiation conditions were done in order to develop a protein compatible photoreactive linker system. In addition, this linker was designed to be immobilised using standard proteinchemistry procedures. Thus, a boc-protected amine on the one hand and a carboxy residue on the other allows to connect the matrix, the linker and the ligand via amide bonds using the same conditions each time.

To evaluate the functionality of the UV light cleavable linker, testosterone and its binding to the androgen receptor (AR) as known interaction was investigated. Figure 21A shows that, the beads themselves without ligand added are capable to bind the AR. Furthermore, none of the commonly used methods to prevent this unspecific AR binding, such as harsh washing conditions or several surface blocking procedures were successful. In fact, when a specific interaction for a certain protein takes place along with strong unspecific binding of the same protein, a selective detection is impossible. The UV reactive linker system reduces the amount of unspecific bound protein and facilitates the specific release of testosterone bound AR.

Although the functionality and benefits of UV reactive linker systems could be demonstrated but exemplary, it was shown that it was possible to establish an effective UV light reactive linker system.

5.1.6 Establishment of the 2D-DIGE approach for pull down assays

Two dimensional gel electrophoresis is the protein separation method with a high separation performance. Nevertheless, its major disadvantage is its poor reproducibility and comparability. By today, the comparison of two different 2D gels is a challenging task. The 2D-DIGE allows to analyse up to three protein samples on the same gel. Thus, the

samples are easily comparable since all samples run under exactly the same conditions. Originally the DIGE technology was developed to compare protein expression patterns within differentially treated cells. This application differs from the target-fishing approach for the buffers used and the amount of proteins obtained. For this reason, novel DIGE conditions had to be evaluated. The conditions we developed resulted in a sufficient CyDye labelling of eluted protein. With BSA as model protein, amounts as low as 5 pg could be detected. Therefore, the optimised DIGE approach offers both high resolution and high sensitivity for the analysis of target-fishing eluates.

Unfortunately, the high sensitivity of the DIGE approach could not be reached with other methods that are required for a reliable target identification and validation. Thus, although a large number of proteins can be quantitatively analysed in DIGE experiments, the subsequent analytical steps are limited to a smaller number of highly abundant target candidates. Considering the remarkable progress in proteomic methodologies, today´s sensitivity of 2D-DIGE analytics will be needed for combination with proteomic methods of tomorrow.

5.1.7 Target-fishing experiments with specific bioactive agents

5.1.7.1 Acetaminophen (ACAP)

ACAP is used for a long time [37-38] as a antipyretic and analgesic drug [38, 40]. Until today, there is a big discrepancy between the wide spread use of ACAP and the knowledge about its pharmacologic action. Although several targets have been discussed [41-47, 51-53] for ACAP, none of these targets could explain the entire pharmacological profile of it. Thus, target-fishing experiments were performed in order to identify new target candidates for ACAP.

For the target-fishing approach using ACAP as ligand, three different immobilisation strategies were applied and fishing experiments were performed in different cell lysates by testing different fishing and elution conditions. Nevertheless, no protein could be identified as potentially new target candidate.

Regarding the therapeutic application, where ACAP is used in doses up to 1000 mg per single dose, it is conceivable that a high dose of an active compound implicates a low affinity to the target. Knowing that molecular interactions like hydrogen bonds, ionic- or hydrophobic interactions are needed for a binding of a drug to a corresponding target allows to predict the binding mode of a molecule. Typically, molecules with more functional groups allow more interactions with a target which results in a higher binding affinity. In addition, size and flexibility of molecules affect their possibility to coordinate functional groups in sterical proximity to interacting groups. Thus, inflexible and large molecules typically show a higher binding selectivity. ACAP possesses only few functional groups and is relatively small. Therefore, the interaction of ACAP and a possible target is expected to have neither a high affinity nor a high selectivity.

The fact that it was not possible to identify new targets for ACAP with the target-fishing approach is caused rather by the chemical nature of ACAP than by methodological deficiencies.

5.1.7.2 Indirubin-3-monoxime

Indirubine-3´-monoxime (IR3MO), is one active ingredient of *Indigo naturalis.* Extracts of *Indigo naturalis* were traditionally used in chinese medcine for the treatment of leukaemic diseases. Although the antileukaemic action of IR3MO seems to bee partially understood [78-79], IR3MO possesses also anti-inflammatory properties that are not understood in detail to this day [82-83]. To expand the knowledge of both: antileukaemic- and anti-inflammatory actions of IR3MO, target-fishing experiments were performed using immobilised IR3MO.

After successful immobilisation of IR3MO, the respective fishing experiments were performed with VSMC, PBMC and PMNL cell lysates. The DIGE analysis of the fishing eluates showed low protein concentrations in general. Thus, although specific fished proteins could be detected in the DIGE experiments subsequent visualisation by silver staining and identification by MS were not possible. Due to the fact that low protein amounts were observed in all IR3MO fishing experiments independent of the type and the concentration of the cell lysate, it may be reasonable that the fishing construct itself is responsible for the low amount of fished protein. Regarding the poor chemical reactivity of the monoxime residue, a moderate immobilisation rate could be the reason for low amounts of bound protein. Thus, a derivatised IR3MO with a more reactive binding side for a higher immobilisation rate would be needed.

5.1.7.3 Myrtucommulone (MC)

MC is an active ingredient of the mediterranian plant *Myrtus communis*. Although remarkable progress on the understanding of the pharmacological actions of MC has been made during the last decade [85-87, 151-152] direct binding partners of MC are still unknown.

DIGE analysis of MC fishing experiments showed exactly the same pattern for the MC fishing construct and its control. Thus, no differences or specific fished proteins could be detected. A possible reason for this result might be an insufficient immobilisation of MC. The fact that the -OH residues of MC are either vinylogue acids or phenolic -OH residues which show poor reactivity in comparison with primary -OH residues could explain an inadequate outcome of MC immobilisation. In addition the reactive groups of

MC are sterically hindered. Thus, there might be too little space for an immobilisation reaction.

To avoid problems regarding poor reactivity and sterical influences MC derivatives containing a linker molecule will be synthesised by our cooperation[IX] partners to allow a sufficient immobilisation.

5.1.8 Betulinic acid (BA)

BA is a pentacyclic triterpene derived from the white birch tree (*Betula alba*). While its antiviral activity is well understood [91, 93, 95] the background of its anti-inflammatory and antitumorous effects remain unclear [88-90, 94]. To identify putative BA targets that are responsible for anti-inflammatory and antitumorous effects, fishing experiments using immobilised BA were performed.

The BA fishing was performed in a semiquantitative way where different amounts of ligand were immobilised to the matrix. Thus, protein bands on a silver stained SDS-PAGE that showed enhanced intensity by increasing the amounts of immobilised BA are meant to be provoked by specific binding events. In contrast, bands that show similar intensities for different amounts of immobilised ligand are considered to be unspecific. This strategy of analysis allows the identification of specific, ligand-bound proteins, even if they bind additionally in an unspecific way to the matrix.

For the BA fishing experiments in PMNL cell lysate, one band with an intensity pattern that correlates to the amount of immobilised BA could be identified. Lupeol was used as control compound because of its similarity with BA. In this way, on one hand less potential targets can be identified, on the other hand this smaller number of target candidates might be more specifically bound.

Massspectrometric identification showed that this band consists of two proteins, proteinase 3 (PR3) and cathepsin G (CG). These results could be confirmed by Western blot experiments. Testing BA in a CG activity assay showed that the activity of CG is not affected at all. In contrast, the activity of PR3 is affected specifically by BA and not by lupeol. Thus, BA can be seen as specific inhibitor for PR3 with an IC_{50} value of about 30 µM.

[IX] Prof. Dr. J. Jauch, Universität des Saarlandes, Organische Chemie II, Saarbrücken, Germany

PR3 like CG and the human leukocyte elastase (HLE) is one of three serine proteases released from neutrophil blood cells [153]. PR3 is a cationic serine protease basically contained in azurophil granules of human polymorphonuclear cells. Indeed, PR3 is also present in other granules of PMN [154] as well as in monocytes, basophils and mast cells [155]. PR3 plays a key role in the pathogenesis of Wegener´s granulomastitis, an inflammatory disease leading to respiratory burst and PMN degranulation and thereby to vascular inflammation and injury [156-157]. Furthermore, PR3 is known to activate precursor forms of cytokines such as TNFα, IL-8 and IL-1β, thus being involved in the regulation of inflammatory response [158-159]. Therefore, anti-inflammatory effects of BA could at least be partially explained by the inhibition of PR3.

5.1.9 Resveratrol

Since Resveratrol (RV) was described as the compound, that is responsible for beneficial effects of red wine [55], RV became a popular compound for medicinal- and pharmacological investigations. Up today, a vast variety of effects of RV were observed in clinical trials and bioassays [58-72, 74-76]. However, most effects of RV can not be explained on the molecular level.

RV fishing experiments and subsequent DIGE analysis led to the identification of a group of spots that were selectively fished with RV. Evaluation of single spots showed a volume ratio up to 1459% showing a very high selectivity for RV. The spots of the identified groups differed in their isoelectric point but not in their size, suggesting that one group consists of one protein in different posttranslational modification forms. Thus, one spot of each of the three identified groups was analysed by MS. All analysed spots were clearly identified as KH-domain splicing regulatory protein (KHSRP). Subsequent Western blot analysis confirmed the MS results and the selectivity of this interaction for RV.

KHSRP also known as far upstream binding protein (FUBP or FBP) belongs to the family of the turnover and translation regulatory mRNA-binding proteins (TTR-RBPs) [160]. Proteins of this family prominently influence oxidant-triggered gene expression. Although detailed mechanisms of TTR-RBPs are not completely understood, they are known to influence mRNA stability and translation [161-162]. KHSRP is known to

cause posttranslational decay of c-fos, c-jun, iNOS, TNF-α and IL-2 mRNA [160, 162-164].

KHSRP is directly phosphorylated by the upstream kinases PI3K and p38 MAPK [161]. Phosporylation by PI3K at Ser 193 promotes the association of KHSRP with 14-3-3 proteins. After association with 14-3-3, KHSRP looses its ability to enter the exosome and thereby its mRNA decay-promoting function. Phosphorylation of KHSRP by p38 MAPK abrogates the binding of KHSRP to its target mRNA [163, 165]. In addition to these effects, KHSRP is known to be a transcriptional activator of c-myc proto-oncogene.

Interestingly KHSRP causes posttranslational decay of iNOS, TNFα and interleukins and RV affects the expression or production of iNOS, TNFα [166-168] and IL-6. Thus, these known effects of RV could be explained by a functional influence of RV with KHSRP. However, the exact mode of interaction between RV and KHSRP requires more detailed evaluation.

5.1.10 Testosterone and progesterone

The classical role of testosterone and progesterone as gender specific steroid hormones is known and understood for a long time [132-133]. Besides this knowledge, only few attention was given to additional effects of these hormones especially regarding their influence on the incidence and progression of inflammatory disease. While healthcare professionals recognised in the last decade, that there are diseases that are closely related to steroid hormone levels [97-99, 101-104, 106, 108], more detailed investigations on the molecular level are matter of current pharmacological research [96]. In 2008 Pergola et. al. found out that leukotriene biosynthesis depends on androgen levels [96]. So further investigations via the target-fishing approach would certainly make sense.

To perform fishing-experiments using testosterone and progesterone as bait, four different immobilisation strategies were tested (see Fig. 43). Since testosterone modifications of C17 led to a loss of biological function in terms of ERK activation, C3 modified steroids have been used for the subsequent experiments.

First fishing experiments using 1D electrophoretic separation methods led to the discovery of HSA and karyopherin β (KPN-β) as binding partners of testosterone. Since the

testosterone/albumin interaction is known for a long time [143], this result shows that testosterone immobilised via the C3 position retains structural features required for interaction with (at least certain) known targets and is at least suitable to confirm known interactions.

Karyopherins are a class of proteins that regulate the import and export of macromolecules through the nuclear membrane. According to the direction of transport they are divided into importins and exportins [169-170]. For an importin mediated transport into the nucleus, proteins need a nuclear localisation signal sequence which is recognised by importin α. Thereafter KPN-β (also named importin β) binds to the imporin α-protein complex and shuttles it through the nuclear envelope. Inside the nucleus, binding of the small GTPase Ran causes the dissociation of the complex and thus, the nuclear release of the imported protein [171-175]. Furthermore KPN-β plays an essential role in nuclear assembly after mitosis [176-177]. Therefore, the interaction between KPN-β and testosterone could give new insights in the regulation of genomic testosterone effects that depend on a nuclear import of testosterone bound androgen receptors. Regarding the role of KPN-β in nuclear assembling after mitosis could be a starting point for an explanation of cellular regulation in testosterone dependent tumours. Nevertheless, the high affinity of KPN-β to the matrix itself impeded a further validation and characterisation of the testosterone KPN-β interaction. Thus, the relevance of this interaction remains unclear.

Comprehensive optimisation processes of the target-fishing approach led to enlarged possibilities in the identification of new target candidates. Above all, the 2D-DIGE approach allowed a high sensitive analysis of complex samples. Pursuing fishing experiments using the DIGE technique were performed in all three major blood cell types that are: PMNL, PBMC and platelets.

For fishing experiments performed in PMNL, vimentin (Vim), the leukocyte elastase inhibitor serpin B1, heat shock protein beta-1 and nicotinamide phosphorybosyltransferase (NAMPT) were identified as potential target candidates. In PBMC cell lysates, the heat shock protein beta- could be identified as potential targets and fishing experiments in platelet lysates again led to the identification of Heat shock protein 27. Subsequent Western blot analysis showed, that Vim is selectively bound to progesterone and not to testosterone in PBMC lysates, whereas fishing results in PMNL cell lysates did not show selectivity for one of both steroids.

The protein Vim as intermediate filament is part of the cytoskeleton. Unlike other components of the cytoskeleton, Vim seems not to be essential for cell viability. The collapsing of Vim networks does not induce cell shape changes [178], nor does it affect mitosis [179], cell growth or proliferation [145, 180-181]. Vim -/- mice show normal growth, cell morphology and physiological properties [182-183]. These findings suggest that the function of Vim is not limited to the classical cytoskeletal functions. In fact, Vim spans from the nucleus to the cell membrane [184] and is known to transmit mechanical signals into biological responses [148, 185]. Furthermore, Vim was shown to be essential for intracellular protein translocation [146] and Vim deficient cells showed decreased motility and chemotactic migration [186]. These findings implicate that Vim plays an important role in subcellular organisation.
It was also found that Vim upregulation is related to the metastatic potential of prostate cancer [187] and serum Vim is discussed as a surrogate marker for tumours [188]. In addition, Vim is involved in lymphocyte adhesion and transmigration [189]. The fact that Vim binds ERK and preserves its activation state while binding it [146] as well as the finding that Vim plays an important role in agonist stimulated ERK activation via β_3-adrenergic receptors [144, 147] gives a connection between Vim and inflammatory diseases. First concrete examples for the involvement of Vim in rheumatic diseases have already been shown [190]. Nevertheless, detailed mechanisms of the observed Vim effects are unclear and methods to analyse and characterise the functionality of Vim are not known by today. Thus, an evaluation of functional effects of a testosterone-Vim interaction is not possible.

Serine protease inhibitors (serpins) are the largest and most widely distributed super family of endogenous protease inhibitors. Serpins are involved in regulating physiological processes such as blood coagulation, complement activation, tumor suppression and inflammation [191-192]. Serpin B1 was initially found in high levels in monocytes and neutrophils as a fast acting elastase inhibitor and is therefore also known as monocyte/neutrophil elastase inhibitor (MNEI) [193]. It is one of the most efficient inhibitors of the neutrophil proteases HLE, CG and PR3 [194-195], thus implicating an important role in inflammatory diseases. In fact, serpin -/- mice are characterised by excessive inflammation and deficient immunological response to bacterial infections [196]. The stimulation of serpin activity or serpin release offers the possibility of anti-inflammatory pharmacological intervention that is yet not considered by today. However, Western

blot analysis of testosterone and progesterone fishing eluates showed that serpin B1 binds to both steroids. Thus, although testosterone and progesterone might have an influence on the Serpin B1 activity, this may not explain gender specific effects or selective sex hormone effects.

Visfatin was originally identified as the protein pre-B-cell colony enhancing factor (PBEF) [197]. In 2005 Fukuhara et al. discovered the adipokine function of PBEF in visceral fat and named it visceral fat adipokine or in brief visfatin (Vis) [198]. They could also show that Vis is mimicking insulin effects. Although it was originally found in visceral fat tissue, Vis is known today as an ubiquitiniously expressed protein [197, 199]. In addition, Vis was previously known as nicotinamide phosphoribosyl transferase (NAMPT) due to its enzymatic activity in the NAD synthesis [200]. The characterisation of this versatile protein can therefore be divided in three parts according to its function. (i) *Transferase activity*; whether the transferase activity of Vis directly correlates with its cytokine-like function is still not clear [201-202]. Nevertheless, it was shown that the inhibition of the transferase activity via FK866 at least, leads to a reduction of cytokine production in inflamatory cells [203]. Inhibition of Vis also caused depletion of intracellular NAD levels resulting in apoptotic cell death [203]. (ii) *Insulin mimicking effects*; it was shown that Vis directly binds to the insulin receptor [198]. Additionally the Vis plasma levels are elevated in type-II diabetes patients [204]. Experiments using Vis +/- mice showed that there is an impaired glucose tolerance in these mice. Taken together, there is an interesting correlation between Vis and glucose metabolism related diseases. The exact role of Vis is however poorly understood. The combination of insulin modulating effects of adipokines and their higher levels in obese people are suggested to explain at least a part of the pathogenesis of the metabolic syndrome. (iii) *Adipokine effects*; adipokines are cytokines classically released from adipocytes and are closely related to inflammatory diseases [201, 205]. Chen et al. showed that there is an increase of inflammatory markers at high Vis plasma levels [204]. Especially the pathogenesis of endothelian dysfunction and rheumatoid arthritis is known to be affected by Vis [206-210]. On the cellular level it was shown that Vis induces production and secretion of cytokines such as IL-1β, IL-6 and TNFα [211]. In addition, Vis causes AKT and ERK phosphorylation as well as PI3K upregulation [149] and thereby activation of eNOS [150]. An increase of NFκB activation by Vis could also be shown [212].

Regarding the gender specific prevalence for inflammatory diseases, Vis could be of interest concerning its role in inflammatory diseases and gender specific regulation. Although some authors excluded gender specific expression of Vis [213], other studies stated that there are gender differences. It was shown that there are higher levels of plasma Vis in girls [214] and that Vis levels elevated during pregnancy [215-216]. In addition, it was shown that testosterone in a nanomolar range decreases Vis expression [217].

Western blot analysis of testosterone and progesterone fishing eluates showed a selective binding of Vis to testosterone. Fishing experiments using isolated recombinant Vis indicated that Vis binds directly to testosterone but not to progesterone. Since Vis, like testosterone, increases the phosphorylation state of ERK [96, 149], synergistic effects of both compounds were evaluated. In fact, the addition of both testosterone and Vis led to a slightly higher phosphorylation state of ERK than one of these compounds alone. Because female plasma contains lower testosterone levels and higher Vis levels compared to male plasma, it may be reasonable that testosterone amplifies the Vis mediated ERK activation to achieve a similar basal ERK phosphorylation level in male. However, additional knowledge is needed to clearly understand the functionality of the testosterone/Vis interaction.

The heatshock protein 27 (HSP27) also known as heat shock protein B1 was first discovered in 1962 [218] and belongs to the family of small HSPs. It is ubiquitously and abundantly expressed [219] and plays a major role in cellular stress response. Furthermore, it is responsible for protein refolding [220] due to its chaperon activity [221-223].

The regulation of HSP27 is poorly understood. It is known that HSP27 dimers form oligomeres up to 1000 kDa [224-225] and phosphorylation causes detachment of dimers leading to decreased size of oligomers [226]. However, it is not clear whether large or small oligomers in phosphorylated or unphosphorylated state are the active form [224, 227-228].

HSP27 can be phosphorylated at Ser 15, 78 and 82 by AKT [229] or MK2 [230-231] via a p38 dependent [232-234] or independent [235-236] pathway. It regulates the integrity of microfilaments [237-238] and intermediate filaments [239] and binds directly to vimentin [240].

It was shown that HSP27 has cytoprotective properties during cellular stress [241] such as heat shock, cytokine release and growth factor release [223, 234, 236, 241-242]. In

addition it was shown that its expression is induced by heat shock, gamma radiation, UV light exposure, infections [243-245] and oxidative stress [246-247].

There is also a close link between HSP27 and inflammation [248-250]. It was shown, that HSP27 regulates the NFκB dependent production of inflammatory mediators TNFα, PGE_2 IL-8, IL-1α [251] and increases NFκB activity via increase of IκB-α degradation [252]. RNAi downregulation of HSP27 leads to an increase of IL-1 induced COX-2, IL-6 and IL-8 levels [249]. It was therefore suggested to be involved in the pathogenesis of atherosclerosis [253] in a gender-dependent manner [254-255]. Moreover HSP27 as potent antiapoptotic factor [246, 256] plays an important role in cancer. High levels of HSP27 in various tumors such as breast [257], gastric [258], ovarian [259], endometrial [260], glial [261], and prostate cancer [262] are correlated with poor prognosis, resistance [257, 263-268] and decreased chemosensitivity [265, 269-270]. As a result of these findings OGX-427 as a HSP27 antisense drug was developed and is currently tested in a phase I study. The role of HSP27 in cancer is closely related to steroid hormone pathways. Thus, the HSP27 gene is one of the most highly expressed genes in androgen independent prostate tumors [271] and is required for translocation [272], transcriptional action [273] and palmitoylation of PR and AR [272]. In turn, androgen bound AR induces rapid HSP27 phosphorylation [233]. Given that the PR [274-275] and AR [127, 276] mediate ERK signalling, connects HSP27 with gender specific regulation of inflammatory diseases.

Interestingly, HSP27 was fished in platelets with both, testosterone and progesterone. HSP27 was identified for two different, clearly separated spots once selectively with testosterone and one with progesterone. These two spots differed not in their size but rather in their isoelectric points. Given, that no isoforms of HSP27 are known so far, a closer look was taken on the phosphorylation state of HSP27 which may cause a shift in the IEP. Western blot analysis of fishing eluates obtained from fishing experiments using PBMC and PMNL cell lysate as protein source showed that HSP27 could be fished with both steroids with only a slightly higher affinity for testosterone. In contrast, the same experiments using platelet lysate as protein source showed a high selectivity for testosterone and it was not possible to pull down HSP27 with progesterone in platelets. Analysing the platelet-derived fishing eluates using a phosphor-specific p(Ser82)HSP27 antibody showed that it is possible to pull down pHSP27 with progesterone. Considering that the common HSP27 antibody recognises both, HSP27 and pHSP27 but the p(Ser82)HSP27 antibody only the phosphorylated form implies that the affinity of

pHSP27 to progesterone is higher than to testosterone, though there is also a prominent band for pHSP27 in the Western blot experiment for the testosterone sample. As mentioned above, it is unknown whether the phosphorylated or the unphosphorylated form of HSP27 can be seen as active form. Thus, it is difficult to speculate about the physiological relevance of phosphorylation dependent affinity of HSP27 to the sex hormones. Nevertheless, using isolated HSP27 for fishing experiments showed that the HSP27 testosterone interaction is a direct interaction. Taking into account that isolated HSP27 is completely unphosphorylated, no signal could be obtained for progesterone in this experiment. To get a closer insight in the physiological relevance of these interactions, HSP27 and pHSP27 levels in platelets from male and female donors were measured. Whereas the ratio between phosphorylated and unphosphorylated HSP27 were similar in platelets from both genders, platelets from female donors turned out to have distinct higher levels of both, HSP27 and pHSP27. Assuming that the interaction between HSP27 and testosterone or progesterone affects physiological procedures it seems to be reasonable that there is a stronger interaction between HSP27 and testosterone to compensate the lower HSP27 levels in male platelets.

To investigate whether steroids immobilised via the C3- or over the C7 position are more suitable for fishing experiments a multiplexed DIGE approach was performed. This way, a statistical evaluation of two 2D gels compared over a pooled internal standard gave insights into the distribution and selectivity of fished proteins. Using the same batch of cell lysate in same amounts for both experiments leads to reliable and comparable results. After exclusion of artificial spots, fishing experiments using C3-immobilised steroids lead to a discovery of 1472 spots whereas C7- derivatives were able to pull down 3937 proteins. In addition, the C7 derivatives showed with 72.0% a lower quota of unspecific bound protein than C3 derivatives with 80.7%. Thus, the combination of both, more fished proteins and more selective fished proteins indicates that the C7 derivatives are more suitable for fishing experiments. Taken together, 282 proteins could be selectively fished with one of the C3 derivatised steroids whereas C7 derivatised steroids were able to fish 1104 proteins selectively in the same cell lysate.

In the course of this study, so far unknown binding partners of testosterone and progesterone could be identified. Furthermore, it could be demonstrated, that the influence of

HSP27 and Vis on inflammation are affected by testosterone and progesterone respectively.

The finding, that testosterone amplifies the visfatin mediated ERK phosphorylation could at least partially explain and affirm the findings of Pergola et. al. [96]. Although, these results can not explain all observed effects regarding gender specific regulation of inflammatory processes, they can be seen as starting point for further investigations such as whole blood assays or in vivo experiments to determine the physiological relevance of these findings. The intention of these investigations is the comprehension of gender specific inflammatory effects that allows a rational, gender specific pharmacotherapy of inflammatory diseases.

6 Conclusion

Pull-down assays are suitable and valuable tools to evaluate drug-target interactions as well as a vast variety of other ligand protein interactions. In so-called target-fishing experiments a drug, covalently bound to an insoluble matrix, is incubated with a cell lysate as source of target proteins. Thus, drug bound proteins can be isolated and identified by appropriate protein analytics.
This work describes essential methodical improvements as well as the exemplary application of this method to identify targets for selected active compounds with so far uncharacterised anti-inflammatory properties.

The methodological part of this work we could achieve: (i) essential improvements of conditions for the target-fishing approach, (ii) innovative strategies for ligand immobilisation, (iii) the development of a biocompatible UV light cleavable linker system, (iv) the development of a semiquantitative fishing approach for determination of selective and unselective bound proteins as well as (v) the development of 2D-difference gelelectrophoresis for analysis of target-fishing eluates.
To improve general fishing conditions the influence of selected buffer systems, elution conditions, matrix modifying procedures and the preparation of cell lysates as source of target proteins was extensively evaluated. For the generation of novel fishing constructs, new immobilisation strategies had to be found. Thus, the immobilisation of compounds over non-reactive monoxime residues could be achieved. Furthermore, a novel method for immobilisation of ligands over keto- and aldehyde residues could successfully be developed. For this purpose a procedure for the production of carboxymethoxylamine activated matrices was established.
Since incubation of matrix-coupled ligands with proteins leads to both: specific protein-ligand interactions as well as unspecific protein-matrix interactions, we developed techniques that either allow the differentiation between selective and unselective bound proteins or essentially bypasses problems related to unspecific protein-matrix interactions. Thus, a semi-quantitative target-fishing approach as well as novel linker strategies were established.
We designed a biocompatible, daylight stable UV light reactive linker system which allows us to cleave off immobilised ligands together with the bound protein(s) simply by UV light exposure. This linker system is based on an o-nitrobenzylic core that can be

cleaved via norrish type II reaction. Using the known testosterone-androgen receptor interaction we could show that the use of this cleavable linker system results particularly in the elution of specific bound proteins.
To advance the analytics of fished proteins, the 2D-DIGE approach was established and modified to the requirements of the target-fishing approach.

In the course of this study the serine proteases proteinase 3 (PR3) and Cathepsin G (CG) were identified as binding partner of betulinic acid (BA). BA was shown to inhibit the enzymatic activity of PR3 with an IC_{50} value of 30 µM, whereas the activity of GC was not affected at all. Thus, BA can be seen as a selective PR3 inhibitor.
The use of a resveratrol (RV) derivative for target-fishing experiments resulted in the identification of the KH-domain splicing regulatory protein (KHSRP) as binding partner. The interaction of RV with KHSRP could be the starting point for the explanation of known in vivo effects of RV.
The steroid hormones testosterone and progesterone were used for target-fishing experiments in order to investigate non-genomic effects and the molecular reason for their influence in inflammatory diseases. The proteins Vimentin, Serin protease B1, Visfatin (Vis) and Heatshock protein 27 (HSP27) were identified as binding partners of steroid hormones. In more detailed experiments Vis was found to bind directly and selectively to testosterone. Furthermore, it could be shown, that testosterone amplifies the ERK activating properties of Vis, which gives new insights in the gender specific regulation of basal ERK phosphorylation levels.
HSP27 was identified as binding partner for both: testosterone and progesterone. It could be shown, that the binding affinity of both steroids to HSP27 depends on the phosphorylation state of HSP27. These findings could explain a stronger interaction between HSP27 and testosterone to compensate the lower HSP27 levels in male platelets.

7 Zusammenfassung

Der Pull-down Assay ist ein nützliches Werkzeug für die Identifizierung und Evaluierung von Arzneistoff Zielstrukturen. In sogenannten “Target-Fishing” Experimenten wird ein Arzneistoff oder eine pharmakologisch aktive Substanz kovalent an eine unlösliche Matrix gebunden und mit einen Zelllysat als Proteinquelle inkubiert. Proteine, die hierbei an den Arzneistoff binden, können isoliert und identifiziert werden. Diese Arbeit beschreibt grundlegende Verbesserungen sowie die beispielhafte Anwendung zur Identifizierung von Zielstrukturen für bislang uncharakterisierte, antientzündliche Wirkungen ausgewählter Substanzen.
Im methodischen Teil dieser Arbeit werden (i) grundlegende Verbesserungen experimenteller Bedingungen, (ii) innovative Strategien der Liganden Immobilisation, (iii) die Entwicklung eines biokompatiblen, UV Licht spaltbaren Linker-Systems, (iv) die Etablierung einer semi-quantitativen Fishing-Methode zur Unterscheidung zwischen selektiv und unselektiv gebundenen Targets sowie (v) die Etablierung der zweidimensionalen-differential Gelelektrophorese für die Analyse von Target-Fishing Eluaten, dargestellt.

Für die Verbesserung grundlegender, experimenteller Bedingungen des Target-Fishings wurde der Einfluss verschiedener Puffer-Systeme, Matrixmodifikationen und Methoden zur Herstellung von Zelllysaten untersucht. Es wurden neuartige Strategien zur Immobilisierung pharmakologisch aktiver Substanzen entwickelt. So konnten Liganden über Monoxim-Funktionen an Epoxy-aktivierte Matrices gebunden werden. Des Weiteren wurde ein Verfahren zur Herstellung Carboxymethoxylamin aktivierter Oberflächen für die Immobilisierung von Liganden über carbonyl Funktionen entwickelt.
Da die Inkubation von Matrix gebundenen Liganden sowohl zu spezifischen als auch zu unspezifischen Protein-Liganden Interaktionen führt, wurden Methoden entwickelt, um zwischen spezifischen und unspezifischen Interaktionen zu unterscheiden oder Probleme hinsichtlich unspezifisch gebundene Proteine generell zu umgehen. So wurden eine semi-quantitative fishing Methode und neuartige Verknüpfungsstrategien etabliert.
Wir konnten ein biokompatibles, Tageslicht stabiles UV Licht spaltbares Linker-System entwickeln, das eine Abspaltung des Liganden-gebundenen Targets durch Bestrahlung mit UV Licht ermöglicht. Die Funktionalität dieses Linker-Systems wurde anhand der bekannten Testosteron- Androgenrezeptor Interaktion unter Beweis gestellt. Um

zusätzlich die Analytik gefischter Proteine zu optimieren, wurde die 2D-DIGE Methode etabliert und an die Anforderungen des Target-Fishings angepasst.

Im Rahmen dieser Arbeit wurden die Serinproteasen Proteinase 3 (PR3) und Cathepsin G (CG) als Bindungspartner für Betulinsäure identifiziert. Es konnte gezeigt werden, dass Betulinsäure die Aktivität der PR3 mit einem IC_{50} Wert von 30 µM inhibieren konnte, während die Aktivität von CG nicht beeinflusst wurde. Damit kann BA als selektiver Inhibitor der PR3 gesehen werden.

Mit der Verwendung von Resveratrol (RV) als Ligand für target-fishing Experimente konnte das KH-domain splicing regulatory protein (KHSRP) als Bindungspartner für RV identifiziert werden. Dies bietet einen neuartiger Ansatzpunkt für die Erklärung bekannter in vivo Effekte des Resveratrols.

Des weiteren wurden die Steroidhormone Testosteron und Progesteron für target-fishing Experimente verwendet, um die physiologischen, nichtgenomischen und anti-inflammatorischen Effekte dieser Substanzen zu untersuchen. Hierbei konnten die Proteine Vimentin, Serin Protease Inhibitor B1, Visfatin (Vis) und Heatshock protein 27 (HSP27) als Bindungspartner dieser Steroidhormone identifiziert werden. In weiteren Experimenten konnte gezeigt werden, dass Vis direkt und selekiv an Testosteron bindet. Wir konnten des Weiteren zeigen, dass Testosteron die ERK aktivierenden Eigenschaften des Vis verstärkt und damit neue Erkenntnisse über die geschlechtsspezifische, basale Regulation der ERK-Phosphorylierung erbracht hat.

HSP27 wurde sowohl als Bindungspartner für Testosteron als auch für Progesteron identifiziert. Es konnte gezeigt werden, dass die Bindungsaffinität beider Steroide vom Phosphorylierungsstatus des HSP27 abhängt und Testosteron eine höhere Affinität zu unphosphoryliertem HSP27 hat, während Progesteron bevorzugt an die phosphorylierte Form bindet.

8 Literature

1. Harrison, P.M., et al., *A question of size: the eukaryotic proteome and the problems in defining it.* Nucleic Acids Res, 2002. **30**(5): p. 1083-90.
2. Castrignano, T., et al., *ASPicDB: a database resource for alternative splicing analysis.* Bioinformatics, 2008. **24**(10): p. 1300-4.
3. Shovman, O., et al., *Antiinflammatory and immunomodulatory properties of statins.* Immunol Res, 2002. **25**(3): p. 271-85.
4. Schonbeck, U. and P. Libby, *Inflammation, immunity, and HMG-CoA reductase inhibitors: statins as antiinflammatory agents?* Circulation, 2004. **109**(21 Suppl 1): p. II18-26.
5. Ezerzer, C., et al., *Chemokine receptor-derived peptides as multi-target drug leads for the treatment of inflammatory diseases.* Peptides, 2009. **30**(7): p. 1296-305.
6. Espinoza-Fonseca, L.M., *Knowledgebase for addiction-related genes: is it possible an extrapolation to rational multi-target drug design?* Bioorg Med Chem, 2008. **16**(20): p. 9346-8.
7. Guruswamy, S. and C.V. Rao, *Multi-Target Approaches in Colon Cancer Chemoprevention Based on Systems Biology of Tumor Cell-Signaling.* Gene Regul Syst Bio, 2008. **2**: p. 163-176.
8. Petrelli, A. and S. Giordano, *From single- to multi-target drugs in cancer therapy: when aspecificity becomes an advantage.* Curr Med Chem, 2008. **15**(5): p. 422-32.
9. Zimmermann, G.R., J. Lehar, and C.T. Keith, *Multi-target therapeutics: when the whole is greater than the sum of the parts.* Drug Discov Today, 2007. **12**(1-2): p. 34-42.
10. Burdine, L. and T. Kodadek, *Target identification in chemical genetics: the (often) missing link.* Chem Biol, 2004. **11**(5): p. 593-7.
11. Tausch, L., et al., *Identification of human cathepsin G as a functional target of boswellic acids from the anti-inflammatory remedy frankincense.* J Immunol, 2009. **183**(5): p. 3433-42.
12. Evans, M.J. and B.F. Cravatt, *Mechanism-based profiling of enzyme families.* Chem Rev, 2006. **106**(8): p. 3279-301.
13. Fonovic, M. and M. Bogyo, *Activity-based probes as a tool for functional proteomic analysis of proteases.* Expert Rev Proteomics, 2008. **5**(5): p. 721-30.
14. Jessani, N. and B.F. Cravatt, *The development and application of methods for activity-based protein profiling.* Curr Opin Chem Biol, 2004. **8**(1): p. 54-9.
15. Uttamchandani, M., et al., *Activity-based protein profiling: new developments and directions in functional proteomics.* Chembiochem, 2008. **9**(5): p. 667-75.
16. Cravatt, B.F., A.T. Wright, and J.W. Kozarich, *Activity-based protein profiling: from enzyme chemistry to proteomic chemistry.* Annual Review of Biochemistry, 2008. **77**: p. 383-414.
17. Sieber, S.A. and B.F. Cravatt, *Analytical platforms for activity-based protein profiling--exploiting the versatility of chemistry for functional proteomics.* Chem Commun (Camb), 2006(22): p. 2311-9.
18. Taunton, J., C.A. Hassig, and S.L. Schreiber, *A mammalian histone deacetylase related to the yeast transcriptional regulator Rpd3p.* Science, 1996. **272**(5260): p. 408-11.
19. Harding, M.W., et al., *A receptor for the immunosuppressant FK506 is a cis-trans peptidyl-prolyl isomerase.* Nature, 1989. **341**(6244): p. 758-60.

20. Allen, R.A., A.J. Jesaitis, and C.G. Cochrane, *Photoaffinity labelling of N-formyl peptide receptors.* Pharmacol Ther, 1987. **33**(2-3): p. 333-48.
21. Holmes, C.P. and D.G. Jones, *Reagents for Combinatorial Organic-Synthesis - Development of a New O-Nitrobenzyl Photolabile Linker for Solid-Phase Synthesis.* Journal of Organic Chemistry, 1995. **60**(8): p. 2318-2319.
22. Norrish, R.G.W., Trans. Faraday Soc., 1937. **33**: p. 1521-1528.
23. Lloyd-Williams, P., F. Albericio, and E. Giralt, *Convergent solid-phase peptide synthesis. VIII. Synthesis, using a photolabile resin, and purification of a methionine-containing protected peptide.* Int J Pept Protein Res, 1991. **37**(1): p. 58-60.
24. Rich, D.H.G., S. K., *Preparation of a New o-Nitrobenzyl Resin for Solid-Phase Synthesis of tert-Butyloxycarbonyl-Protected Peptide Acids.* JOURNAL OF THE AMERICAN CHEMICAL SOCIETY, 1974. **97**(6): p. 1575-1579.
25. Laemmli, U.K., *Cleavage of structural proteins during the assembly of the head of bacteriophage T4.* Nature, 1970. **227**(5259): p. 680-5.
26. Unlu, M., M.E. Morgan, and J.S. Minden, *Difference gel electrophoresis: a single gel method for detecting changes in protein extracts.* Electrophoresis, 1997. **18**(11): p. 2071-7.
27. Minden, J.S., et al., *Difference gel electrophoresis.* Electrophoresis, 2009. **30 Suppl 1**: p. S156-61.
28. Marouga, R., S. David, and E. Hawkins, *The development of the DIGE system: 2D fluorescence difference gel analysis technology.* Anal Bioanal Chem, 2005. **382**(3): p. 669-78.
29. Bernocco, S., et al., *Sequential detergent fractionation of primary neurons for proteomics studies.* Proteomics, 2008. **8**(5): p. 930-8.
30. Schmidt, H., et al., *2-D DIGE analyses of enriched secretory lysosomes reveal heterogeneous profiles of functionally relevant proteins in leukemic and activated human NK cells.* Proteomics, 2008. **8**(14): p. 2911-25.
31. Islinger, M., et al., *Insights into the membrane proteome of rat liver peroxisomes: microsomal glutathione-S-transferase is shared by both subcellular compartments.* Proteomics, 2006. **6**(3): p. 804-16.
32. Lilley, K.S. and P. Dupree, *Methods of quantitative proteomics and their application to plant organelle characterization.* J Exp Bot, 2006. **57**(7): p. 1493-9.
33. Aggarwal, B.B., *Inflammation, a silent killer in cancer is not so silent!* Curr Opin Pharmacol, 2009. **9**(4): p. 347-50.
34. Karin, M., *Nuclear factor-kappaB in cancer development and progression.* Nature, 2006. **441**(7092): p. 431-6.
35. de Martel, C. and S. Franceschi, *Infections and cancer: established associations and new hypotheses.* Crit Rev Oncol Hematol, 2009. **70**(3): p. 183-94.
36. Soberman, R.J. and P. Christmas, *The organization and consequences of eicosanoid signaling.* J Clin Invest, 2003. **111**(8): p. 1107-13.
37. Morse, H., *Ueber eine neue Dartellungsmethode der Acetylamidophenole.* Ber Deutscher Chem Ges, 1878. **11**: p. 232-233.
38. Mering, v., *Beitraege zur Kenntniss der Antipyretica.* Ther Monatsch, 1893. **7**: p. 577-587.
39. Robert, C., et al., *Quantitative analysis of the scientific literature on acetaminophen in medicine and biology: a 2003-2005 study.* Fundam Clin Pharmacol, 2009. **23**(2): p. 159-68.
40. Tripathy, D. and P. Grammas, *Acetaminophen inhibits neuronal inflammation and protects neurons from oxidative stress.* J Neuroinflammation, 2009. **6**: p. 10.

41. Lee, Y.S., et al., *Acetaminophen selectively suppresses peripheral prostaglandin E2 release and increases COX-2 gene expression in a clinical model of acute inflammation.* Pain, 2007. **129**(3): p. 279-86.
42. Flower, R.J. and J.R. Vane, *Inhibition of prostaglandin synthetase in brain explains the anti-pyretic activity of paracetamol (4-acetamidophenol).* Nature, 1972. **240**(5381): p. 410-1.
43. Graham, G.G. and K.F. Scott, *Mechanism of action of paracetamol.* Am J Ther, 2005. **12**(1): p. 46-55.
44. Kis, B., J.A. Snipes, and D.W. Busija, *Acetaminophen and the cyclooxygenase-3 puzzle: sorting out facts, fictions, and uncertainties.* J Pharmacol Exp Ther, 2005. **315**(1): p. 1-7.
45. Pickering, G., et al., *Analgesic effect of acetaminophen in humans: first evidence of a central serotonergic mechanism.* Clin Pharmacol Ther, 2006. **79**(4): p. 371-8.
46. Sandrini, M., et al., *Effect of acute and repeated administration of paracetamol on opioidergic and serotonergic systems in rats.* Inflamm Res, 2007. **56**(4): p. 139-42.
47. Aronoff, D.M., J.A. Oates, and O. Boutaud, *New insights into the mechanism of action of acetaminophen: Its clinical pharmacologic characteristics reflect its inhibition of the two prostaglandin H2 synthases.* Clin Pharmacol Ther, 2006. **79**(1): p. 9-19.
48. Ruggieri, V., et al., *Differential involvement of opioidergic and serotonergic systems in the antinociceptive activity of N-arachidonoyl-phenolamine (AM404) in the rat: comparison with paracetamol.* Naunyn Schmiedebergs Arch Pharmacol, 2008. **377**(3): p. 219-29.
49. Hogestatt, E.D., et al., *Conversion of acetaminophen to the bioactive N-acylphenolamine AM404 via fatty acid amide hydrolase-dependent arachidonic acid conjugation in the nervous system.* J Biol Chem, 2005. **280**(36): p. 31405-12.
50. Zygmunt, P.M., et al., *The anandamide transport inhibitor AM404 activates vanilloid receptors.* Eur J Pharmacol, 2000. **396**(1): p. 39-42.
51. Chandrasekharan, N.V., et al., *COX-3, a cyclooxygenase-1 variant inhibited by acetaminophen and other analgesic/antipyretic drugs: cloning, structure, and expression.* Proc Natl Acad Sci U S A, 2002. **99**(21): p. 13926-31.
52. Davies, N.M., et al., *Cyclooxygenase-3: axiom, dogma, anomaly, enigma or splice error?--Not as easy as 1, 2, 3.* J Pharm Pharm Sci, 2004. **7**(2): p. 217-26.
53. Boutaud, O., et al., *Determinants of the cellular specificity of acetaminophen as an inhibitor of prostaglandin H(2) synthases.* Proc Natl Acad Sci U S A, 2002. **99**(10): p. 7130-5.
54. Nonomura, A., H. Kanagawa, and A. Makimoto, *Chemical constituents of polygonaceus plants. I. Studies on the components of Ko-jo-kon (Polygonu cuspidatum SIEB et ZUCC).* Yakugaku Zasshi, 1963. **83**: p. 988-90.
55. Siemann, E.H. and L.L. Creasy, *Concentration of the Phytoalexin Resveratrol in Wine.* American Journal of Enology and Viticulture, 1992. **43**(1): p. 49-52.
56. Ferrieres, J., *The French paradox: lessons for other countries.* Heart, 2004. **90**(1): p. 107-11.
57. Constant, J., *Alcohol, ischemic heart disease, and the French paradox.* Clin Cardiol, 1997. **20**(5): p. 420-4.
58. Rubiolo, J.A., G. Mithieux, and F.V. Vega, *Resveratrol protects primary rat hepatocytes against oxidative stress damage: activation of the Nrf2 transcription*

factor and augmented activities of antioxidant enzymes. Eur J Pharmacol, 2008. **591**(1-3): p. 66-72.
59. Li, Y., Z. Cao, and H. Zhu, *Upregulation of endogenous antioxidants and phase 2 enzymes by the red wine polyphenol, resveratrol in cultured aortic smooth muscle cells leads to cytoprotection against oxidative and electrophilic stress.* Pharmacol Res, 2006. **53**(1): p. 6-15.
60. Orallo, F., *Comparative studies of the antioxidant effects of cis- and trans-resveratrol.* Curr Med Chem, 2006. **13**(1): p. 87-98.
61. Murias, M., et al., *Antioxidant, prooxidant and cytotoxic activity of hydroxylated resveratrol analogues: structure-activity relationship.* Biochem Pharmacol, 2005. **69**(6): p. 903-12.
62. Haider, U.G., et al., *Resveratrol increases serine15-phosphorylated but transcriptionally impaired p53 and induces a reversible DNA replication block in serum-activated vascular smooth muscle cells.* Mol Pharmacol, 2003. **63**(4): p. 925-32.
63. Tyagi, A., et al., *Resveratrol causes Cdc2-tyr15 phosphorylation via ATM/ATR-Chk1/2-Cdc25C pathway as a central mechanism for S phase arrest in human ovarian carcinoma Ovcar-3 cells.* Carcinogenesis, 2005. **26**(11): p. 1978-87.
64. Fontecave, M., et al., *Resveratrol, a remarkable inhibitor of ribonucleotide reductase.* FEBS Lett, 1998. **421**(3): p. 277-9.
65. Sun, N.J., et al., *DNA polymerase and topoisomerase II inhibitors from Psoralea corylifolia.* J Nat Prod, 1998. **61**(3): p. 362-6.
66. Udenigwe, C.C., et al., *Potential of resveratrol in anticancer and anti-inflammatory therapy.* Nutr Rev, 2008. **66**(8): p. 445-54.
67. Das, S. and D.K. Das, *Anti-inflammatory responses of resveratrol.* Inflamm Allergy Drug Targets, 2007. **6**(3): p. 168-73.
68. Haider, U.G., et al., *Resveratrol suppresses angiotensin II-induced Akt/protein kinase B and p70 S6 kinase phosphorylation and subsequent hypertrophy in rat aortic smooth muscle cells.* Mol Pharmacol, 2002. **62**(4): p. 772-7.
69. Haider, U.G., et al., *Resveratrol inhibits angiotensin II- and epidermal growth factor-mediated Akt activation: role of Gab1 and Shp2.* Mol Pharmacol, 2005. **68**(1): p. 41-8.
70. Koeberle, A. and O. Werz, *Inhibitors of the microsomal prostaglandin E(2) synthase-1 as alternative to non steroidal anti-inflammatory drugs (NSAIDs)--a critical review.* Curr Med Chem, 2009. **16**(32): p. 4274-96.
71. Marambaud, P., H. Zhao, and P. Davies, *Resveratrol promotes clearance of Alzheimer's disease amyloid-beta peptides.* J Biol Chem, 2005. **280**(45): p. 37377-82.
72. Baur, J.A., et al., *Resveratrol improves health and survival of mice on a high-calorie diet.* Nature, 2006. **444**(7117): p. 337-42.
73. Sharafkhaneh, A., et al., *The potential role of natural agents in treatment of airway inflammation.* Ther Adv Respir Dis, 2007. **1**(2): p. 105-20.
74. Culpitt, S.V., et al., *Inhibition by red wine extract, resveratrol, of cytokine release by alveolar macrophages in COPD.* Thorax, 2003. **58**(11): p. 942-6.
75. Bishayee, A., et al., *Resveratrol Suppresses Oxidative Stress and Inflammatory Response in Diethylnitrosamine-Initiated Rat Hepatocarcinogenesis.* Cancer Prev Res (Phila Pa), 2010.
76. Wood, L.G., P.A. Wark, and M.L. Garg, *Antioxidant and Antiinflammatory Effects of Resveratrol in Airway Disease.* Antioxid Redox Signal, 2010.
77. *Chinese Pharmacopoeia*. 1995, People´s Health Publisher: Beijing.

78. Damiens, E., et al., *Anti-mitotic properties of indirubin-3'-monoxime, a CDK/GSK-3 inhibitor: induction of endoreplication following prophase arrest.* Oncogene, 2001. **20**(29): p. 3786-97.
79. Hoessel, R., et al., *Indirubin, the active constituent of a Chinese antileukaemia medicine, inhibits cyclin-dependent kinases.* Nat Cell Biol, 1999. **1**(1): p. 60-7.
80. Li, C., *The synthesis, antileukemic activity, and crystal structures of indirubin derivates.* Bull. Chem. Soc. Jpn, 1996. **69**: p. 1621-1627.
81. Ji, X.J. and F.R. Zhang, *[Studies on antineoplastic action of indirubin derivatives and analogs and their structure-activity relationships].* Yao Xue Xue Bao, 1985. **20**(2): p. 137-9.
82. Lin, Y.K., et al., *Anti-inflammatory effects of the extract of indigo naturalis in human neutrophils.* J Ethnopharmacol, 2009. **125**(1): p. 51-8.
83. Kunikata, T., et al., *Indirubin inhibits inflammatory reactions in delayed-type hypersensitivity.* Eur J Pharmacol, 2000. **410**(1): p. 93-100.
84. Appendino, G., et al., *Oligomeric acylphloroglucinols from myrtle (Myrtus communis).* J Nat Prod, 2002. **65**(3): p. 334-8.
85. Koeberle, A., et al., *Myrtucommulone, a natural acylphloroglucinol, inhibits microsomal prostaglandin E(2) synthase-1.* Br J Pharmacol, 2009. **156**(6): p. 952-61.
86. Feisst, C., et al., *Identification of molecular targets of the oligomeric nonprenylated acylphloroglucinols from Myrtus communis and their implication as anti-inflammatory compounds.* J Pharmacol Exp Ther, 2005. **315**(1): p. 389-96.
87. Tretiakova, I., et al., *Myrtucommulone from Myrtus communis induces apoptosis in cancer cells via the mitochondrial pathway involving caspase-9.* Apoptosis, 2008. **13**(1): p. 119-31.
88. Alakurtti, S., et al., *Pharmacological properties of the ubiquitous natural product betulin.* Eur J Pharm Sci, 2006. **29**(1): p. 1-13.
89. Mullauer, F.B., J.H. Kessler, and J.P. Medema, *Betulinic acid, a natural compound with potent anticancer effects.* Anticancer Drugs, 2010. **21**(3): p. 215-27.
90. Fulda, S., *Betulinic acid: a natural product with anticancer activity.* Mol Nutr Food Res, 2009. **53**(1): p. 140-6.
91. Fujioka, T., et al., *Anti-AIDS agents, 11. Betulinic acid and platanic acid as anti-HIV principles from Syzigium claviflorum, and the anti-HIV activity of structurally related triterpenoids.* J Nat Prod, 1994. **57**(2): p. 243-7.
92. Connor, A., et al., *An oral human drug absorption study to assess the impact of site of delivery on the bioavailability of bevirimat.* J Clin Pharmacol, 2009. **49**(5): p. 606-12.
93. Smith, P.F., et al., *Phase I and II study of the safety, virologic effect, and pharmacokinetics/pharmacodynamics of single-dose 3-o-(3',3'-dimethylsuccinyl)betulinic acid (bevirimat) against human immunodeficiency virus infection.* Antimicrob Agents Chemother, 2007. **51**(10): p. 3574-81.
94. Pisha, E., et al., *Discovery of betulinic acid as a selective inhibitor of human melanoma that functions by induction of apoptosis.* Nat Med, 1995. **1**(10): p. 1046-51.
95. Reutrakul, V., et al., *Anti-HIV-1 and anti-inflammatory lupanes from the leaves, twigs, and resin of Garcinia hanburyi.* Planta Med, 2010. **76**(4): p. 368-71.
96. Pergola, C., et al., *ERK-mediated regulation of leukotriene biosynthesis by androgens: a molecular basis for gender differences in inflammation and asthma.* Proc Natl Acad Sci U S A, 2008. **105**(50): p. 19881-6.

97. Sears, M.R., et al., *Atopy in childhood. I. Gender and allergen related risks for development of hay fever and asthma.* Clin Exp Allergy, 1993. **23**(11): p. 941-8.
98. Zandman-Goddard, G., E. Peeva, and Y. Shoenfeld, *Gender and autoimmunity.* Autoimmun Rev, 2007. **6**(6): p. 366-72.
99. Gissler, M., et al., *Boys have more health problems in childhood than girls: follow-up of the 1987 Finnish birth cohort.* Acta Paediatr, 1999. **88**(3): p. 310-4.
100. Ensom, M.H., *Gender-based differences and menstrual cycle-related changes in specific diseases: implications for pharmacotherapy.* Pharmacotherapy, 2000. **20**(5): p. 523-39.
101. Brower, V., *Sex matters. In sickness and in health, men and women are clearly different.* EMBO Rep, 2002. **3**(10): p. 921-3.
102. Dodge, R.R. and B. Burrows, *The prevalence and incidence of asthma and asthma-like symptoms in a general population sample.* Am Rev Respir Dis, 1980. **122**(4): p. 567-75.
103. Nelson, J.L. and M. Ostensen, *Pregnancy and rheumatoid arthritis.* Rheum Dis Clin North Am, 1997. **23**(1): p. 195-212.
104. Confavreux, C., et al., *Rate of pregnancy-related relapse in multiple sclerosis. Pregnancy in Multiple Sclerosis Group.* N Engl J Med, 1998. **339**(5): p. 285-91.
105. Wilder, R.L., *Neuroendocrine-immune system interactions and autoimmunity.* Annu Rev Immunol, 1995. **13**: p. 307-38.
106. Griffin, A.C. and C.C. Whitacre, *Sex and strain differences in the circadian rhythm fluctuation of endocrine and immune function in the rat: implications for rodent models of autoimmune disease.* J Neuroimmunol, 1991. **35**(1-3): p. 53-64.
107. Hermes, G.L., et al., *Social isolation and the inflammatory response: sex differences in the enduring effects of a prior stressor.* Am J Physiol Regul Integr Comp Physiol, 2006. **290**(2): p. R273-82.
108. Bouman, A., M.J. Heineman, and M.M. Faas, *Sex hormones and the immune response in humans.* Hum Reprod Update, 2005. **11**(4): p. 411-23.
109. House, J.S., C. Robbins, and H.L. Metzner, *The association of social relationships and activities with mortality: prospective evidence from the Tecumseh Community Health Study.* Am J Epidemiol, 1982. **116**(1): p. 123-40.
110. Wang, J., et al., *Is lipstick associated with the development of systemic lupus erythematosus (SLE)?* Clin Rheumatol, 2008. **27**(9): p. 1183-7.
111. Zhou, Z.X., et al., *The androgen receptor: an overview.* Recent Prog Horm Res, 1994. **49**: p. 249-74.
112. Heinlein, C.A. and C. Chang, *Androgen receptor (AR) coregulators: an overview.* Endocr Rev, 2002. **23**(2): p. 175-200.
113. Beato, M., *Gene regulation by steroid hormones.* Cell, 1989. **56**(3): p. 335-44.
114. Roy, A.K., et al., *Regulation of androgen action.* Vitam Horm, 1999. **55**: p. 309-52.
115. Mangelsdorf, D.J., et al., *The nuclear receptor superfamily: the second decade.* Cell, 1995. **83**(6): p. 835-9.
116. Kastner, P., et al., *Two distinct estrogen-regulated promoters generate transcripts encoding the two functionally different human progesterone receptor forms A and B.* EMBO J, 1990. **9**(5): p. 1603-14.
117. Wilson, C.M. and M.J. McPhaul, *A and B forms of the androgen receptor are expressed in a variety of human tissues.* Mol Cell Endocrinol, 1996. **120**(1): p. 51-7.

118. Lieberherr, M. and B. Grosse, *Androgens increase intracellular calcium concentration and inositol 1,4,5-trisphosphate and diacylglycerol formation via a pertussis toxin-sensitive G-protein.* J Biol Chem, 1994. **269**(10): p. 7217-23.
119. Gorczynska, E. and D.J. Handelsman, *Androgens rapidly increase the cytosolic calcium concentration in Sertoli cells.* Endocrinology, 1995. **136**(5): p. 2052-9.
120. Steinsapir, J., R. Socci, and P. Reinach, *Effects of androgen on intracellular calcium of LNCaP cells.* Biochem Biophys Res Commun, 1991. **179**(1): p. 90-6.
121. Benten, W.P., et al., *Testosterone induces Ca2+ influx via non-genomic surface receptors in activated T cells.* FEBS Lett, 1997. **407**(2): p. 211-4.
122. Duval, D., S. Durant, and F. Homo-Delarche, *Non-genomic effects of steroids. Interactions of steroid molecules with membrane structures and functions.* Biochim Biophys Acta, 1983. **737**(3-4): p. 409-42.
123. Van Bommel, T., T. Marsen, and H. Bojar, *Effects of high-dose medroxyprogesterone acetate and various other steroid hormones on plasma membrane lipid mobility in CAMA-1 mammary cancer cells.* Anticancer Res, 1987. **7**(6): p. 1217-23.
124. Madden, T.D., D. Chapman, and P.J. Quinn, *Cholesterol modulates activity of calcium-dependent ATPase of the sarcoplasmic reticulum.* Nature, 1979. **279**(5713): p. 538-41.
125. Yeagle, P.L., J. Young, and D. Rice, *Effects of cholesterol on (Na+,K+)-ATPase ATP hydrolyzing activity in bovine kidney.* Biochemistry, 1988. **27**(17): p. 6449-52.
126. Deliconstantinos, G., *Structure activity relationship of cholesterol and steroid hormones with respect to their effects on the Ca2+-stimulated ATPase and lipid fluidity of synaptosomal plasma membranes from dog and rabbit brain.* Comp Biochem Physiol B, 1988. **89**(3): p. 585-94.
127. Migliaccio, A., et al., *Steroid-induced androgen receptor-oestradiol receptor beta-Src complex triggers prostate cancer cell proliferation.* EMBO J, 2000. **19**(20): p. 5406-17.
128. Cheng, J., S.C. Watkins, and W.H. Walker, *Testosterone activates mitogen-activated protein kinase via Src kinase and the epidermal growth factor receptor in sertoli cells.* Endocrinology, 2007. **148**(5): p. 2066-74.
129. Fortunati, N., *Sex hormone-binding globulin: not only a transport protein. What news is around the corner?* J Endocrinol Invest, 1999. **22**(3): p. 223-34.
130. Fortunati, N., et al., *Sex steroid binding protein exerts a negative control on estradiol action in MCF-7 cells (human breast cancer) through cyclic adenosine 3',5'-monophosphate and protein kinase A.* Endocrinology, 1996. **137**(2): p. 686-92.
131. Wiemann, J.N., D.K. Clifton, and R.A. Steiner, *Gonadotropin-releasing hormone messenger ribonucleic acid levels are unaltered with changes in the gonadal hormone milieu of the adult male rat.* Endocrinology, 1990. **127**(2): p. 523-32.
132. Cicero, T.J., B.A. Schainker, and E.R. Meyer, *Endogenous opioids participate in the regulation of the hypothalamus-pituitary-luteinizing hormone axis and testosterone's negative feedback control of luteinizing hormone.* Endocrinology, 1979. **104**(5): p. 1286-91.
133. Shin, S.H. and C.J. Howitt, *Effect of testosterone on hypothalamic LH-RH content.* Neuroendocrinology, 1976. **21**(2): p. 165-74.
134. Huang, X. and R.E. Harlan, *Absence of androgen receptors in LHRH immunoreactive neurons.* Brain Res, 1993. **624**(1-2): p. 309-11.

135. Herbison, A.E., et al., *Androgen receptor-immunoreactive cells in ram hypothalamus: distribution and co-localization patterns with gonadotropin-releasing hormone, somatostatin and tyrosine hydroxylase.* Neuroendocrinology, 1996. **63**(2): p. 120-31.
136. Werz, O., et al., *Activation of 5-lipoxygenase by cell stress is calcium independent in human polymorphonuclear leukocytes.* Blood, 2002. **99**(3): p. 1044-52.
137. Merrifield, r.B., *SOLID PHASE PEPTIDE SYNTHESIS .1. SYNTHESIS OF A TETRAPEPTIDE.* JOURNAL OF THE AMERICAN CHEMICAL SOCIETY, 1963. **85**.
138. Merrifield, B., *Solid-Phase Synthesis.* Science, 1986. **232**(4748): p. 341-347.
139. Hoschle, B., V. Gnau, and D. Jendrossek, *Methylcrotonyl-CoA and geranyl-CoA carboxylases are involved in leucine/isovalerate utilization (Liu) and acyclic terpene utilization (Atu), and are encoded by liuB/liuD and atuC/atuF, in Pseudomonas aeruginosa.* Microbiology, 2005. **151**(Pt 11): p. 3649-56.
140. Grady, J.K., N.D. Chasteen, and D.C. Harris, *Radicals from "Good's" buffers.* Anal Biochem, 1988. **173**(1): p. 111-5.
141. Holmes, C.P., *Model studies for new o-nitrobenzyl photolabile linkers: Substituent effects on the rates of photochemical cleavage.* Journal of Organic Chemistry, 1997. **62**(8): p. 2370-2380.
142. Kurbanov, S., *Investigation of the alkylation of aldoximes and ketoximes with α-epoxides.* Organic Preparations and Procedures Inc., 1999. **31**(6): p. 681-688.
143. Eik-Nes, K., et al., *The binding of steroids to protein. I. Solubility determinations.* J Biol Chem, 1954. **206**(1): p. 411-9.
144. Kumar, N., et al., *Requirement of vimentin filament assembly for beta3-adrenergic receptor activation of ERK MAP kinase and lipolysis.* J Biol Chem, 2007. **282**(12): p. 9244-50.
145. Moisan, E., S. Chiasson, and D. Girard, *The intriguing normal acute inflammatory response in mice lacking vimentin.* Clin Exp Immunol, 2007. **150**(1): p. 158-68.
146. Perlson, E., et al., *Vimentin-dependent spatial translocation of an activated MAP kinase in injured nerve.* Neuron, 2005. **45**(5): p. 715-26.
147. Shen, W.J., et al., *Vimentin is a functional partner of hormone sensitive lipase and facilitates lipolysis.* Journal of Proteome Research, 2010. **9**(4): p. 1786-94.
148. Wang, N. and D. Stamenovic, *Mechanics of vimentin intermediate filaments.* J Muscle Res Cell Motil, 2002. **23**(5-6): p. 535-40.
149. Adya, R., et al., *Visfatin induces human endothelial VEGF and MMP-2/9 production via MAPK and PI3K/Akt signalling pathways: novel insights into visfatin-induced angiogenesis.* Cardiovasc Res, 2008. **78**(2): p. 356-65.
150. Lovren, F., et al., *Visfatin activates eNOS via Akt and MAP kinases and improves endothelial cell function and angiogenesis in vitro and in vivo: translational implications for atherosclerosis.* Am J Physiol Endocrinol Metab, 2009. **296**(6): p. E1440-9.
151. Rossi, A., et al., *Myrtucommulone from Myrtus communis exhibits potent anti-inflammatory effectiveness in vivo.* J Pharmacol Exp Ther, 2009. **329**(1): p. 76-86.
152. Blaesius, D., *Elucidation of molecular mechanisms of apoptosis induction by myrtucommulone from Myrtus communis.* Dissertation, 2009.
153. Owen, C.A. and E.J. Campbell, *The cell biology of leukocyte-mediated proteolysis.* J Leukoc Biol, 1999. **65**(2): p. 137-50.

154. Witko-Sarsat, V., et al., *Presence of proteinase 3 in secretory vesicles: evidence of a novel, highly mobilizable intracellular pool distinct from azurophil granules.* Blood, 1999. **94**(7): p. 2487-96.
155. Braun, M.G., et al., *Proteinase 3, the target antigen of anticytoplasmic antibodies circulating in Wegener's granulomatosis. Immunolocalization in normal and pathologic tissues.* Am J Pathol, 1991. **139**(4): p. 831-8.
156. Jennette, J.C., J.R. Hoidal, and R.J. Falk, *Specificity of anti-neutrophil cytoplasmic autoantibodies for proteinase 3.* Blood, 1990. **75**(11): p. 2263-4.
157. Falk, R.J., et al., *Anti-neutrophil cytoplasmic autoantibodies induce neutrophils to degranulate and produce oxygen radicals in vitro.* Proc Natl Acad Sci U S A, 1990. **87**(11): p. 4115-9.
158. Padrines, M., et al., *Interleukin-8 processing by neutrophil elastase, cathepsin G and proteinase-3.* FEBS Lett, 1994. **352**(2): p. 231-5.
159. Coeshott, C., et al., *Converting enzyme-independent release of tumor necrosis factor alpha and IL-1beta from a stimulated human monocytic cell line in the presence of activated neutrophils or purified proteinase 3.* Proc Natl Acad Sci U S A, 1999. **96**(11): p. 6261-6.
160. Abdelmohsen, K., et al., *Posttranscriptional gene regulation by RNA-binding proteins during oxidative stress: implications for cellular senescence.* Biol Chem, 2008. **389**(3): p. 243-55.
161. Briata, P., et al., *p38-dependent phosphorylation of the mRNA decay-promoting factor KSRP controls the stability of select myogenic transcripts.* Mol Cell, 2005. **20**(6): p. 891-903.
162. Chen, C.Y., et al., *AU binding proteins recruit the exosome to degrade ARE-containing mRNAs.* Cell, 2001. **107**(4): p. 451-64.
163. Gherzi, R., et al., *A KH domain RNA binding protein, KSRP, promotes ARE-directed mRNA turnover by recruiting the degradation machinery.* Mol Cell, 2004. **14**(5): p. 571-83.
164. Linker, K., et al., *Involvement of KSRP in the post-transcriptional regulation of human iNOS expression-complex interplay of KSRP with TTP and HuR.* Nucleic Acids Res, 2005. **33**(15): p. 4813-27.
165. Ruggiero, T., et al., *Identification of a set of KSRP target transcripts upregulated by PI3K-AKT signaling.* BMC Mol Biol, 2007. **8**: p. 28.
166. Leiro, J.M., et al., *The anti-inflammatory activity of the polyphenol resveratrol may be partially related to inhibition of tumour necrosis factor-alpha (TNF-alpha) pre-mRNA splicing.* Molecular Immunology, 2010. **47**(5): p. 1114-1120.
167. Wang, M.J., et al., *Resveratrol inhibits interleukin-6 production in cortical mixed glial cells under hypoxia/hypoglycemia followed by reoxygenation.* Journal of Neuroimmunology, 2001. **112**(1-2): p. 28-34.
168. Youn, J., et al., *Resveratrol and piceatannol inhibit iNOS expression and NF-kappaB activation in dextran sulfate sodium-induced mouse colitis.* Nutr Cancer, 2009. **61**(6): p. 847-54.
169. Fried, H. and U. Kutay, *Nucleocytoplasmic transport: taking an inventory.* Cellular and Molecular Life Sciences, 2003. **60**(8): p. 1659-1688.
170. Macara, I.G., *Transport into and out of the nucleus.* Microbiol Mol Biol Rev, 2001. **65**(4): p. 570-94, table of contents.
171. Harel, A. and D.J. Forbes, *Importin beta: conducting a much larger cellular symphony.* Mol Cell, 2004. **16**(3): p. 319-30.
172. Askjaer, P., et al., *Ran GTPase cycle and importins alpha and beta are essential for spindle formation and nuclear envelope assembly in living Caenorhabditis elegans embryos.* Mol Biol Cell, 2002. **13**(12): p. 4355-70.

173. Gorlich, D., et al., *Isolation of a protein that is essential for the first step of nuclear protein import.* Cell, 1994. **79**(5): p. 767-78.
174. Gorlich, D. and R.A. Laskey, *Roles of importin in nuclear protein import.* Cold Spring Harb Symp Quant Biol, 1995. **60**: p. 695-9.
175. Gorlich, D., et al., *Two different subunits of importin cooperate to recognize nuclear localization signals and bind them to the nuclear envelope.* Curr Biol, 1995. **5**(4): p. 383-92.
176. Walther, T.C., et al., *RanGTP mediates nuclear pore complex assembly.* Nature, 2003. **424**(6949): p. 689-94.
177. Harel, A., et al., *Importin beta negatively regulates nuclear membrane fusion and nuclear pore complex assembly.* Mol Biol Cell, 2003. **14**(11): p. 4387-96.
178. Klymkowsky, M.W., *Intermediate filaments in 3T3 cells collapse after intracellular injection of a monoclonal anti-intermediate filament antibody.* Nature, 1981. **291**(5812): p. 249-51.
179. Gawlitta, W., M. Osborn, and K. Weber, *Coiling of intermediate filaments induced by microinjection of a vimentin-specific antibody does not interfere with locomotion and mitosis.* Eur J Cell Biol, 1981. **26**(1): p. 83-90.
180. Venetianer, A., et al., *Cessation of cytokeratin expression in a rat hepatoma cell line lacking differentiated functions.* Nature, 1983. **305**(5936): p. 730-3.
181. Hedberg, K.K. and L.B. Chen, *Absence of intermediate filaments in a human adrenal cortex carcinoma-derived cell line.* Exp Cell Res, 1986. **163**(2): p. 509-17.
182. Holwell, T.A., S.C. Schweitzer, and R.M. Evans, *Tetracycline regulated expression of vimentin in fibroblasts derived from vimentin null mice.* J Cell Sci, 1997. **110 (Pt 16)**: p. 1947-56.
183. Colucci-Guyon, E., et al., *Mice lacking vimentin develop and reproduce without an obvious phenotype.* Cell, 1994. **79**(4): p. 679-94.
184. Djabali, K., *Cytoskeletal proteins connecting intermediate filaments to cytoplasmic and nuclear periphery.* Histol Histopathol, 1999. **14**(2): p. 501-9.
185. Coulombe, P.A., et al., *The 'ins' and 'outs' of intermediate filament organization.* Trends Cell Biol, 2000. **10**(10): p. 420-8.
186. Eckes, B., et al., *Impaired mechanical stability, migration and contractile capacity in vimentin-deficient fibroblasts.* J Cell Sci, 1998. **111 (Pt 13)**: p. 1897-907.
187. Wu, M., et al., *Proteome analysis of human androgen-independent prostate cancer cell lines: variable metastatic potentials correlated with vimentin expression.* Proteomics, 2007. **7**(12): p. 1973-83.
188. Sun, S., et al., *Proteomics of Hepatocellular Carcinoma: Serum Vimentin As a Surrogate Marker for Small Tumors (<= 2 cm).* Journal of Proteome Research, 2010. **9**(4): p. 1923-1930.
189. Nieminen, M., et al., *Vimentin function in lymphocyte adhesion and transcellular migration.* Nat Cell Biol, 2006. **8**(2): p. 156-62.
190. Moisan, E. and D. Girard, *Cell surface expression of intermediate filament proteins vimentin and lamin B1 in human neutrophil spontaneous apoptosis.* J Leukoc Biol, 2006. **79**(3): p. 489-98.
191. Gettins, P., P.A. Patston, and M. Schapira, *Structure and Mechanism of Action of Serpins.* Hematology-Oncology Clinics of North America, 1992. **6**(6): p. 1393-1408.
192. Gooptu, B. and D.A. Lomas, *Conformational Pathology of the Serpins: Themes, Variations, and Therapeutic Strategies.* Annual Review of Biochemistry, 2009. **78**: p. 147-176.

193. Remold-O'Donnell, E., J.C. Nixon, and R.M. Rose, *Elastase inhibitor. Characterization of the human elastase inhibitor molecule associated with monocytes, macrophages, and neutrophils.* J Exp Med, 1989. **169**(3): p. 1071-86.
194. Benarafa, C. and E. Remold-O'Donnell, *The ovalbumin serpins revisited: perspective from the chicken genome of clade B serpin evolution in vertebrates.* Proc Natl Acad Sci U S A, 2005. **102**(32): p. 11367-72.
195. Cooley, J., et al., *The serpin MNEI inhibits elastase-like and chymotrypsin-like serine proteases through efficient reactions at two active sites.* Biochemistry, 2001. **40**(51): p. 15762-70.
196. Benarafa, C., G.P. Priebe, and E. Remold-O'Donnell, *The neutrophil serine protease inhibitor serpinb1 preserves lung defense functions in Pseudomonas aeruginosa infection.* J Exp Med, 2007. **204**(8): p. 1901-9.
197. Samal, B., et al., *Cloning and characterization of the cDNA encoding a novel human pre-B-cell colony-enhancing factor.* Mol Cell Biol, 1994. **14**(2): p. 1431-7.
198. Fukuhara, A., et al., *Visfatin: a protein secreted by visceral fat that mimics the effects of insulin.* Science, 2005. **307**(5708): p. 426-30.
199. Kitani, T., S. Okuno, and H. Fujisawa, *Growth phase-dependent changes in the subcellular localization of pre-B-cell colony-enhancing factor.* FEBS Lett, 2003. **544**(1-3): p. 74-8.
200. Burgos, E.S. and V.L. Schramm, *Weak coupling of ATP hydrolysis to the chemical equilibrium of human nicotinamide phosphoribosyltransferase.* Biochemistry, 2008. **47**(42): p. 11086-96.
201. Garten, A., et al., *Nampt: linking NAD biology, metabolism and cancer.* Trends Endocrinol Metab, 2009. **20**(3): p. 130-8.
202. Romacho, T., et al., *Extracellular PBEF/NAMPT/visfatin activates pro-inflammatory signalling in human vascular smooth muscle cells through nicotinamide phosphoribosyltransferase activity.* Diabetologia, 2009. **52**(11): p. 2455-63.
203. Busso, N., et al., *Pharmacological inhibition of nicotinamide phosphoribosyltransferase/visfatin enzymatic activity identifies a new inflammatory pathway linked to NAD.* PLoS One, 2008. **3**(5): p. e2267.
204. Chen, M.P., et al., *Elevated plasma level of visfatin/pre-B cell colony-enhancing factor in patients with type 2 diabetes mellitus.* J Clin Endocrinol Metab, 2006. **91**(1): p. 295-9.
205. Maury, E. and S.M. Brichard, *Adipokine dysregulation, adipose tissue inflammation and metabolic syndrome.* Mol Cell Endocrinol, 2010. **314**(1): p. 1-16.
206. Otero, M., et al., *Changes in plasma levels of fat-derived hormones adiponectin, leptin, resistin and visfatin in patients with rheumatoid arthritis.* Ann Rheum Dis, 2006. **65**(9): p. 1198-201.
207. Nowell, M.A., et al., *Regulation of pre-B cell colony-enhancing factor by STAT-3-dependent interleukin-6 trans-signaling: implications in the pathogenesis of rheumatoid arthritis.* Arthritis Rheum, 2006. **54**(7): p. 2084-95.
208. Brentano, F., et al., *Pre-B cell colony-enhancing factor/visfatin, a new marker of inflammation in rheumatoid arthritis with proinflammatory and matrix-degrading activities.* Arthritis Rheum, 2007. **56**(9): p. 2829-39.
209. Takebayashi, K., et al., *Association between plasma visfatin and vascular endothelial function in patients with type 2 diabetes mellitus.* Metabolism, 2007. **56**(4): p. 451-8.

210. Yilmaz, M.I., et al., *Normalization of endothelial dysfunction following renal transplantation is accompanied by a reduction of circulating visfatin/NAMPT. A novel marker of endothelial damage?* Clin Transplant, 2009. **23**(2): p. 241-8.
211. Moschen, A.R., et al., *Visfatin, an adipocytokine with proinflammatory and immunomodulating properties.* J Immunol, 2007. **178**(3): p. 1748-58.
212. Lee, W.J., et al., *Visfatin-induced expression of inflammatory mediators in human endothelial cells through the NF-kappaB pathway.* Int J Obes (Lond), 2009. **33**(4): p. 465-72.
213. Malamitsi-Puchner, A., et al., *Blood visfatin concentrations in normal full-term pregnancies.* Acta Paediatr, 2007. **96**(4): p. 526-9.
214. Ibanez, L., et al., *Gender specificity of body adiposity and circulating adiponectin, visfatin, insulin, and insulin growth factor-I at term birth: relation to prenatal growth.* J Clin Endocrinol Metab, 2008. **93**(7): p. 2774-8.
215. Morgan, S.A., J.B. Bringolf, and E.R. Seidel, *Visfatin expression is elevated in normal human pregnancy.* Peptides, 2008. **29**(8): p. 1382-9.
216. Mazaki-Tovi, S., et al., *Maternal visfatin concentration in normal pregnancy.* J Perinat Med, 2009. **37**(3): p. 206-17.
217. MacLaren, R., W. Cui, and K. Cianflone, *Visfatin expression is hormonally regulated by metabolic and sex hormones in 3T3-L1 pre-adipocytes and adipocytes.* Diabetes Obes Metab, 2007. **9**(4): p. 490-7.
218. Ritossa, P., *[Problems of prophylactic vaccinations of infants.].* Riv Ist Sieroter Ital, 1962. **37**: p. 79-108.
219. Ciocca, D.R., et al., *Biological and clinical implications of heat shock protein 27,000 (Hsp27): a review.* J Natl Cancer Inst, 1993. **85**(19): p. 1558-70.
220. Dudich, I.V., et al., *Dimer structure as a minimum cooperative subunit of small heat-shock proteins.* Biochim Biophys Acta, 1995. **1253**(2): p. 163-8.
221. Jakob, U., et al., *Small heat shock proteins are molecular chaperones.* J Biol Chem, 1993. **268**(3): p. 1517-20.
222. Ehrnsperger, M., et al., *Binding of non-native protein to Hsp25 during heat shock creates a reservoir of folding intermediates for reactivation.* EMBO J, 1997. **16**(2): p. 221-9.
223. Haslbeck, M. and J. Buchner, *Chaperone function of sHsps.* Prog Mol Subcell Biol, 2002. **28**: p. 37-59.
224. Bruey, J.M., et al., *Differential regulation of HSP27 oligomerization in tumor cells grown in vitro and in vivo.* Oncogene, 2000. **19**(42): p. 4855-63.
225. Garrido, C., *Size matters: of the small HSP27 and its large oligomers.* Cell Death Differ, 2002. **9**(5): p. 483-5.
226. Kato, K., et al., *Dissociation as a result of phosphorylation of an aggregated form of the small stress protein, hsp27.* J Biol Chem, 1994. **269**(15): p. 11274-8.
227. Charette, S.J., et al., *Inhibition of Daxx-mediated apoptosis by heat shock protein 27.* Mol Cell Biol, 2000. **20**(20): p. 7602-12.
228. Theriault, J.R., et al., *Essential role of the NH2-terminal WD/EPF motif in the phosphorylation-activated protective function of mammalian Hsp27.* J Biol Chem, 2004. **279**(22): p. 23463-71.
229. Rane, M.J., et al., *Heat shock protein 27 controls apoptosis by regulating Akt activation.* J Biol Chem, 2003. **278**(30): p. 27828-35.
230. Stokoe, D., et al., *Identification of MAPKAP kinase 2 as a major enzyme responsible for the phosphorylation of the small mammalian heat shock proteins.* FEBS Lett, 1992. **313**(3): p. 307-13.

231. Rouse, J., et al., *A novel kinase cascade triggered by stress and heat shock that stimulates MAPKAP kinase-2 and phosphorylation of the small heat shock proteins.* Cell, 1994. **78**(6): p. 1027-37.
232. Widmann, C., et al., *Mitogen-activated protein kinase: conservation of a three-kinase module from yeast to human.* Physiol Rev, 1999. **79**(1): p. 143-80.
233. Zoubeidi, A., et al., *Cooperative interactions between androgen receptor (AR) and heat-shock protein 27 facilitate AR transcriptional activity.* Cancer Res, 2007. **67**(21): p. 10455-65.
234. Yuan, J. and E. Rozengurt, *PKD, PKD2, and p38 MAPK mediate Hsp27 serine-82 phosphorylation induced by neurotensin in pancreatic cancer PANC-1 cells.* Journal of Cellular Biochemistry, 2008. **103**(2): p. 648-62.
235. Maizels, E.T., et al., *Heat-shock protein-25/27 phosphorylation by the delta isoform of protein kinase C.* Biochem J, 1998. **332 (Pt 3)**: p. 703-12.
236. Evans, I.M., G. Britton, and I.C. Zachary, *Vascular endothelial growth factor induces heat shock protein (HSP) 27 serine 82 phosphorylation and endothelial tubulogenesis via protein kinase D and independent of p38 kinase.* Cell Signal, 2008. **20**(7): p. 1375-84.
237. Gerthoffer, W.T. and S.J. Gunst, *Invited review: focal adhesion and small heat shock proteins in the regulation of actin remodeling and contractility in smooth muscle.* J Appl Physiol, 2001. **91**(2): p. 963-72.
238. Welsh, M.J. and M. Gaestel, *Small heat-shock protein family: function in health and disease.* Ann N Y Acad Sci, 1998. **851**: p. 28-35.
239. Perng, M.D., et al., *Intermediate filament interactions can be altered by HSP27 and alphaB-crystallin.* J Cell Sci, 1999. **112 (Pt 13)**: p. 2099-112.
240. Lee, J.S., et al., *Heat shock protein 27 interacts with vimentin and prevents insolubilization of vimentin subunits induced by cadmium.* Exp Mol Med, 2005. **37**(5): p. 427-35.
241. Parcellier, A., et al., *Heat shock proteins, cellular chaperones that modulate mitochondrial cell death pathways.* Biochem Biophys Res Commun, 2003. **304**(3): p. 505-12.
242. Belka, C., et al., *Interleukin (IL)-6 signaling leads to phosphorylation of the small heat shock protein (Hsp)27 through activation of the MAP kinase and MAPKAP kinase 2 pathway in monocytes and monocytic leukemia cells.* Leukemia, 1995. **9**(2): p. 288-94.
243. Wong, H.R. and J.R. Wispe, *The stress response and the lung.* Am J Physiol, 1997. **273**(1 Pt 1): p. L1-9.
244. Polla, B.S., et al., *Stress proteins in inflammation.* Ann N Y Acad Sci, 1998. **851**: p. 75-85.
245. Concannon, C.G., A.M. Gorman, and A. Samali, *On the role of Hsp27 in regulating apoptosis.* Apoptosis, 2003. **8**(1): p. 61-70.
246. Arrigo, A.P., *Hsp27: novel regulator of intracellular redox state.* IUBMB Life, 2001. **52**(6): p. 303-7.
247. Rogalla, T., et al., *Regulation of Hsp27 oligomerization, chaperone function, and protective activity against oxidative stress/tumor necrosis factor alpha by phosphorylation.* J Biol Chem, 1999. **274**(27): p. 18947-56.
248. Jacquier-Sarlin, M.R. and B.S. Polla, *Dual regulation of heat-shock transcription factor (HSF) activation and DNA-binding activity by H2O2: role of thioredoxin.* Biochem J, 1996. **318 (Pt 1)**: p. 187-93.
249. Alford, K.A., et al., *Heat shock protein 27 functions in inflammatory gene expression and transforming growth factor-beta-activated kinase-1 (TAK1)-mediated signaling.* J Biol Chem, 2007. **282**(9): p. 6232-41.

250. Polla, B.S., et al., *Heat shock proteins in inflammation and asthma: Dr Jekyll or Mr Hyde?* Clin Exp Allergy, 1998. **28**(5): p. 527-9.
251. Sur, R., P.A. Lyte, and M.D. Southall, *Hsp27 regulates pro-inflammatory mediator release in keratinocytes by modulating NF-kappaB signaling.* J Invest Dermatol, 2008. **128**(5): p. 1116-22.
252. Parcellier, A., et al., *HSP27 is a ubiquitin-binding protein involved in I-kappaBalpha proteasomal degradation.* Mol Cell Biol, 2003. **23**(16): p. 5790-802.
253. Miller, H., et al., *Modulation of estrogen signaling by the novel interaction of heat shock protein 27, a biomarker for atherosclerosis, and estrogen receptor beta: mechanistic insight into the vascular effects of estrogens.* Arterioscler Thromb Vasc Biol, 2005. **25**(3): p. e10-4.
254. Rayner, K., et al., *Extracellular release of the atheroprotective heat shock protein 27 is mediated by estrogen and competitively inhibits acLDL binding to scavenger receptor-A.* Circ Res, 2008. **103**(2): p. 133-41.
255. Rayner, K., et al., *Heat shock protein 27 protects against atherogenesis via an estrogen-dependent mechanism: role of selective estrogen receptor beta modulation.* Arterioscler Thromb Vasc Biol, 2009. **29**(11): p. 1751-6.
256. Garrido, C., et al., *Heat shock proteins 27 and 70: anti-apoptotic proteins with tumorigenic properties.* Cell Cycle, 2006. **5**(22): p. 2592-601.
257. Conroy, S.E. and D.S. Latchman, *Do heat shock proteins have a role in breast cancer?* Br J Cancer, 1996. **74**(5): p. 717-21.
258. Kapranos, N., et al., *Expression of the 27-kDa heat shock protein (HSP27) in gastric carcinomas and adjacent normal, metaplastic, and dysplastic gastric mucosa, and its prognostic significance.* J Cancer Res Clin Oncol, 2002. **128**(8): p. 426-32.
259. Arts, H.J., et al., *Heat-shock-protein-27 (hsp27) expression in ovarian carcinoma: relation in response to chemotherapy and prognosis.* Int J Cancer, 1999. **84**(3): p. 234-8.
260. Wataba, K., et al., *Over-expression of heat shock proteins in carcinogenic endometrium.* Int J Cancer, 2001. **91**(4): p. 448-56.
261. Zhang, R., et al., *Identification of differentially expressed proteins in human glioblastoma cell lines and tumors.* Glia, 2003. **42**(2): p. 194-208.
262. Cornford, P.A., et al., *Heat shock protein expression independently predicts clinical outcome in prostate cancer.* Cancer Res, 2000. **60**(24): p. 7099-105.
263. Garrido, C., et al., *HSP27 as a mediator of confluence-dependent resistance to cell death induced by anticancer drugs.* Cancer Res, 1997. **57**(13): p. 2661-7.
264. Song, H., et al., *Stat3 modulates heat shock 27kDa protein expression in breast epithelial cells.* Biochem Biophys Res Commun, 2004. **314**(1): p. 143-50.
265. Vargas-Roig, L.M., et al., *Heat shock protein expression and drug resistance in breast cancer patients treated with induction chemotherapy.* Int J Cancer, 1998. **79**(5): p. 468-75.
266. Thanner, F., et al., *Heat shock protein 27 is associated with decreased survival in node-negative breast cancer patients.* Anticancer Res, 2005. **25**(3A): p. 1649-53.
267. Jaattela, M., *Over-expression of hsp70 confers tumorigenicity to mouse fibrosarcoma cells.* Int J Cancer, 1995. **60**(5): p. 689-93.
268. Garrido, C., et al., *Heat shock protein 27 enhances the tumorigenicity of immunogenic rat colon carcinoma cell clones.* Cancer Res, 1998. **58**(23): p. 5495-9.

269. Kang, S.H., et al., *Upregulated HSP27 in human breast cancer cells reduces Herceptin susceptibility by increasing Her2 protein stability.* BMC Cancer, 2008. **8**: p. 286.
270. Hansen, R.K., et al., *Hsp27 overexpression inhibits doxorubicin-induced apoptosis in human breast cancer cells.* Breast Cancer Res Treat, 1999. **56**(2): p. 187-96.
271. Rocchi, P., et al., *Heat shock protein 27 increases after androgen ablation and plays a cytoprotective role in hormone-refractory prostate cancer.* Cancer Res, 2004. **64**(18): p. 6595-602.
272. Razandi, M., A. Pedram, and E.R. Levin, *Heat Shock Protein 27 is required for sex steroid receptor trafficking to and functioning at the plasma membrane.* Mol Cell Biol, 2010.
273. Chen, H., M. Hewison, and J.S. Adams, *Control of estradiol-directed gene transactivation by an intracellular estrogen-binding protein and an estrogen response element-binding protein.* Mol Endocrinol, 2008. **22**(3): p. 559-69.
274. Boonyaratanakornkit, V., et al., *The role of extranuclear signaling actions of progesterone receptor in mediating progesterone regulation of gene expression and the cell cycle.* Mol Endocrinol, 2007. **21**(2): p. 359-75.
275. Skildum, A., E. Faivre, and C.A. Lange, *Progesterone receptors induce cell cycle progression via activation of mitogen-activated protein kinases.* Mol Endocrinol, 2005. **19**(2): p. 327-39.
276. Haas, D., et al., *The modulator of nongenomic actions of the estrogen receptor (MNAR) regulates transcription-independent androgen receptor-mediated signaling: evidence that MNAR participates in G protein-regulated meiosis in Xenopus laevis oocytes.* Mol Endocrinol, 2005. **19**(8): p. 2035-46.

9 Publications

9.1 Poster presentations

- **Behnke, F.**, Kutter T., Golkowski M., Ziegler, T., Werz, O. (2009) Improved Drug Target Discovery Strategies: The Target-Fishing Approach. Posterpräsentation, *Frontiers in medicinal Chemistry* 2009, Heidelberg

- **Behnke, F.**, Kutter T., Golkowski M., Ziegler, T., Werz, O. (2009) Drug Target Identification: UV-Light Cleavable Linker Systems For Pull-Down Assays. Posterpräsentation, *DPhG Jahrestagung*, Jena

- Etzel, Y., **Behnke, F.**, Golkowski M., Ziegler, T., Werz, O., Dodt, G. (2009) Discovering Drug-Target Interactions: The Target Fishing Approach. Posterpräsentation, *EMBO Meeting*, Amsterdam

- Etzel, Y., **Behnke, F.**, Golkowski M., Ziegler, T., Werz, O., Dodt, G. (2009) Discovering Drug-Target Interactions: The Target Fishing Approach. Posterpräsentation, *IFIB Postersession*, Tübingen

- Dittrich, M., Zettl, H., Greiner, C., **Behnke, F.**, Werz, O., Schubert-Zsilavecz, M. (2009) Use Of The „Target Fishing“ Approach For Identification Of Further Proteins Affected By Pirinixic Acid Derivatives. Posterpräsentation, *DPhG Jehrestagung*, Jena

- Dittrich, M., Zettl, H., Greiner, C., **Behnke, F.**, Werz, O., Schubert-Zsilavecz, M. (2009) Use Of The „Target Fishing“ Approach For Identification Of Further Proteins Affected By Pirinixic Acid Derivatives. Posterpräsentation, *Frontiers In Medicinal Chemistry*, Barcelona

9.2 Patents/ Invention disclosures

- **Behnke, F.**, Kutter T., Golkowski M., Ziegler, T., Werz, O. (2008) UV-Licht spaltbare Linker für das Target-Fishing. Erfindungsmeldung

- **Behnke, F.**, Golkowski M., Ziegler, T., Werz, O. (2008). Carboxymethoxylamin aktivierte Beads zur Immobilisierung von Ketonen und Aldehyden für Pull-Down Assays. Erfindungsmeldung

9.3 Others

- **Behnke, F.** (2009) Mass spectrometry based Proteomics. Oral presentation, *Summerschool of the Pharmaceutical Institute*, Oberjoch

- Editorial contribution at: Ammon H. T. P. (Hrsg.) Hunnius Pharmazeutisches Wörterbuch, 11. Auflage. Berlin: de Gruyter

10 Acknowledgements

Mein besonderer Dank gilt Herrn Prof. Dr. Werz für das entgegengebrachte Vertrauen, und die mir gebotenen Möglichkeiten.
Bei Herrn Prof. Dr. Laufer möchte ich mich ganz herzlich für die Übernahme des Zweitgutachtens bedanken.
Aufs Herzlichste möchte ich mich bei meinen Mitstreitern des Arbeitskreises bedanken, die zu einem außergewöhnlich motivierenden, produktiven und kreativen Laboralltag beigetragen haben und auch darüberhinaus stets mit Rat und Tat zur Seite standen.

Bei allen Prüfern und Gutachtern möchte ich mich für die investierte Zeit und Arbeit, vor allem aber für kritische Fragen und Denkanstöße bedanken.
Bei den Kollegen des Promotionsverbundes möchte ich mich ganz herzlich für die äußerst produktive und unkomplizierte Zusammenarbeit bedanken, ohne die diese Arbeit so nicht möglich gewesen wäre: bei den Professoren Ziegler, Maier, Dodt und Laufer, die stets mit Ihrem Rat zur Seite standen, bei Yvonne, Martin, Kutti, Marc und Pramod für die umfangreiche Unterstützung, die Kooperation, die Anregungen und für die weisen Ratschläge.
Prof. Dr. A. Norheim und Dr. T. Lamkemeyer aus dem Proteom-Center Tübingen für die Beratung und Unterstützung bei massenspektrometrischen Analysen.
Bei Frau Prof. Dirsch möchte ich mich ganz herzlich für die Bereitstellung des Indirubin-3´-Monoximes bedanken. Ihr und Herrn Prof. Erker möchte ich des Weiteren für die Unterstützung im Resveratrol Projekt ganz herzlichst danken.
Herrn Prof. Dr. H. Northoff und dem Team der Transfusionsmedizin der Universitätsklinik Tübingen gilt mein besonderer Dank für die Bereitstellung der Buffy-Coats.

Mein größter Dank gilt jedoch meiner Familie, ohne deren Unterstützung ich diesen Weg nicht hätte gehen können.